A DEVELOPMENT OF HI-PERFORMANCE INDUSTRIAL RUBBER ROLLERS BASED ON NEOPRENE RUBBER

YOTWADEE CHOKANANDSOMBAT

A THESIS SUBMITTED IN PARTIAL FULFILLMENT
OF THE REQUIREMENTS FOR
THE DEGREE OF MASTER OF SCIENCE
(POLYMER SCIENCE AND TECHNOLOGY)
FACULTY OF GRADUATE STUDIES
MAHIDOL UNIVERSITY
2010

Thesis
entitled

A DEVELOPMENT OF HI-PERFORMANCE INDUSTRIAL RUBBER ROLLERS BASED ON NEOPRENE RUBBER

....
Miss Yotwadee Chokanandsombat
Candidate

....
Assoc. Prof. Chakrit Sirisinha,
Ph. D.
Major-advisor

Pongdhorn Saeoui
....
Mr. Pongdhorn Sae-Oui,
Ph. D.
Co-advisor

....
Prof. Banchong Mahaisavariya,
M. D., Dip Thai Board of Orthopedics
Dean
Faculty of Graduate Studies
Mahidol University

P. Sunintaboon
....
Lect. Panya Sunintaboon,
Ph. D.
Program Director
Master of Science Program in
Polymer Science and Technology
Faculty of Science
Mahidol University

Thesis
entitled

A DEVELOPMENT OF HI-PERFORMANCE INDUSTRIAL RUBBER ROLLERS BASED ON NEOPRENE RUBBER

was submitted to the Faculty of Graduate Studies, Mahidol University
for the degree of Master of Science (Polymer Science and Technology)
on
October 5, 2010

Miss Yotwadee Chokanandsombat
Candidate

Kanoktip Boonkerd

Lect. Kanoktip Boonkerd,
Ph. D.
Chair

Assoc. Prof. Chakrit Sirisinha,
Ph. D.
Member

Pongdhorn Saeoui

Mr. Pongdhorn Sae-Oui,
Ph. D.
Member

B. Mahai

Prof. Banchong Mahaisavariya,
M. D., Dip Thai Board of Orthopedics
Dean
Faculty of Graduate Studies
Mahidol University

Prof. Skorn Mongkolsuk,
Ph. D.
Dean
Faculty of Science
Mahidol University

ACKNOWLEDGEMENTS

This research project would not have been succeeded without the extensive support and assistance from my admirable advisor, Assoc. Prof. Chakrit Sirisinha. I would like to express my sincere gratitude, for his valuable suggestion, encouragement, kind supervision and supporting as well as attentive interest throughout the course of this research. My appreciation and sincerity pass to Dr. Pongdhorn Sae-Oui for his helpful suggestion and inspiring guidance for completion of this thesis. Furthermore, the sincere thankfulness is given to Dr. Kanoktip Boonkerd, who is the external examiner of this thesis defense, for her valuable comment and advice.

For the cooperation, I would like to thanks Polymer Science and Technology Program in Department of Chemistry, Faculty of Science, Mahidol University and Research and Development Centre for Thai Rubber Industry (RDCTRI) for the use of their machine and other facilities.

I would like to pass my gratitude to the Thailand Research Fund–Master Research Grants (TRF–MAG) and Thai Industrial Rollers Co., Ltd. for the financial support of this research.

Furthermore, my thankfulness go to teachers and staffs of this program for their assistance and suggestion and I wish to heartfelt thanks my nice friends and polymer graduate students whose names are not mentioned here, for their help, kindness, suggestion, and encouragement.

Finally, I take this opportunity to express my sincere gratitude to my lovely family for their encouragement, understanding, inspiration and giving my best thing all times.

Yotwadee Chokanandsombat

A DEVELOPMENT OF HI-PERFORMANCE INDUSTRIAL RUBBER ROLLERS BASED ON NEOPRENE RUBBER

YOTWADEE CHOKANANDSOMBAT 5036072 SCPO/M

M.Sc. (POLYMER SCIENCE AND TECHNOLOGY)

THESIS ADVISORY COMMITTEE: CHAKRIT SIRISINHA, Ph.D. (RUBBER ENGINEERING), PONGDHORN SAE-OUI, Ph.D. (RUBBER ENGINEERING)

ABSTRACT

Polychloroprene (CR), commonly referred to “Neoprene”, is widely used in many applications requiring good mechanical properties and oil resistance. For some engineering products including rubber roll applications, an optimal state-of-cure is desired in order to achieve good dynamic mechanical properties and chemical resistance. Consequently, CR vulcanizates with various loadings of zinc oxide (ZnO), magnesium oxide (MgO) and lead oxide (PbO) were prepared, and their properties were investigated.

Results obtained reveal that a crosslink density increases with increasing loadings of MgO and ZnO, and reaches the maximum value at 4 and 5 phr of MgO and ZnO, respectively. In the case of PbO, crosslink density is relatively low, implying that the MgO and ZnO contribute to the crosslink of CR more effectively than PbO. The development in crosslink density leads to the improvement of most of mechanical properties. However, the compression set and heat build-up (HBU) show unexpected results which disagree with the crosslink density results. Such results are believed to be caused by the occurrence of post-curing effect and molecular restriction, respectively. Additionally, the role of sulfur on properties in CR compounds and vulcanizates was also investigated, and the results indicate that sulfur plays a significant role in CR vulcanization process.

Furthermore, two different types of reinforcing fillers, namely, carbon black (CB) and precipitated silica (PSi), were incorporated into CR compounds with various loadings. Crosslink density appears to increase with increasing filler loading, which is due to the development of CR-filler interaction. The addition of filler leads to the improvement in most of mechanical properties. However, the compression set and heat build-up of PSi-filled CR are apparently poor. It is therefore interesting to investigate the role of silane coupling agent (SCA) on properties of PSi-filled CR. Results obtained reveal that the use of SCA in PSi-filled CR vulcanizates appears to significantly improve the compression set and heat- build up properties of CR.

KEY WORDS: POLYCHLOROPRENE/ METAL OXIDE/ CURING/ MECHANICAL PROPERTIES/ SILANE

172 pages

การพัฒนายางลูกกลิ้งอุตสาหกรรมสมรรถนะสูงจากยางนีโอพรีน

A DEVELOPMENT OF HI-PERFORMANCE INDUSTRIAL RUBBER ROLLERS BASED ON NEOPRENE RUBBER

ยศวดี โชคอนันต์สมบัติ 5036072 SCPO/M

วท.ม. (วิทยาศาสตร์และเทคโนโลยีพอลิเมอร์)

คณะกรรมการที่ปรึกษาวิทยานิพนธ์ : ชาคริต สิริสิงห, Ph.D. (RUBBER ENGINEERING), พงษ์ธร แซ่อุย, Ph.D. (RUBBER ENGINEERING)

บทคัดย่อ

ยางพอลีคลอโรพรีน มีชื่อทางการค้าว่ายางนีโอพรีน ซึ่งเป็นยางสังเคราะห์ที่นิยมใช้กันอย่างแพร่หลายในการผลิต ผลิตภัณฑ์ที่ต้องการสมบัติเชิงกลที่ดีและมีความทนทานต่อน้ำมัน สำหรับชิ้นงานที่ใช้งานในเชิงวิศวกรรมรวมถึงลูกกลิ้ง ผู้ผลิตจำเป็นต้องปรับสภาวะการคงรูปยางที่เหมาะสม เพื่อให้ได้ยางที่มีคุณสมบัติเชิงพลวัตและทนต่อสารเคมีที่ดี ดังนั้นในงานนี้ยางพอลีคลอโรพรีนผลิตภัณฑ์ ที่มีปริมาณของ ซิงค์ออกไซค์ แมกนีเซียมออกไซค์ และตะกั่วออกไซค์ต่างกันจึงถูกเตรียมขึ้น และสมบัติต่างๆของยางผลิตภัณฑ์จะถูกพิจารณา ผลการศึกษาที่ได้ชี้ให้เห็นว่าทั้งซิงค์ออกไซค์และแมกนีเซียมออกไซค์ต่างมีอิทธิพลต่อการสุกตัวของยางพอลีคลอโรพรีน กล่าวคือปริมาณการเชื่อมขวางของยางเพิ่มขึ้นตามปริมาณของโลหะออกไซค์ทั้งสองที่เพิ่มขึ้น โดยเฉพาะอย่างยิ่งที่ปริมาณ ซิงค์ออกไซค์ 5 phr และแมกนีเซียมออกไซค์ 4 phr ส่วนในกรณีของตะกั่วออกไซค์นั้น พบว่าปริมาณการเชื่อมขวางของยางมีระดับที่ต่ำ เมื่อเทียบกับโลหะออกไซค์ทั้งสอง จึงอาจกล่าวได้ว่าโลหะออกไซค์ทั้งสองมีผลต่อการเชื่อมขวางของยางพอลีคลอโรพรีนมากกว่าตะกั่วออกไซค์ การเพิ่มขึ้นของปริมาณการเชื่อมขวางส่งผลให้ยางมีสมบัติเชิงกลหลายๆอย่างที่ดีขึ้น อย่างไรก็ตามค่าการเสียรูปถาวรจากแรงกดอัดและค่าอุณหภูมิก่อตัวของยาง กลับให้ผลที่สวนทางกับปริมาณการเชื่อมขวางของยาง ทั้งนี้เชื่อว่าเป็นผลมาจากการเกิดการเชื่อมขวางขณะทดสอบที่อุณหภูมิสูง และการเกิดการจำกัดการเคลื่อนไหวของโมเลกุลตามลำดับ นอกจากนี้ได้ทำการศึกษาบทบาทของซัลเฟอร์ในยางพอลีคลอโร พรีน ซึ่งผลที่ได้ชี้ให้เห็นว่าซัลเฟอร์มีบทบาทที่สำคัญ ต่อปฏิกิริยาวัลคาไนซ์เซชันของยางพอลีคลอโรพรีน

ยิ่งไปกว่านี้ยังทำการศึกษาเรื่องการเสริมแรงยางผลิตภัณฑ์โดยใช้สารตัวเติมสองชนิดได้แก่ เขม่าดำและซิลิกา โดยมีการปรับเปลี่ยนปริมาณสารตัวเติมดังกล่าว โดยพบว่าปริมาณการเชื่อมขวางของยางจะเพิ่มขึ้นตามปริมาณสารตัวเติมที่มากขึ้น ทั้งนี้เกิดเนื่องจากอันตรกิริยาระหว่างยางและสารตัวเติมที่มากขึ้นนั่นเอง ซึ่งการเติมสารตัวเติมลงไปในยางนั้นจะส่งผลให้ยางมีคุณสมบัติเชิงกลที่ดีขึ้น อย่างไรก็ตามในยางที่ใช้ซิลิกาเป็นสารตัวเติม จะให้ค่าการเสียรูปถาวรจากแรงกดอัดและค่าอุณหภูมิก่อตัวของยางที่ไม่ดี จึงทำให้มีความสนใจในบทบาทของสารคู่ควบไซเลนในยางที่เสริมแรงด้วยซิลิกา จากผลการทดลองพบว่า การเติมสารคู่ควบไซเลนลงไปในยางที่เสริมแรงด้วยซิลิกาจะช่วยปรับปรุงสมบัติค่าการเสียรูปถาวรจากแรงกดอัดและค่าอุณหภูมิก่อตัวของยางให้ดีขึ้น

172หน้า

CONTENTS

CONTENTS (cont.)

CONTENTS (cont.)

CONTENTS (cont.)

CONTENTS (cont.)

CONTENTS (cont.)

LIST OF TABLES

Table **Page**

LIST OF TABLES (cont.)

Table **Page**

LIST OF TABLES (cont.)

LIST OF TABLES (cont.)

LIST OF TABLES (cont.)

LIST OF TABLES (cont.)

LIST OF FIGURES

LIST OF FIGURES (cont.)

LIST OF FIGURES (cont.)

LIST OF FIGURES (cont.)

LIST OF FIGURES (cont.)

LIST OF FIGURES (cont.)

LIST OF FIGURES (cont.)

LIST OF FIGURES (cont.)

LIST OF ABBREVIATIONS

CR	Polychloroprene
ZnO	Zinc oxide
MgO	Magnesium oxide
PbO	Lead oxide
Pb_2O_3	Red lead
CB	Carbon black
PSi	Precipitated silica
S	Sulfur
ETU	Ethylene thiourea
6-PPD	N-(1, 3-dimethylbutyl)-N'-phenyl-p-phenylenediamine
DOP	Dioctyl phthalate
Si-69	Bis-(3-triethoxysilylpropyl) Tetrasulfane; TESPT
Si264	3-thiocyanatopropyl triethoxysilane; TCPTS
Cl	Chlorine
Si	Silica
C	Carbon
Zn	Zinc
Mg	Magnesium
Pb	Lead
O	Oxygen
NR	Natural rubber

LIST OF ABBREVIATIONS (cont.)

CSM	Chlorosulfonated polyethylene
ENR	Epoxidized natural rubber
XNBR	Carboxylated nitrile rubber
SCA	Silane coupling agent
phr	Part per hundred of rubber
DDE	Dupont dow elastomers
MW	Molecular weight
MWD	Molecular weight distribution
ASTM	American Society for Testing and Materials
ISO	International Organization for Standardization
MDR	Moving die rheometer
RPA	Rubber processing analyzer
DMA	Dynamic mechanical analysis
HBU	Heat build-up
SEM	Scanning electron microscope
EDS	Energy dispersive X-ray spectroscopy
M100	Modulus at 100 % strain

CHAPTER I

INTRODUCTION

Rubber rollers, frequently known as rubber rolls, are cylindrical tubes used to provide support and transportation of materials through the machine. In rubber roller industry, a variety of rubber materials are used depending on final properties required. Polychloroprene (CR) or neoprene is one of specialty elastomers used for a wide variety of technical rubber goods, including rubber roll industry [1, 2]. CR is a general purpose material having a wide variety of properties, such as good mechanical properties, remarkable resistance to oils and moderate resistance to most chemicals [2-4]. Furthermore, CR is relatively flame resistant and is not affected by ozone, weather and heat [3-4].

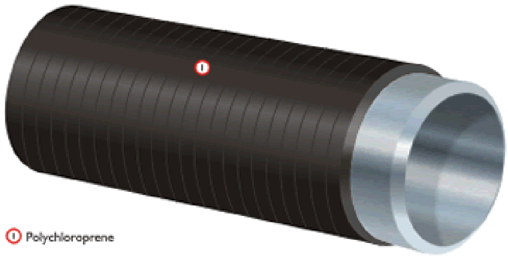

Figure 1.1 Schematic of Neoprene rubber coating roll [5]

Unlike most diene rubber, CR is not vulcanizable by sulfur alone, due to the polarity of chlorine atom causing a reduction in the reactivity of the double bond on its backbone [6]. There are many published papers suggesting the curing agents for CR [7-15]. However, the most widely used curing agent for CR is metal oxide, including zinc oxide (ZnO) in the combination with magnesium oxide (MgO) [6, 16-17]. Apart from MgO and ZnO, CR can be vulcanized with several other metallic oxides [18]. With the use of lead oxide (PbO) or red lead (Pb_2O_3), vulcanizates reveal low absorption and high acid resistance, but with much greater tendency to scorch than ones with MgO and ZnO [6, 19]. For some engineering products as rubber roll applications, the optimal state-of-cure is desired in order to achieve good dynamic mechanical properties and chemical resistance. Therefore, present work aims to investigate the effects of ZnO, MgO and PbO on cure characteristics and mechanical properties of CR. Apart from metal oxides, the effect of sulfur is of interest.

Additionally, to improve mechanical properties of CR vulcanizates, reinforcing fillers are thus incorporated. Carbon black (CB) is one of the widely used reinforcing filler providing enhancement in mechanical properties with the expense of dark color. As for light color products, precipitated silica (PSi) is usually selected as a non-black reinforcing filler. It should be noted that PSi could interact strongly with functionalized polymers including CR [20]. In this work, the influences of loading and type of filler on the cure and mechanical properties of CR composites were also studied. Furthermore, the roles of the two widely used silane coupling agents, i.e., bis-(3-triethoxysilylpropyl) tetrasulfane (Si-69) and 3-thiocyanatopropyl triethoxysilane (Si-264), on properties of PSi-filled CR vulcanizates were also studied.

CHAPTER II

OBJECTIVES

The main objectives of this work are to investigate cure characteristics, rheological properties, phase morphology and dynamic as well as static mechanical properties of polychloroprene (CR). The scope of this research consists of four main parts, as follows:

1. A study of metal oxide effect on cure characteristics and mechanical properties of CR vulcanizates.

For this part, the metal oxides commonly used with CR, i.e., magnesium oxide (MgO), zinc oxide (ZnO) and lead oxide (PbO), were chosen as curatives. The effects of type and loading of each metal oxide on cure characteristics and mechanical properties are determined. Afterward, the suitable loading and type of metal oxide are selected for the subsequent study. The loading ratio of metal oxide was multiplied. The cure characteristics and mechanical properties were investigated.

2. A study of sulfur effect on cure characteristics and mechanical properties of CR vulcanizates.

The main purpose of this part is to investigate the influence of sulfur on rheological properties, cure characteristics and mechanical properties of CR vulcanizates.

3. A study of reinforcing filler effect on cure characteristics, mechanical properties and phase morphology of CR vulcanizates.

The most widely used reinforcing fillers, i.e., carbon black (CB) and precipitated silica (PSi) were used. The effects of type and loading of both reinforcing fillers on cure characteristic, rheological properties, mechanical properties and phase morphology of CR vulcanizates were examined.

4. A study of silane coupling agent (SCA) effect on cure characteristics, mechanical properties and phase morphology of CR vulcanizates.

The final section, aims to investigate the role of silane coupling agent (SCA) on properties of PSi-filled CR vulcanizates. Two SCA selected in this study were bis-(3-triethoxysilylpropyl) tetrasulfane (Si-69) and 3-thiocyanatopropyl triethoxy silane (Si-264). The effects of both SCAs on cure characteristic, rheological characteristics, mechanical properties as well as phase morphology of PSi-filled CR were determined.

CHAPTER III

LITERATURE REVIEW

3.1 Introduction

Polychloroprene (chloroprene rubbers; CR) or chlorobutadiene is one of the earliest synthetic elastomer that is widely used in many technological applications. ‘Neoprene’ is a trade name of CR, which was registered by Dupont Dow Elastomer (DDE) who is the first CR manufacture. Polychloroprene has played an important role in the development of the rubber industry as a whole, attributed to its favorable combination of technical properties. In terms of consumption, the current worldwide capacity of CR is approximately 239,230 ton with a value of more than $1.5 billion [15].

3.2 Polymerization, Structures, Application and Properties of CR

3.2.1 Polymerization, Structures and Application of CR

Polychloroprene was discovered in 1930 at E. I. DuPont de Nemours & Co. in Wilmington Delaware [15]. The first successful polymerization under economically feasible conditions was discovered by Carothers, Collins and coworkers using emulsion polymerization techniques [1]. Afterward, in 1933, DuPont marketed this commercially synthetic elastomer under the trade name ‘Duprene’ which was then changed to ‘Neoprene’ in 1936 [15]. Nowadays, the commercial acceptable generic name for this elastomer is CR or chloroprene rubber.

In principle, it is possible to polymerize chloroprene by anionic-, cationic-, and Ziegler Natta catalysis techniques, but because of the lack of useful properties, production safety and economical considerations, the free radical emulsion polymerization of 2 – chloro – 1, 3 – butadiene is exclusively used [1, 21].

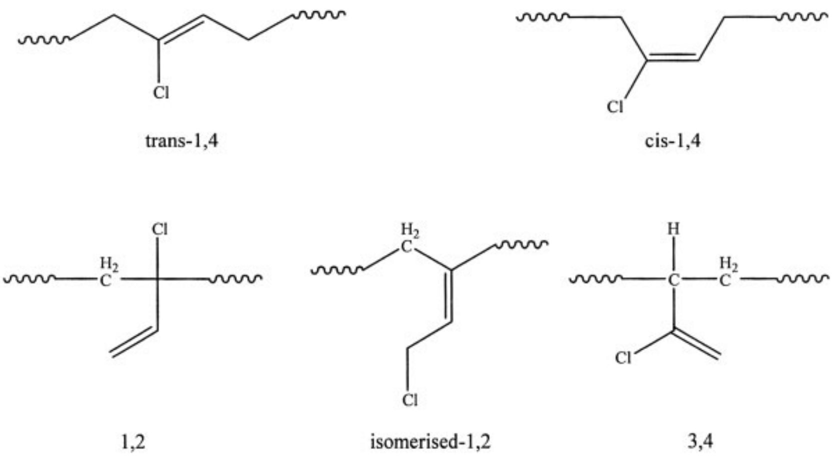

Figure 3.1 Isomeric structures typically found in CR [18]

The individual monomeric repeating units can take up to five basic configurations, as illustrated in Figure 3.1, typically 88 – 92 % trans configuration, 7 – 12 % cis configuration, 1% 3, 4 addition and 1.5 % of 1, 2 addition configuration [22]. It should be noted that the 1, 2 addition is believed to provide the principal sites of vulcanization [18, 23-24].

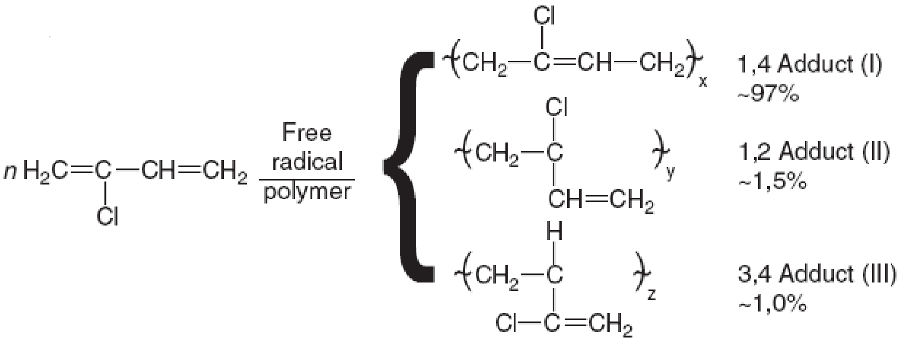

Figure 3.2 Structural units in the polychloroprene chain (typical commercial rubber grade) [1]

Some compounders have called CR “chlorinated butural rubber” because its structure is similar to that of natural rubber (NR) except that the chlorine has replaced the methyl groups [16, 25]. The addition of chlorine also increases the polarity of CR relative to that of NR.

The high content of trans 1, 4 configuration is responsible for crystallinity of CR under stress and strain, sometimes known as strain induced crystallization, similar to the case of NR [21-22, 26- 29]. This leads to the high strength of CR. The small amounts of 3, 4 and 1, 2 addition configurations lead to lower crystallinity of CR, and could be the vulcanizable sites of CR backbone, especially the 1, 2 addition configuration [18, 23, 28-29].

3.2.2 Properties of CR

CR is categorized as a multipurpose elastomer since CR does offer an excellent balance of overall properties. The CR combines both environmental resistance and toughness, especially in dynamic applications involving heat build-up and resistance to flex cracking. The high structural regularity (i.e. high trans content) of CR allows the occurrence of strain induced crystallization phenomenon giving high mechanical strength [21-22, 26- 29].

In addition, the presence of chlorine (Cl) in the polymer structure makes CR polar, which improves resistances to oil, weathering, ozone and heat [16, 22-23]. The chlorine atom not only reduces reactivity of the double bonds in CR backbone leading to the improved oxidation resistance of CR vulcanizates, but also yields the ability to retard flame [23, 28-30]. Since the time of its introduction to the marketplace, CR has been more than a simple replacement for natural rubber [15]. Furthermore, this unique combination of properties of CR makes it widely used in various applications, including automotives, construction, footwear, specialty apparel, transportation, wire and cable industry.

3.2.3 Applications of CR

As mentioned earlier, CR has a well-balanced combination of properties including processibility, strength, flex and tear resistance, flame resistance especially in the combination with chlorinated wax and adhesion, together with sufficient heat, weather and ozone resistances for most applications [29]. Consequently, CR is usually chosen for using in numerous applications. The estimated consumption of CR is approximately 250,000 tons per year, mainly in dry-rubber applications [1, 15].

Examples of CR products include power transmission, timing belting, industrial belts, mining conveyor belts, industrial rolls, vibration isolators, tank lining and hydraulic hoses. In the construction industry, CR has been replaced by EPDM for cost reasons; however, CR is still the preferred polymer if flame retardant and some oil resistance properties are required [1].

3.2.4 Grades and types of polychloroprene

A broad range of CR grades has been developed to meet changing market demands. A first subdivision of CR types is between those supplied for adhesives and dry rubber application, the latter are divided into three classes which are differentiated by the use of an appended letter (i.e., G, W and T types). These designations not only reflect the composition of the polymer, but also are derived from the manufacturing and process conditions [29].

The polymer structure can be modified by copolymerizing chloroprene monomers with sulfur and/or 2, 3 – dichloro – 1, 3 – butadiene to yield a family of materials with a broad range of chemical and physical properties [21]. Because DuPont Dow Elastomers (DDE) is the first production and the most capacity of all CR grades, it is easiest to break down the various types of polychloroprenes by using DDE’s classification [1, 15-16].

3.2.4.1 Neoprene G family

The so-called “G type” was the first grade of CR developed in which the chloroprene monomer is polymerized with sulfur (S) to control its molecular weight (MW). The polymerization and of “G type” is shown schematically in Figure 3.3 [15]. In general, “G type” possesses poor storage stability, i.e., an increase in viscosity with storage time if not stored in a cool environment [16]. However, the advantage of “G type” is its ability to be vulcanized without additional sulfur or accelerators through the uses of metal oxides (zinc oxide (ZnO), magnesium oxide (MgO) or lead oxide

(PbO)) alone. Furthermore, the “G type” can break down during mixing or milling via cleavage at the S_x group, i.e., the decrease in MW and the elasticity (or nerve during processing) [23].

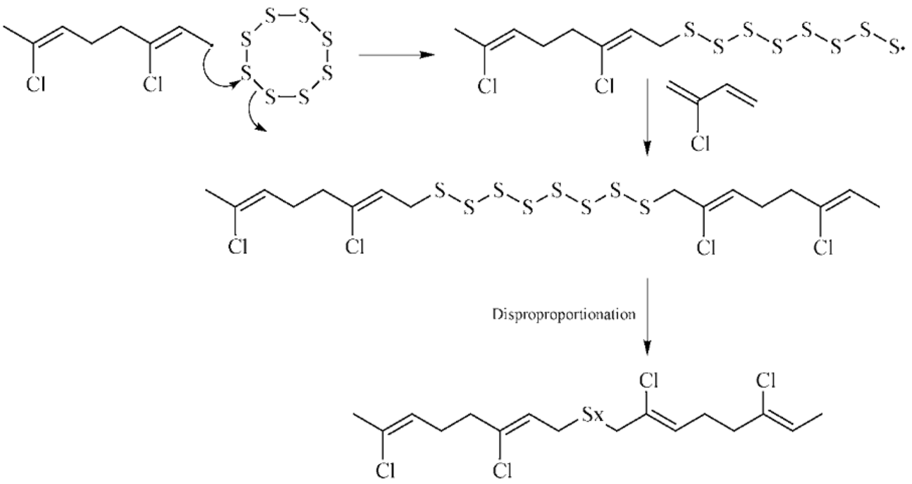

Figure 3.3 Polymerization of polychloroprene “G-type” (S_x represents one or more sulfur atoms) [15]

In general, “G type” polymers have much broaden molecular weight distribution (MWD) ranges than are found in the “W- and T- types” [16, 31]. The “G type” offers fast curing with processing safety. In terms of mechanical properties, the “G type” provides the best flex resistance, tear strength and rebound properties among all CR grades, which makes the “G-type” an excellent choice for dynamic applications.

3.2.4.2 Neoprene W family

The neoprene W is the crystalline resistance grade of CR with the high molecular weight controlled by the use of a mercaptan [23]. Thus, this grade is sometimes known as the “mercaptane modified grade”. The “W type” is chloroprene homopolymers or copolymers of chloroprene and 2, 3 – dichloro – 1, 3 – butadiene, as illustrated in Figure 3.4 [16, 31].

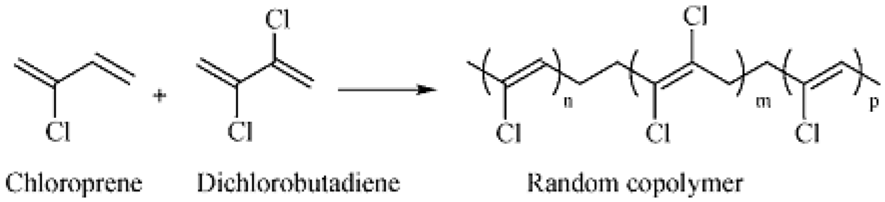

Figure 3.4 Schematic of Polychloroprene “W type” [15]

Generally, the mercaptan modified grade possesses excellent storage stability, as well as low compression set due to the length of sulfur crosslinks can be controlled better, compared with the case that the sulfur and accelerators are added during mixing [29].

The “W type” is known to have more uniform MWD than the “G type”, and is therefore not broken down during mixing [16]. This leads to the easy in mixing process, i.e., CR can be milled without sticking to the rolls. In short, one might say that the vulcanizates of W family have excellent resistances to heat, compression set, storage hardening and mechanical loads.

However, the “W type” requires additional accelerator, and a derivative of thiourea, in which the ethylene thiourea (ETU), is widely used for this purpose. The vulcanizates of “W type” obtained exhibit excellent mechanical properties, good aging resistance and very good sealing properties. It must be noted that, the main limitation for the use of ETU is its carcinogenic characteristics, and hence, the effective substitution for ETU has been extensively explored. Sulfur is sometimes used to increase the degree of cure in the CR “W type”, but this detracts from the aging performance of the vulcanizates.

3.2.4.3 Neoprene T family

The “T type”, sometimes known as the “precrosslinked grades”, is similar to the “W type”, except that a highly crosslinked microscopic “gel” of CR could act as an internal processing aid [16]. In most of their chemical composition and performance characteristics, the “T type” is similar to the “W type”, i.e., the chemical structure with chloroprene homopolymers or copolymers of chloroprene and 2, 3 –

dichloroprene – 1, 3 – butadiene, without element of sulfur and other chemicals which can decompose and act as curative [16]. In addition, the "T type" contains no staining stabilizer, and has much more uniform MWD than the "G type" with greater processability than both the "G and W types", i.e., good storage stability and flow ability, due to the presence of microscopic gel which act as processing aid [31]. Therefore, these grades are particularly suitable for the extrusion and calendaring processes [29, 31]. Furthermore, these types have very low nerve and shrinkage [1].

All three families of Neoprene; "G, W and T types", are available for dry rubber applications, and offer a broad range of physical properties and processability. By proper selecting and formulating of these elastomers, the compounder is capable of achieving the optimum performance for a given end use.

3.2.5 Compounding and processing of CR

Chloroprene rubber (CR) can generally be crosslinked by metal oxides alone, i.e. zinc oxide (ZnO), magnesium oxide (MgO) and, lead oxide (PbO) [6, 16, 32]. In addition to metal oxides, the ethylene thiourea (ETU) is a traditional accelerator of choice for attaining maximum physical properties in CR vulcanizates [6, 15, 17, 32-33]. Sulfur (S) is also used as a co-curative, raising the state-of-cure of CR vulcanizates. Other ingredients such as fillers, plasticizers, antioxidants, and processing aids, can be used commonly similar to the cases of diene rubber compounding systems.

Chloroprene rubber (CR) is typically supplied in chip form normally coated with talc to prevent blocking during shipping and storage [21]. These chips can be processed on either open mills or internal mixers. The crystallized chips are melted at temperatures above 40°C–60°C [1].

Figure 3.5 Typical polychloroprene “chips” [21]

For processing safety, the two – stage mixing is recommended [1]. In the 1st mixing stage, the rubber is added first and allowed to mix alone to reduce any hardening caused by the presence of crystallization. Significantly, the G-type or sulfur modified grade always shows a tendency to mill sticking, which could be overcome by allowing CR to mix longer in order to lower the viscosity [1, 29]. In addition, low friction ratios and processing temperature are recommended to solve the effect.

It is suggested that the MgO and antioxidant (if any) should be charged in the early stage of the mixing cycle [1, 15, 23, 29]. Remarkably, the state-of-mix in CR is highest when the shear force is kept greatest. Reinforcing fillers and plasticizers are generally added at about optimal period before damping. The compound should then be sheeted off and cooled as quickly as possible. In Stage II of mixing, the ZnO, ETU and other chemicals such as sulfur are added. The compound is quickly mixed in order to control compound temperatures. For the internal mixer, the compound should be dumped with the batch temperature approximately of 110 °C and 130 °C in the cases of black- and silica-filled compounds, respectively, in order to prevent scorch [29].

3.3 Vulcanization of polychloroprene

A vulcanization chemistry of CR is different from other diene rubbers. The processes involved, (unlike normal vulcanization with sulfur) are due to the polarity of chorine atom causing a reduction in the reactivity of the double bond on its backbone

[6]. The CR rubbers are generally vulcanized by the action of metallic oxides. The widely used curing agent is ZnO, in conjunction with MgO [6, 16-17].

However, CR can be vulcanized in the presence of ZnO alone giving a relatively fast onset of vulcanization with flat stress/strain curve [6, 17]. This means poor process safety and mechanical properties [6]. In contrast, the use of MgO alone offers good process – safety with the long cure time [6, 16]. The degree of crosslink is only moderate giving rise to moderate magnitude of mechanical properties. In the system with a combination of MgO and ZnO, the vulcanizates demonstrate good balance of mechanical properties and process safety [6, 18].

Apart from MgO and ZnO, the CR can be vulcanized with several other metallic oxides [18]. With the use of lead oxide (PbO) or red lead (Pb_2O_3), vulcanizates reveal low absorption and high acid resistance, but with much stronger tendency to scorch than ones with MgO and ZnO [6, 19].

As mentioned previously, the neoprene “G type” can be vulcanized without additional sulfur or accelerators though the use of metal oxides alone, while the Neoprene “W and T types” require organic accelerator for assisting vulcanization system. Most accelerators used in the accelerated-sulfur vulcanization of other high-diene rubbers are not applicable to the vulcanization of CR rubbers. An exception to this is the use of the so-called “mixed curing system” for CR, in which metal oxide vulcanization is combined with organic accelerators. The accelerator which has been most widely used with metal oxide cures is ethylene thiourea (ETU) or 2-mercaptoimidazoline [6, 16, 23, 27, 33]. It has been reported that the use of ETU as accelerator for assisting vulcanized system for CR could result in additional crosslinks in the rubber vulcanizates [14]. Apart from increased crosslink density, increases in cure rate, modulus, hardness and aging resistance of rubber vulcanizates could be resulted by increasing ETU loading [14, 23]. Furthermore, it has been reported that the system with ETU (0.3-l phr)/ZnO (5 phr)/MgO (4 phr) is recommended for the most heat-resistant properties [33].

However, ETU is a potent carcinogenic compound, and so its replacement is required. A numbers of efforts have been made to develop the non-carcinogenic compounds as vulcanizing accelerators for CR [7-10]. One of the explored researches is the use of cetyltrimethylammonium maleate (CTMAM) [11]. The results show that the scorch time and cure time appear to decrease with increasing CTMAM content. In other words, the CTMAM is capable of functioning as a crosslinking agent for CR. Apart from CTMAM, the dimethyl l-crystine, an amino acid containing a disulfide linkage, is reported to act as a crosslinking agent for CR [12]. Furthermore, the use of nano-filler, Zn ion-coated nanosilica filler, as crosslinker for CR compound has been reported to improve the state-of-cure and thus the modulus as well as tensile strength of CR products [13]. Apart from the metal oxides and other curatives mentioned previously, sulfur is also used together with the curing agent, significantly raising the state-of-cure of CR vulcanizates [6, 16].

3.3.1 Vulcanization mechanism

The knowledge of the CR crosslinking processes has still been very little [6]. Several possibilities of ZnO crosslinking reaction of CR mechanisms have been proposed in the literature [24]. Some works suggest that the crosslinking mechanism involves an ether linkage, as illustrated in Figure 3.6 [24].

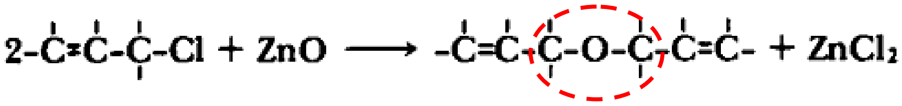

$$2\text{-C=C-C-Cl} + \text{ZnO} \longrightarrow \text{-C=C-C-O-C-C=C-} + \text{ZnCl}_2$$

Figure 3.6 Ether linkage as a crosslink in CR [34]

It is widely agreed that an important step in the vulcanization of CR involves the allylic rearrangement of 1, 2-polymerized units in CR giving the ether linkage is shown in Figure 3.7 [17, 24, 27].

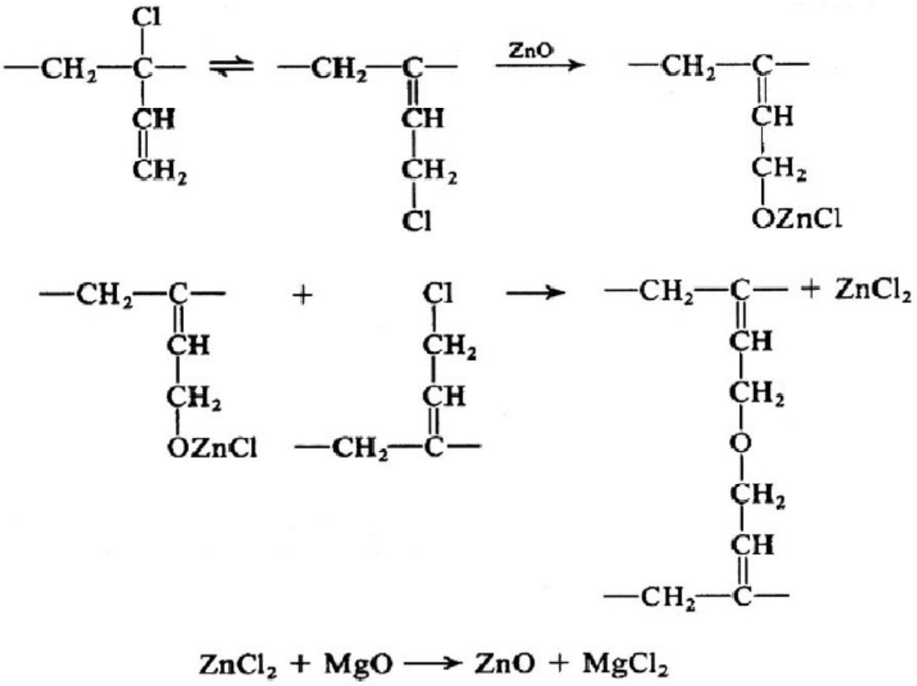

Figure 3.7 Vulcanization mechanism involving ether crosslink of CR by ZnO [27]

On the other hand, Desai and his coworker have proposed another mechanism in a way that the vulcanization system of CR by ZnO involves the reaction between a cation formed on isoprenoid unit and alkene (which must be in close proximity to the cation) on the CR polymer chain as illustrated in Figure 3.8 [18].

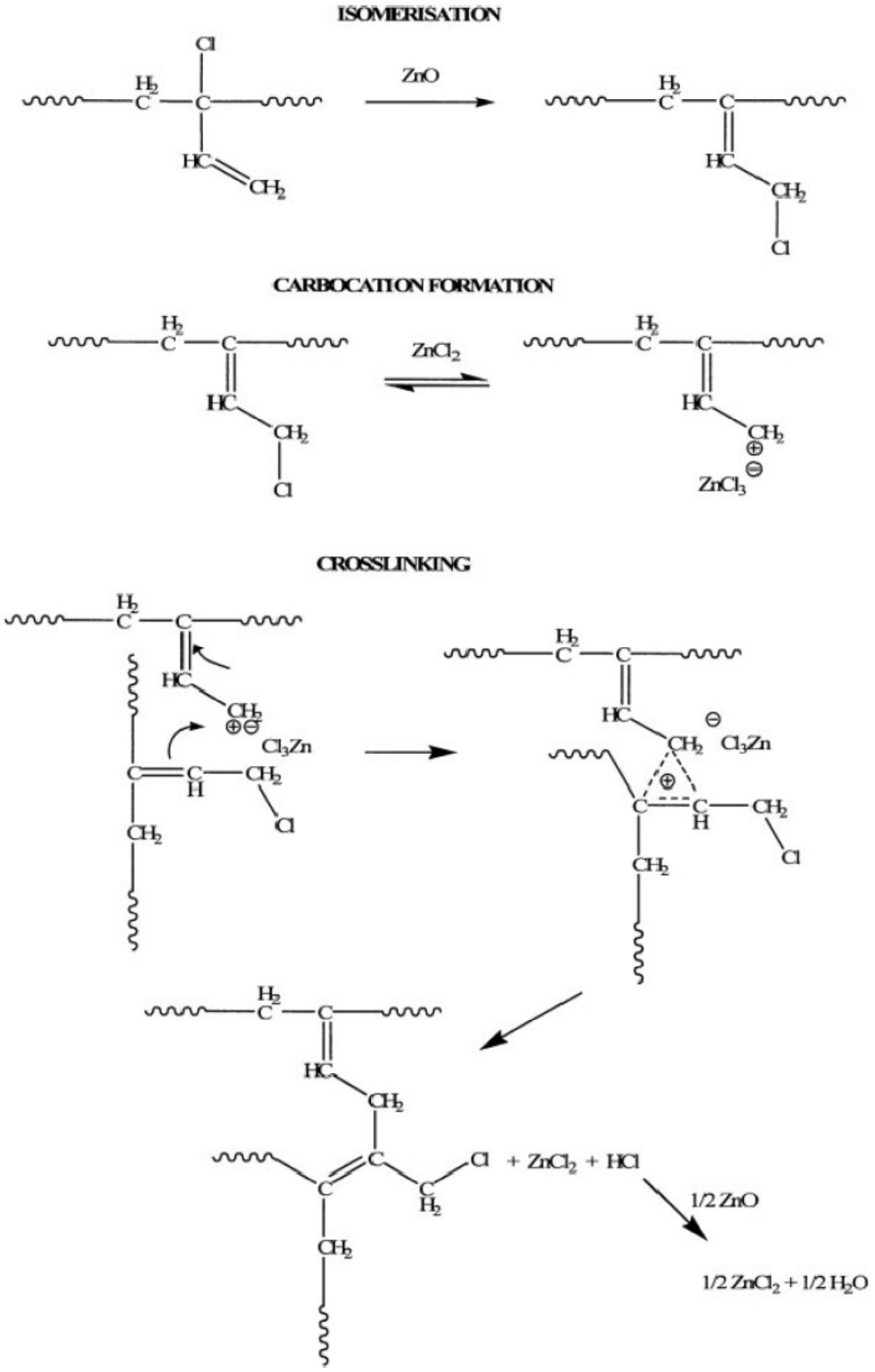

Figure 3.8 Cationic mechanism proposed by Desai et al. for the vulcanization of 1, 2-units in CR by ZnO [18]

The mechanism for the ETU acceleration has been given by Pariser, as illustrated in Figure 3.9 [27]. By this mechanism, the sulfidic linkage is gained.

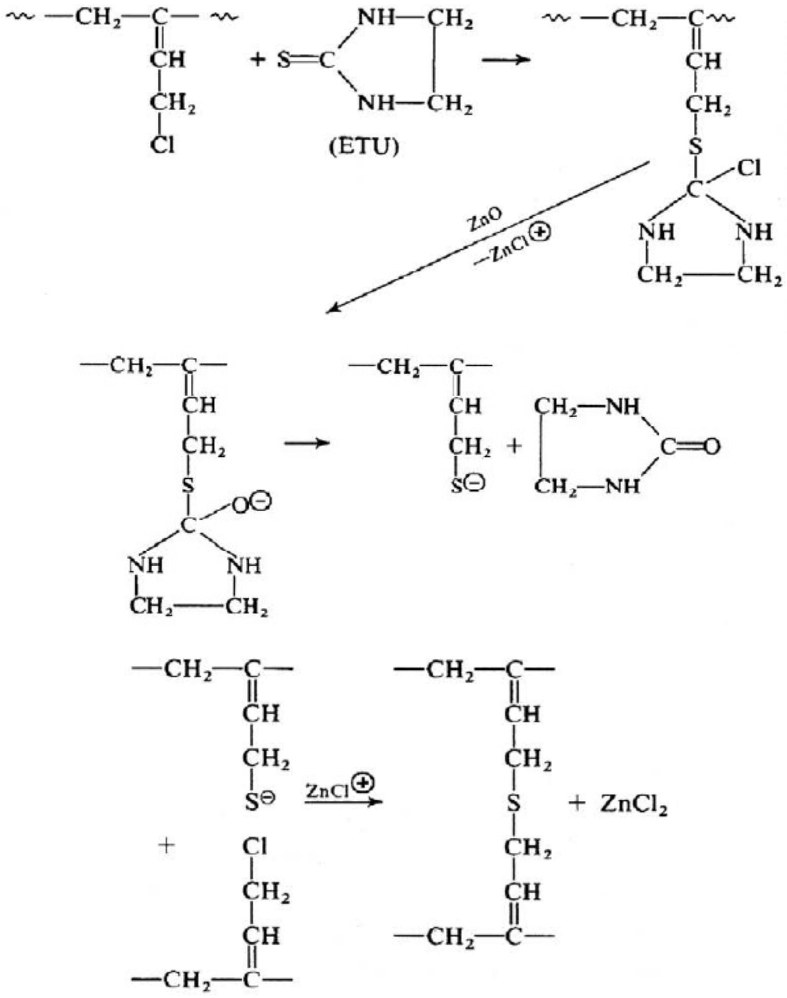

Figure 3.9 Vulcanization mechanism of CR by ethylene thiourea [27]

Moreover, CR, as compared with natural rubber, styrene-butadiene rubber and nitrile rubber, has a stronger tendency to crosslink, which is demonstrated by its ability to vulcanize at sufficiently high temperature, even when curatives are not present. In other word, CR could be vulcanized in the absence of curative. The basic crosslinking reaction without metallic oxides acting as curative for CR can be expressed as in Figure 3.10 [6].

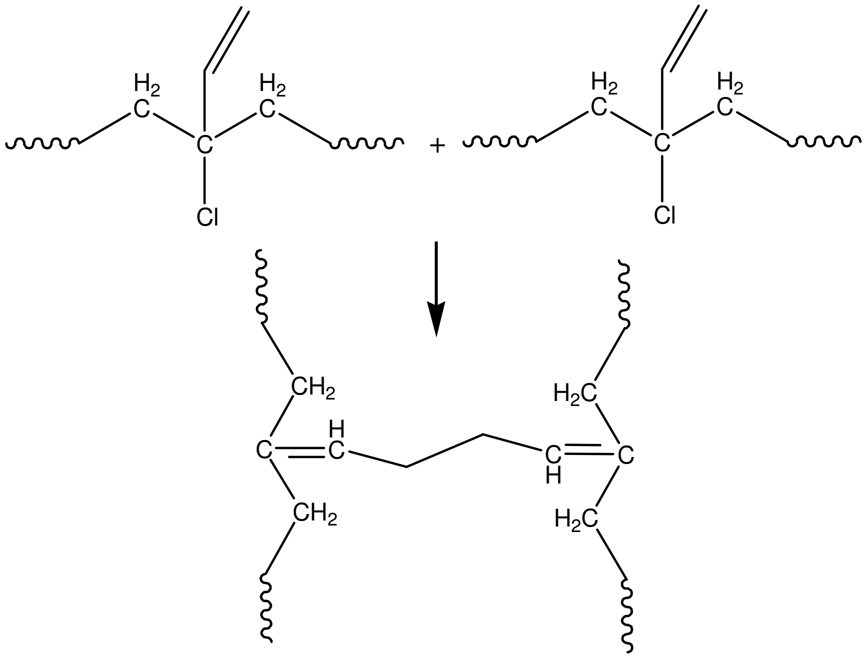

Figure 3.10 Crosslinking mechanism of CR in the absence of metal oxide curing agents [6]

3.4 Post vulcanization phenomenon of CR

By definition, vulcanization is the process of treating an elastomer with chemicals to increase its elasticity via a conversion of a viscous entanglement of long-chain molecules into a three-dimensional elastic network by chemically joining (cross-linking) these molecules at various points along the chain [28].

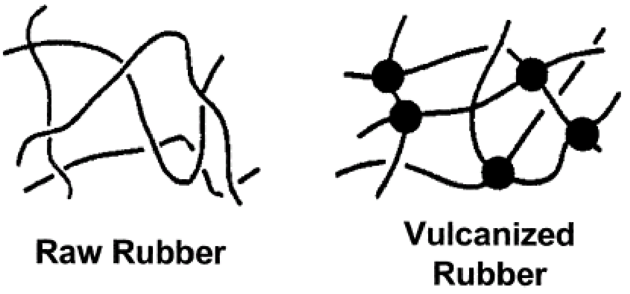

Figure 3.11 Model of randomly oriented chains of raw rubber (left) and the crosslinked polymer (right) [28]

State-of-cure refers to the degree of crosslinking or crosslink density which could be measured by the torque difference as a function of time at a given temperature as measured from rheometer (as illustrated in Figure 3.12) [32, 35-36].

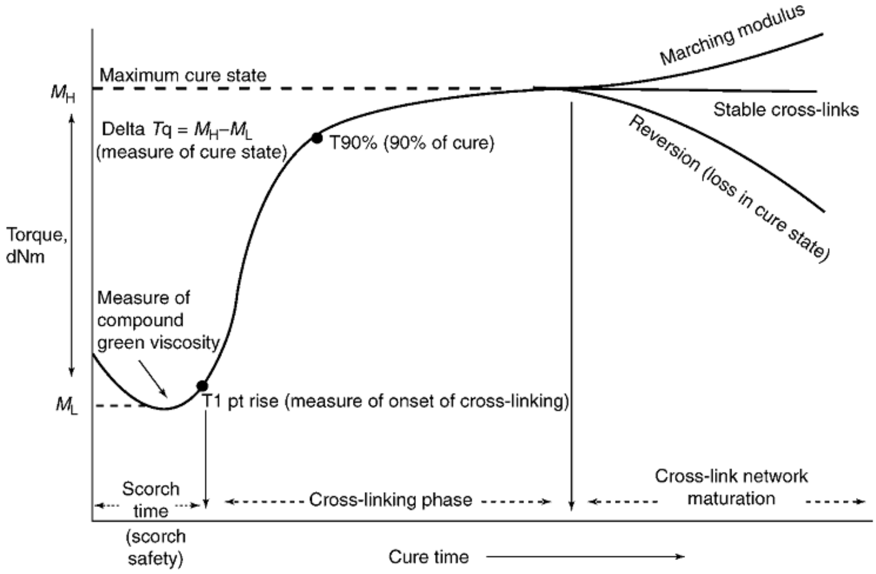

Figure 3.12 Rheometer cure curve illustrating major cure attributes. [37]

Figure 3.13 exhibits the difference between cure curve that plateaus, one that reverts, and one that marches [36]. Curve “a” represents a cure that forms the perfect plateaus. Rubber compounds in this type reach the definitive state of cure without any additional chemical crosslinking reactions occurring. Curve “b” is the example of rubber compound with ‘reversion’, in which, the depolymerization takes place more quickly than the crosslink reaction, so that, as the vulcanization time increases, the total number of crosslinks fall. Lastly, Curve “c” represents the cure curve with ‘marching phenomenon’, in which, modulus never reaches the fully plateau but progressively increases with time [30]. As stated elsewhere, CR could be vulcanized in the absence of curative. Thus, cure characteristics of CR compounds exhibit the marching behavior [17, 38]. The marching phenomenon in cure curve is sometimes known as the ‘post cure phenomenon’. The compounds with an occurrence of post vulcanization during prolonged storage, at room temperature could exhibit the marching phenomenon in cure curves [6].

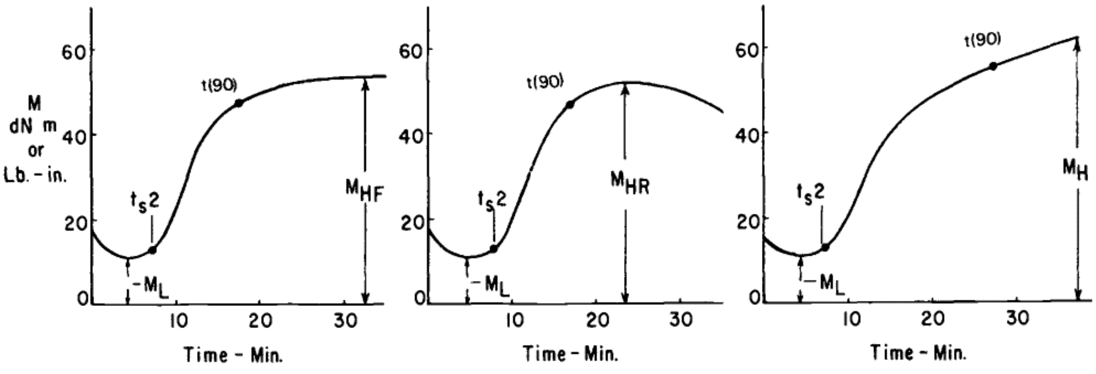

(a) *(b)* *(c)*

Figure 3.13 Typical characteristics of cure curves: stable curve (a); reversion (b); and marching (c) [36]

3.5 Reinforcing fillers

By definition, fillers are used to give designable product properties with minimal cost [39]. In general, there are 2 two main types of fillers, namely, reinforcing and non-reinforcing fillers. Common reinforcing fillers used in rubber industry are silica (Si) and carbon black (CB) offering enhancement in mechanical properties of rubber vulcanizates such as tear strength, abrasion resistance, etc. The other type of filler is non-reinforcing fillers, including calcium carbonate, providing color or opacity or probably lowering the price of the final products. Typically, the reinforcement magnitude of filler usually depends mainly on average particle size of filler, as illustrated in Figure 3.14 [40]. Reinforcing fillers, when added to an elastomer, would provide a composite product with high strength, and therefore are particularly important for synthetic rubbers whose properties of unfilled state are relatively low [29].

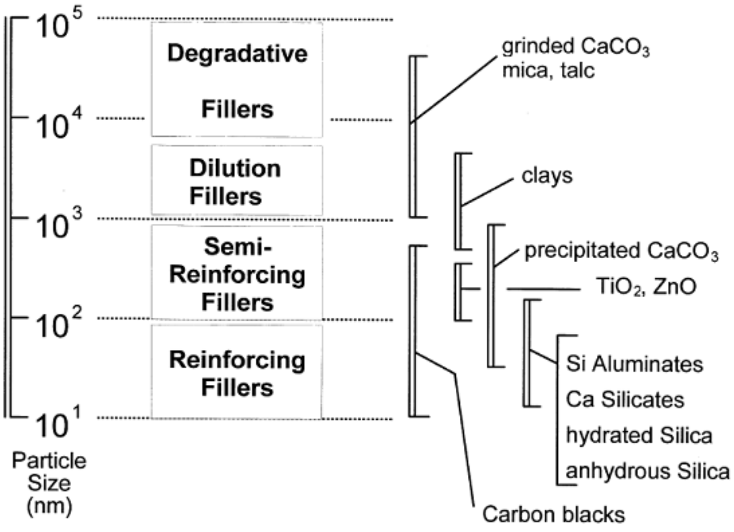

Figure 3.14 Classification of filler according to average particle size [40]

From Figure 3.15, when stress is applied to polymer matrix, such stress will transfer from polymer matrix to the strong and stiff filler phase. This stress transfer will be more efficient if the filler particles are smaller, because the greater surface is thereby exposed for a given filler concentration [41]. Thus, the most importance is the development of a strong filler-rubber interface [23]. However, almost all fillers do not exist as the discrete individual particles of their primary structure, but rather aggregates, i.e., secondary structure, which can agglomerate into tertiary structures in the matrix [39].

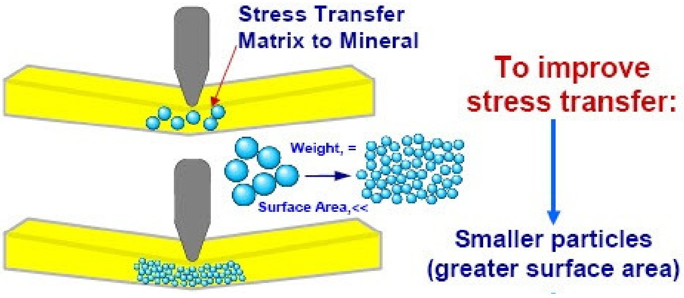

Figure 3.15 Relationship of stress transfer and filler characteristics [41]

By definition, the aggregate is a group of primary particles which strongly fused together which could not be broken down by conventional mixing techniques used in rubber processing [16, 39]. The surface area of an aggregate is less than the sum of surface areas of all primary particles in that aggregate [39]. The combination of aggregates, although weakly associated through physical interactions, leads to the agglomerate. Fillers often exist as agglomerates in their natural state [39]. The total surface area of agglomerate is similar to the sum of individual surface areas of aggregates in that agglomerate.

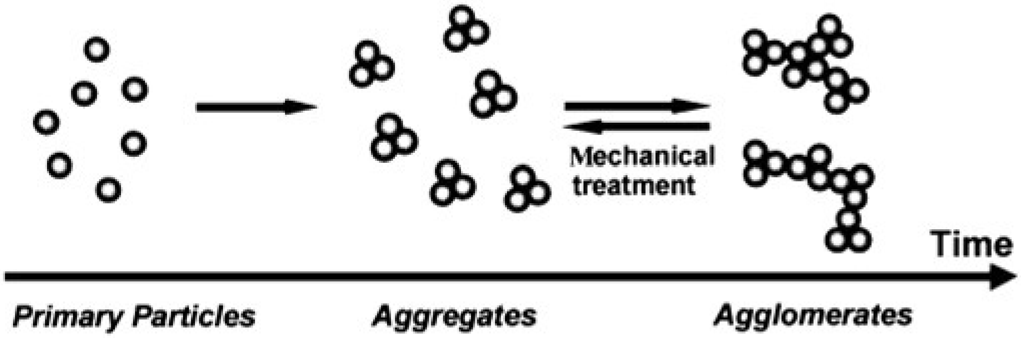

Figure 3.16 Structure formations of filler [28]

3.5.1 Carbon black (CB)

Carbon black (CB) added to rubber compounds could not only cheapen the compounds by reducing the proportion of the more expensive polymer component, but also improve the physical properties of a rubber compound [42]. In terms of rubber reinforcement, the surface activity of the CB may be defined as the capacity for restricting the mobility of the rubber molecules in contact with its surfaces having 90 – 99% elemental carbon with combined hydrogen and oxygen [23]. Typical functional groups which are located on the surfaces of CB are phenol, carboxyl, lactol, quinine, ketone, pyrone, and lactone [23].

Commonly, similar to other rigid fillers, CB is capable of increasing the hardness and viscosity of rubber compounds. The CB owes its reinforcing characteristics to the size, shape and surface chemistry of aggregated structures which consist of primary particles essentially spherical in shape that are chemically bonded to one another [16].

The size of the CB particle has a profound influence on its dispersion characteristics within a rubber matrix, and determines the final vulcanizate properties

[23]. Fortunately, the N550 CB having relatively low surface reactivity could be easily incorporated into CR compounds [1].

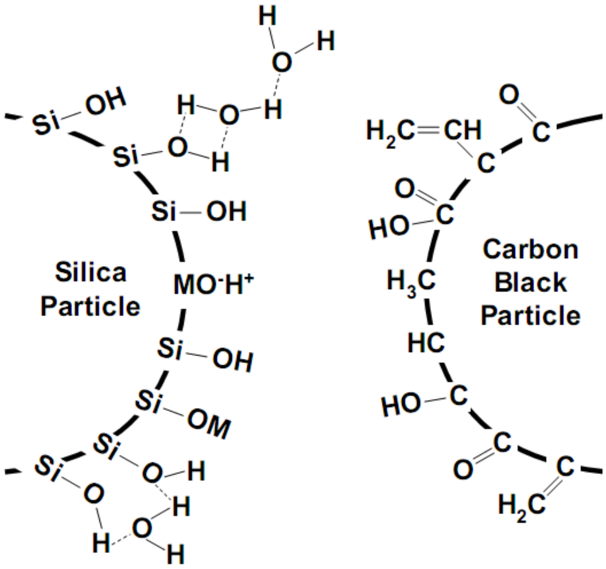

Figure 3.17 Hydrophilic silica surface (left) and hydrophobic carbon black surface (right) [35]

3.5.2 Silica (Si)

Although the use of carbon black results in outstanding high reinforcement, non-black fillers such as clays, carbonates, silicates, and precipitated silica (PSi) are still needed for manufacturing the light color products. Common non-black reinforcing fillers used in rubber industry, are silicas (Si) having strongly polar surfaces. The functional groups found on the surfaces of silcas are principally silanol (SiOH), and reaction products of the silanol with various hydrous oxides, as illustrated in Figure 3.18 [23]. The silanols produce the hydrophilic reactivity of PSi which is incapable of forming a strong bond with most diene elastomer [35].

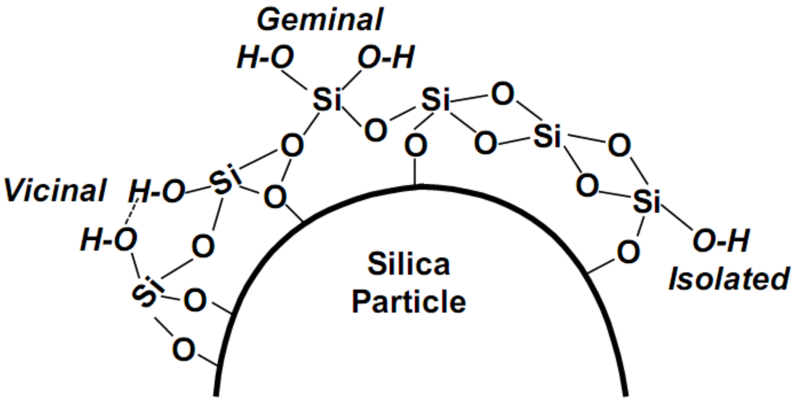

Figure 3.18 Model of surface of silica with silanol group [35]

It should be noted that the PSi with proper surface treatment usually with silane could offer final products with low dynamic heat build-up, i.e., low hysteresis loss. This property is very useful to automotive tire compound design. Low hysteresis with high modulus could be translated into low rolling resistance of tires which means low fuel consumption [30]. Thus, the tires with PSi as reinforcing filler in their compounds are sometimes called "green" tires.

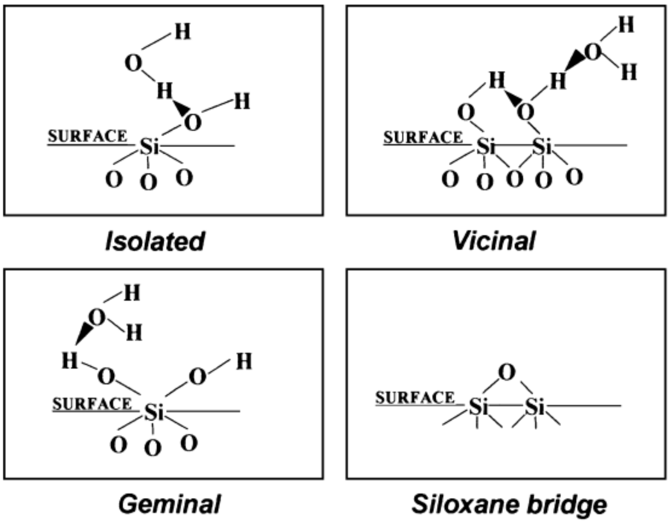

Figure 3.19 Silanol configurations found in silica: geminal, isolated, vicinal, siloxane bridges [28]

As mentioned earlier, the silanol groups on surfaces of PSi are responsible for the hydrophilic nature of silica and its unique (versus carbon black) reactivity with water, soluble zinc and other compounding ingredients as well as elastomers [35]. Three positions are recognized: isolated, vicinal and geminal, as modeled in Figure 3.19.

A vicinal grouping refers to adjacent silanols (-SiOH), hydrogen bonded. Geminal refers to two -OH groups attached to other silicons. The isolated silanol is the most reactive. This silanol type leads not only to hydrogen bonding between rubber and filler surfaces, but also to bonding to soluble zinc, amine derivatives, glycols and other additives.

Many published papers have revealed that PSi could interact strongly via primary chemical bond between functionalized polymer such as chlorosulfonated polyethylene (CSM), epoxidized natural rubber (ENR), carboxylated nitrile rubber (XNBR) [43-47] and polychloroprene [14]. Recently, it has been reported that the PSi could react with CR via silanol group of silica and chlorine atom of CR, as exhibited in Figure 3.20. The interaction development leads to the additional crosslinks in the rubber vulcanizates. Cure rate and crosslink density are therefore found to increase with increasing silica loading in those polar elastomers.

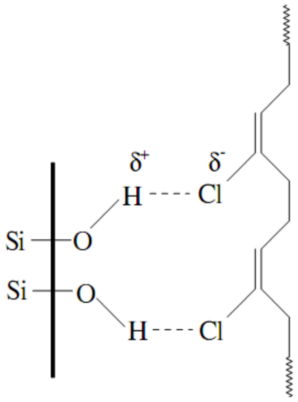

Figure 3.20 Interaction between CR and silica (H-bonds) [14]

3.5.3 Silane coupling agent (SCA)

Surface chemistry plays an importance role on the interaction of silicas and polymers. In other words, the interaction between the polar silanol on silica surfaces and non-polar groups (i.e. methyl, alkenyl, aryl) of hydrocarbon elastomer is weak compared to the dipole-dipole interactions resulting from hydrogen bonding between surface silanol groups in silica aggregates. Thus, the dispersive forces between a non-polar rubber molecule and polar silica are low while those between a non-polar rubber molecule and carbon black are high [16]. Furthermore, the polar surfaces of silicas could strongly interact with other chemicals in the rubber compound, particularly active metal oxides, curatives, and antidegradants [23, 35]. Thus, materials that improve the compatibility between hydrocarbon elastomers and mineral fillers are of considerable interest. The important surface modification for PSi, as well as for many silanol containing mineral extender fillers, has been the treatment by organo silane to enhance filler-polymer adhesion and, thereby, reinforcement [35].

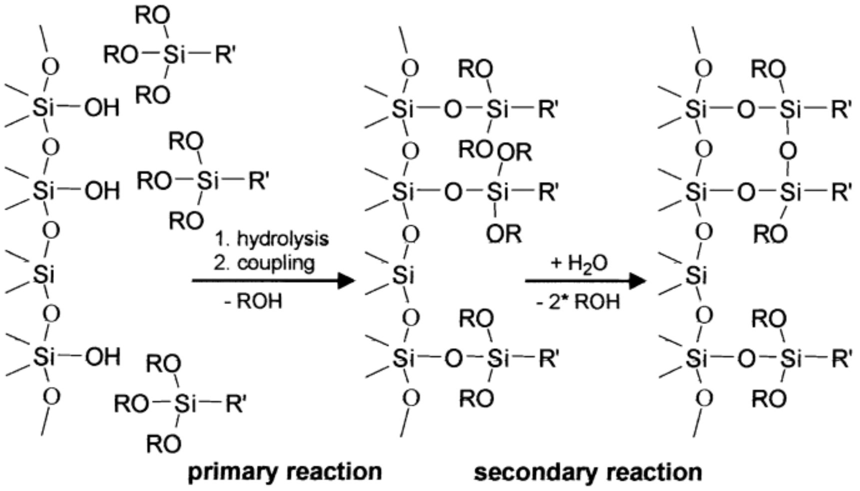

Figure 3.21 Simplified silica–silane coupling reaction [28]

Silane coupling agent (SCA) is usually a bi-functional substance which is composed of two functionally active end groups [16, 28]. The reactive silanol group on silica surface will be treated with the readily hydrolysable alkoxy group to form stable siloxane linkage. The other group is organo-functional group which is relatively non-polar and more compatible with rubber. SCA apparently acts as a bridge between silica and rubber to enhance the rubber–filler interaction and, thus, gives a significant improvement in properties of silica filled compounds. Furthermore, the presence of SCA leads to the increment in silica dispersion and also prevents the adsorption of curatives on the silica surfaces.

Although silica filled CR compounds exhibit their strong interaction between allylic chlorine atom and silanol group, the role of SCA in silica filled CR is still of interest. Recently, it has been reported that the SCA play a significant role in silica filled CR compounds [48]. The presence of SCA improves significantly the processability of the rubber compounds, as well as the mechanical properties of CR vulcanizates due to the combined effects of improved filler dispersion, enhanced rubber-filler interaction and increased crosslink density.

3.6 Strain-dependent behavior (Payne effect)

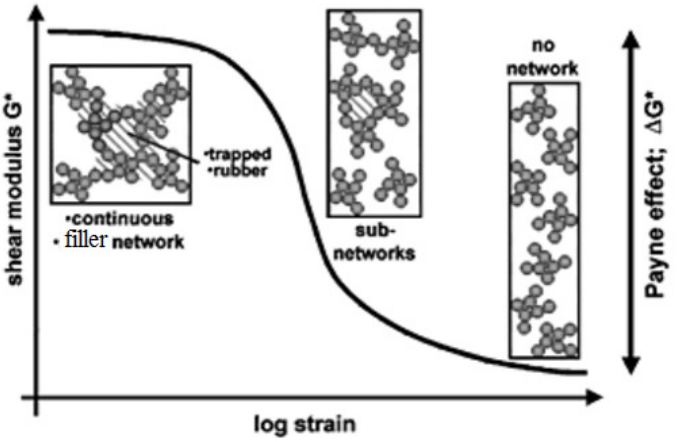

Figure 3.22 The dramatic drop in modulus with strain as a result of the destruction of the filler network is known as the Payne Effect [28]

The Payne effect is widely accepted as the mechanical consequence of the progressive destruction of the “filler network” under shear strain [27]. Practically, the Payne effect could be defined as the difference in modulus values measured at low and high strains [49]. The various contributions to the modulus are illustrated in Figure 3.22. It could be observed that the storage modulus appears to decrease with increasing strain amplitude.

The increment of modulus is due to variable factors, as shown in Figure 3.23. The increase in modulus by polymer network, hydrodynamic effect (due to the addition of a rigid filler), and the ‘‘in-rubber structure’’ (or trapped rubber which defined by the possibility of a filler preventing part of the rubber from being deformed as illustrated in Figure 3.22) are *“strain-independent”*. In addition to these contributions, the addition of an active filler results in the formation of a filler transient network, which also increases the modulus. However, the contribution of the filler network is *"strain-dependent"* [28]. Thus, the rise in strain leads to a successive breakdown of the filler network into sub networks until, at high deformation, the network is completely destroyed (as exhibited in Figure 3.22). The disruption of such filler network would release the rubber which is trapped in the network. Hence, the effective filler volume fraction and the modulus would decrease [28].

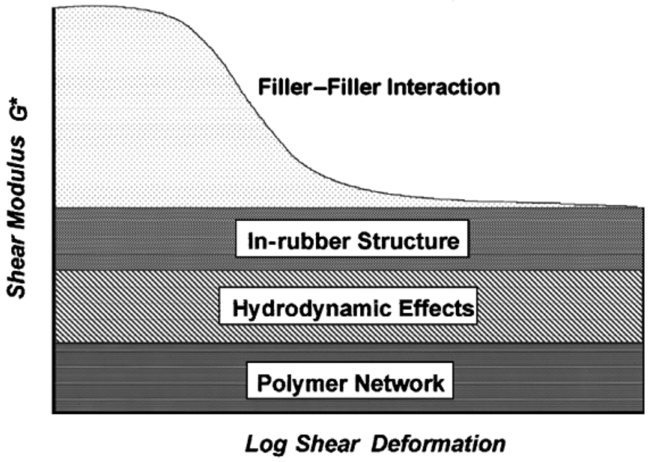

Figure 3.23 Contributions to the modulus of filled compounds according to Payne. [28]

Several works have suggested relationships between modulus and filler loading, and the most successful approach being the one called "Guth-Gold expression" which is based on the hydrodynamic effect and mutual disturbance caused by sphere particles, as illustrated in Equation 3.1 [49].

$$G_f = G_{gum} (1 + 2.5\phi + 14.1\phi^2) \ldots\ldots\ldots\ldots\ldots\ldots\ldots\ldots\ldots [3.1]$$

where as

G_f = shear modulus of filled rubber,

G_{gum} = shear modulus of gum rubber and

ϕ = volume fraction of the filler

It should be noted that the Guth-Gold equation is appropriate at small strain. By substituting the values of filler volume fraction in the equation, the theoretical values are obtained [50]. As illustrated in Figure 3.24, the positive deviation from calculated Guth-Gold results is observed [51].

This positive deviation at any given of filler volume fraction is related to be the results of the additional reinforcement provided by the pseudo-network via filler–filler and/or filler–rubber interaction [52].

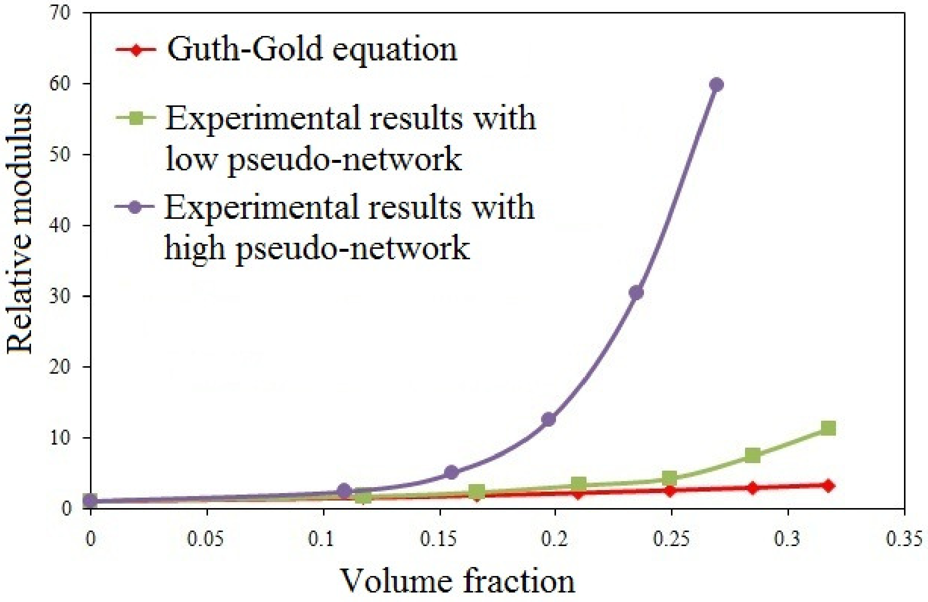

Figure 3.24 Positive deviation of relative modulus from the Guth-Gold equation at low strain

CHAPTER IV

MATERIALS AND METHODS

4.1 Materials

The materials used in present study are summarized in Table 4.1, as shown below.

Table 4.1 Materials used in the present work

Chemical Name	Use as	Grade/Manufacturer or Supplier
Polychloroprene (CR)	Raw Material	W-type / Dupont Dow Elastomer Co., Ltd., USA
Zinc oxide (ZnO)	Cure activator	Enery Product Co., Ltd., Thailand
Magnesium oxide (MgO)	Cure activator	Starmag # 150/ Konoshima Chemical Co., Ltd, Osaka, Japan
Lead oxide (PbO)	Curative/acid receptor	Behnmeyer Co., Ltd., Thailand
Carbon black	Reinforcing filler	N550 / Thai carbon product Co.,Ltd., Thailand
Precipitated silica	Reinforcing filler	TOKUSIL® 233/ Tukuyama Siam Silica Co., Ltd., Thailand
Sulfur (S_8)	Vulcanizing agent	Commercial grade / Chemmin Co., Ltd., Thailand
Ethylene thiourea (ETU)	Vulcanizing agent	ETU 22S / Kawakushi Co., Ltd., Japan

Table 4.1 Materials used in the present study (cont.)

Chemical Name	Use as	Grade/Supplier
N-(1, 3-dimethylbutyl)-N'-phenyl-p-phenylenediamine (6-PPD)	Antioxidant	Santoflex 6-PPD / Flexsys Co.,Ltd., USA
Stearic acid	Cure activator	Commercial grade / Petch Thai Chemical Co., Ltd., Thailand
Dioctyl phthalate (DOP)	Plasticizer	A.O. Chemical Co., Ltd., Thailand
Bis-(3-triethoxysilylpropyl) tetrasulfane (Si-69, TESPT)	Silane coupling agent	JJ-Degussa (Thailand) Co., Ltd., Thailand
3-thiocyanatopropyl triethoxy silane (Si-264, TCPTS)		

4.2 Instruments

The apparatus used in this work are summarized in Table 4.2, as shown below.

Table 4.2 List of apparatus used in the present work

Instruments	Model	Manufacture
Laboratory 2 – roll mill	LRM 150 W	Labtech Engineering Company Ltd., Thailand
Compression molding	G30H	Wabash Genesis Series, USA
Rubber process analyzer	RPA 2000	Alpha Technology, USA
Dynamic mechanical analysis	Model Eplexor 25N	Gabo Qualimeter, Germany
Moving die rheometer	Rheo TECH MD+	TechPro, USA

Table 4.2 List of apparatus used in the present work (cont.)

Instruments	Model	Manufacture
Tensile tester	Model 5566	Instron, USA
Shore A hardness tester	H17A	Cogenix Wallace, England
Heat buildup flexometor	BF Goodrich flexometor Model II	Hurst Mfg., Div. of Emerson Electric Co., USA
DIN-type abrasion tester	Model 6102	Zwick Materialf*ü*ng, Germany
Scanning electron microscopy (SEM)	Model S-2500	Hitachi , Japan
	JSM-6400	JEOL, Japan
Energy Dispersive X-ray Spectrometer (EDS)	Link ISIS series 300	Oxford, England
Microtome	Model 1400	Leitz, Germany

4.3 Compound formulation

4.3.1. A study on metal oxide effect

4.3.1.1. Magnesium Oxide (MgO)

Compounding ingredients used for the study of MgO effect are illustrated in Table 4.3.1.

Table 4.3.1 Compound formulation used for the study of MgO effect

Ingredients	Amount (phr[*])
Polychloroprene (CR)	100.0
Magnesium oxide (MgO)	Variable: 2.0-6.0
Zinc oxide (ZnO)	5.0
Sulfur (S_8)	0.5

Table 4.3.1 Compound formulation used for the study of MgO effect (cont.)

Ingredients	**Amount (phr[*])**
Carbon black	50.0
Ethylene thiourea (ETU)	1.0
Stearic acid	2.0
Antioxidant (6-PPD)	2.0
Plasticizer (DOP)	10.0

* = part per hundred of rubber

4.3.1.2. Zinc oxide (ZnO)

Compounding ingredients used for the study of ZnO effect are exhibited in Table 4.3.2.

Table 4.3.2 Compound formulation used for the study of ZnO effect

Ingredients	**Amount (phr[*])**
Polychloroprene (CR)	100.0
Magnesium oxide (MgO)	4.0
Zinc oxide (ZnO)	Variable: 2.0-6.0
Sulfur (S_8)	0.5
Carbon black	50.0
Ethylene thiourea (ETU)	1.0
Stearic acid	2.0
Antioxidant (6-PPD)	2.0
Plasticizer (DOP)	10.0

* = part per hundred of rubber

4.3.1.3. Lead oxide (PbO)

Compounding ingredients used for the study of PbO effect are tabulated in Table 4.3.3.

Table 4.3.3 Compound formulation used for the study of PbO effect

Ingredients	**Amount (phr[*])**
Polychloroprene (CR)	100.0
Zinc oxide (ZnO)	5.0
Lead oxide (PbO)	Variable: 2.0-6.0
Sulfur (S_8)	0.5
Carbon black	50.0
Ethylene thiourea (ETU)	1.0
Stearic acid	2.0
Antioxidant (6-PPD)	2.0
Plasticizer (DOP)	10.0

* = part per hundred of rubber

4.3.1.4. Multiple of fixed MgO:ZnO ratio

In this part, the loading ratio of MgO and ZnO (at constant MgO: ZnO loading ratio of 4:5) was multiplied. The cure characteristics as well as mechanical properties were investigated.

Compounding ingredients used for the study of ZnO and MgO effects in combined curing system are exhibited in Table 4.3.4.

Table 4.3.4 Compound formulation used for the study of ZnO and MgO effects

Ingredients	**Amount (phr[*])**
Polychloroprene (CR)	100.0
Magnesium oxide (MgO)	Variable: 4.0-20.0
Zinc oxide (ZnO)	Variable: 5.0-25.0

Table 4.3.4 Compound formulation used for the study of ZnO and MgO effects (cont.)

Ingredients	**Amount (phr*)**
Sulfur (S_8)	0.5
Carbon black	50.0
Ethylene thiourea (ETU)	1.0
Stearic acid	2.0
Antioxidant (6-PPD)	2.0
Plasticizer (DOP)	10.0

* = part per hundred of rubber

4.3.2. Effect of Sulfur

Compounding ingredients used for the study of sulfur effect are shown in Table 4.3.5.

Table 4.3.5 Compound formulation used for the study of sulfur effect

Ingredients	**Amount (phr*)**
Polychloroprene (CR)	100.0
Magnesium oxide (MgO)	Variable: 2.0-6.0
Zinc oxide (ZnO)	Variable: 2.0-6.0
Sulfur (S_8)	0, 0.5
Carbon black	50.0
Ethylene thiourea (ETU)	1.0
Stearic acid	2.0
Antioxidant (6-PPD)	2.0
Plasticizer (DOP)	10.0

* = part per hundred of rubber

4.3.3. Effect of reinforcing filler

4.3.3.1. Carbon black (CB)

As stated elsewhere, the N550 CB (size of black particle is about 40-48 nm and surface area is about 36-52 m^2g^{-1}) having relatively low surface reactivity could be easily incorporated into CR compounds [1, 29]. Thus, in this present work, CB N550 is selected to study the effect.

Compounding ingredients used for the study of (CB) effect are presented in Table 4.3.6.

Table 4.3.6 Compound formulation used for the study of CB effect

Ingredients	**Amount (phr*)**
Polychloroprene (CR)	100
Magnesium oxide (MgO)	4.0
Zinc oxide (ZnO)	5.0
Sulfur (S_8)	0.5
Carbon black (CB; N550)	Variable: 20-70
Ethylene thiourea (ETU)	1.0
Stearic acid	2.0
Antioxidant (6-PPD)	2.0
Plasticizer (DOP)	10.0

* = part per hundred of rubber

4.3.3.2. Precipitated silica (PSi)

The PSi used in this work is Tokusil 233 grade of having the bulk density and BET surface area of 0.240 ± 0.025 g cm^{-3} and 135 m^2g^{-1}, respectively [53, 54].

Compounding ingredients used for the study of PSi effect are illustrated in Table 4.3.7.

Table 4.3.7 Compound formulation used for the study of PSi effect

Ingredients	**Amount (phr*)**
Polychloroprene (CR)	100.0
Magnesium oxide (MgO)	4.0
Zinc oxide (ZnO)	5.0
Sulfur (S_8)	0.5
Precipitated silica (PSi; Tokusil 233)	Variable: 20-60
Ethylene thiourea (ETU)	1.0
Stearic acid	2.0
Antioxidant (6-PPD)	2.0
Plasticizer (DOP)	10.0

* = part per hundred of rubber

4.3.4. Effect of silane coupling agent (SCA)

Silane coupling agent (SCA) is used extensively to improve reinforcing efficiency of silica. In the present study, roles of the two widely used SCA, i.e., bis-(3-triethoxysilylpropyl) tetrasulfane (Si-69) and 3-thiocyanatopropyl triethoxy silane (Si-264), on properties of PSi-filled CR vulcanizates were investigated.

Compounding ingredients used for the study of SCA (i.e., Si-69 and Si-264) effect are exhibited in Table 4.3.8.

Table 4.3.8 Compound formulation used for the study of Si-69 and Si-264 effects

Ingredients	**Amount (phr*)**
Polychloroprene (CR)	100.0
Magnesium oxide (MgO)	4.0
Zinc oxide (ZnO)	5.0
Sulfur (S_8)	0.5
Precipitated silica	Variable: 20-60
Ethylene thiourea (ETU)	1.0
Stearic acid	2.0

Table 4.3.8 Compound formulation used for the study of Si-69 and Si-264 effects (cont.)

Ingredients	Amount (phr*)
Antioxidant (6-PPD)	2.0
Plasticizer (DOP)	10.0
Si – 69 or Si – 264	10 % wt of PSi

* = part per hundred of rubber

4.4 Mixing Procedures

The compounding ingredients as illustrated in Tables 4.3.1-4.3.8 were mixed using 2 – roll mill (LabTech model LRM 150) with two-stage mixing technique at set temperature of 50 °C. In the first stage, MgO, stearic acid, 6-PPD, reinforcing filler and DOP were incorporated sequentially into raw rubber with total mixing time of 17 minutes. In the second stage, the rubber mix gained from the first stage of mixing was masticated on 2 – roll mill for 2 minutes at 50 °C, and then the vulcanizing agents (i.e., ZnO, ETU and sulfur) were charged into the rubber mix, and allowed 8 minutes for achieving good distribution and dispersion of ingredients.

4.5 Determination of cure characteristics of rubber compounds

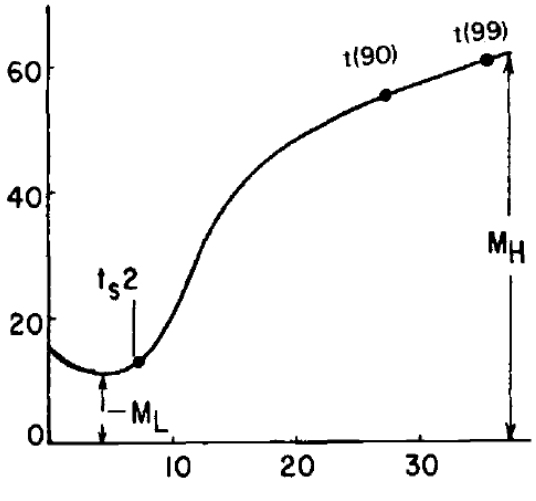

Figure 4.1 A typical characteristic of cure behavior [36]

Cure characteristics including scorch time (t_{s2}), cure time (t_{c99}), minimum torque (M_L) and maximum torque (M_H) of rubber compounds were measured using a moving die rheometer (MDR) at 155°C. Torque difference (M_H – M_L) was also determined as an indication of crosslink density of the vulcanizates [32, 35-36].

According to ASTM D5289 – 95, approximately 5 g of rubber compound was placed in the rheometer cavity and deformed under oscillating force. The t_{cx} is simply the time to reach a given x% of state-of-cure. Mathematically, t_{cx} could be calculated, as follows:

$$t_{cx} = [(\frac{x}{100}) \times (M_H - M_L)] + M_L \quad \text{........................}[4.1]$$

where :

t_{cx} = time to a given percent (x) state-of-cure

M_L = minimum torque

M_H = maximum torque

x = percentage of state-of-cure

4.6 Preparation of rubber vulcanizates

The compounds were compression molded with the hydraulic hot press (Wabash model G30H) under pressure of 12 MPa at 155^{0}C for the optimum cure time (t_{c99}) as predetermined from the moving die rheometer (MDR). In order to eliminate air bubbles in cured products, bumping technique was used.

4.7 Determination of rheological properties

4.7.1 Rubber process analyzer (RPA2000)

With the use of rubber process analyzer (RPA; Alpha Technology, USA) at 100°C under strain sweep tests, approximately 5 g of rubber compounds were placed between the dies. By applying the preset strain (0.5-1200%) and frequency

(0.99 radians /second) to the test specimens, viscoelastic behavior could be monitored. Values of storage and loss moduli were determined.

4.7.2 Dynamic mechanical analyzer (DMA)

Dynamic mechanical analysis (DMA) enables simultaneous study of both elastic and viscous flow types of behavior [55]. DMA scanning tests in tension mode of deformation were performed on rectangular specimens (in this present study the samples were cut in rectangular size of 40 mm × 10 mm). In order to investigate the vulcanizate dynamic behavior affected by temperature, the temperature was varied in the range of 25-100 °C at a frequency of 10 Hertz and a scanning rate of 2 °C/minutes. The temperature-dependent storage modulus and tanδ were investigated.

4.8 Flory-Rehner equation

The degree of swelling could be used to determine the magnitude of crosslink density in rubber vulcanizates [56]. In general, crosslinked polymer, when placed in a good solvent, rather than dissolving completely, will absorb a portion of the solvent and subsequently swell. The Flory-Rehner equation is widely used to relate the amount of swelling to the crosslink density of polymer [19].

The vulcanized rubber sheets were cut into the dimension of approximately 1.5cm ×1.5cm ×1mm. Then, the test samples were weighed by electric balance and were immersed in 60 ml toluene for seven days at room temperature. After 7 days, the test specimens were removed from the toluene and were weighed accurately. It must be noted that the excess toluene on specimen after removed from the toluene was eliminated by towel paper. The number average molecular weight between crosslinks, *n*, can be calculated from the Flory – Rehner equation as shown in Equation 4. 2 [47, 57-58].

$$-[\ln(1-\upsilon_2)+\upsilon_2+\chi\upsilon_2^2] = V_1 n[\upsilon_2^{1/3} - \frac{\upsilon_2}{2}] \ldots\ldots\ldots\ldots [4.2]$$

where :

n = number of elastically active chains per unit volume

υ_2 = volume fraction of polymer in the swollen gel at equilibrium

χ = polymer - solvent interaction parameter

V_1 = the molar volume of the solvent

In the experiment, toluene is employed as the liquid-medium. A polymer–solvent interaction parameter (χ) of 0.386 for the CR–toluene system was calculated from the literature data [18, 59]. The volume fraction of polymer in the swollen gel at equilibrium, υ_2, could be calculated from the Equation 4.3, as shown below [57]. It should be noted that the density of toluene and CR are 0.87 and 1.23 g/cm^3, respectively [7, 60-61].

$$\upsilon_2 = \frac{M_1 d_s}{M_1(d_s+d_r)+M_2 d_r} \quad \ldots\ldots\ldots\ldots\ldots\ldots\ldots [4.3]$$

where :

M_1 = the weight of the polymer before swelling

M_2 = the weight of the polymer after swelling

d_s = the density of solvent

d_r = the density of polymer

4.9 Mechanical property measurement

4.9.1 Shore A hardness

A so-called durometer measures the hardness of a cured rubber specimen quickly from the penetration of a special indentor. Hardness is a measure of resistance to deformation of vulcanizates as per ASTM D2240 and ISO 7619, using Cogenix Wallace Hardness tester (Durometer) model H17A.

The test specimen shall be at least 6.0 mm (0.24 in) in thickness. The surfaces of the specimen shall be flat and parallel over an area to permit the presser foot to contact the specimen over an area having a radius of at least 6.0 mm (0.24 in) from the indentor point. The specimen shall be suitably supported to provide for positioning and stability.

4.9.2 Heat build-up (HBU)

The prime object of heat build-up (HBU) test is to measure a temperature rise in the test specimens as a result of the viscoelastic nature of polymers. Some of the applied stress is dissipated by viscous flow between molecules and converted into thermal energy. The Goodrich flexometer operates by superimposing a cyclic compression strain onto the static deformation caused by a constant force. For the HBU test given in ASTM D623**,** the cylindrical specimen with the dimension of 17.8 mm in diameter and 25 mm in height is cycled at 1800 cycles/minute with a full stroke of 4.45 mm for 25 minutes, and the temperature rise at the base of specimens was recorded.

4.9.3 Tensile properties

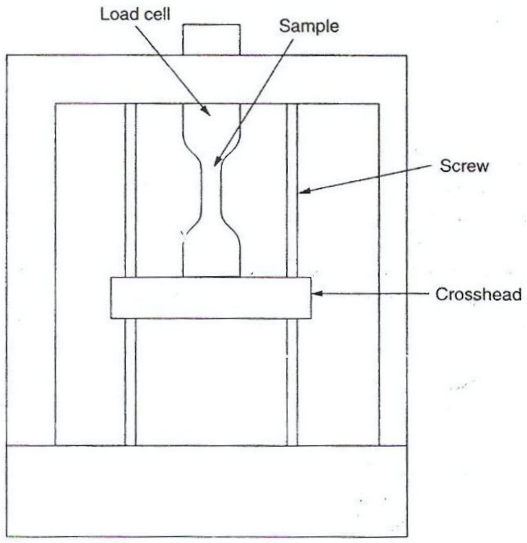

Figure 4.2 The main components of a tensile tester apparatus [62]

Tensile testing machines are designed to elongate specimens at a constant rate. Figure 4.2 illustrates the main components of a tensile testing apparatus. This method simply consists of cutting out dumbbells from cured sheets, using a cutting die (as per ASTM D412-92, Die C), and pulling them apart with a tensile tester at a standard rate of 500 mm/minutes. During the test, the deformation occurs to the narrowed central region of the sample which has a uniform cross-sectional area along its length. The load cell measures the magnitude of applied load on the sample, while the extensometer measures the elongation of the sample. Figure 4.3 shows the dimensions of the die used to cut the dumbbells from standard cured sheets.

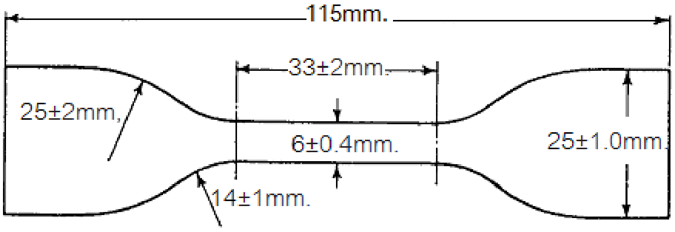

Figure 4.3 A dumbbell-bone tensile test sample

4.9.4 Compression set

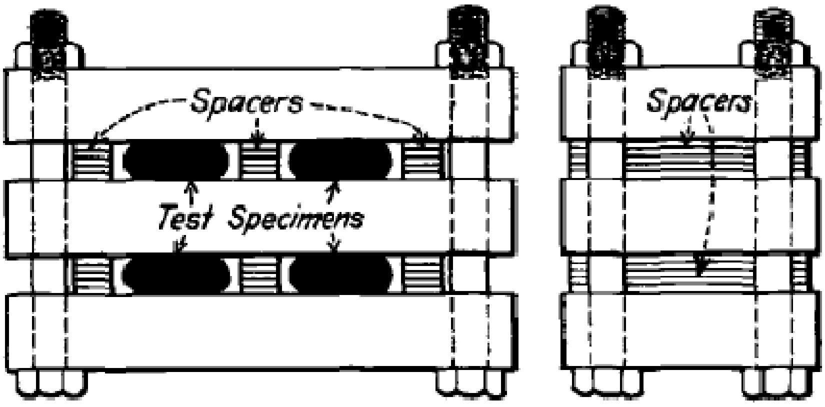

Figure 4.4 Device for compression set test under constant deflection. [36]

A cured test specimen is measured for its tendency to take a set from a constant strain under preselected standard conditions of temperature, time, percent deflection and recovery time as per ASTM D395 (Method B) at 70 °C and 100 °C. Figure 4.4 shows the apparatus used to condition rubber specimens for compression set measurement by applying a constant strain. The test specimen is a disc with 13 mm. in diameter and 6.3 mm in thickness. The compression set could be calculated from the following equation.

$$C_B = \left[\frac{(t_o - t_i)}{(t_o - t_n)}\right] \times 100 \qquad [4.4]$$

where :

C_B = compression set (Test Method B) expressed as percentage of the original deflection

t_o = original thickness of specimen

t_i = final thickness of specimen

t_n = thickness of the spacer bar used (in the present study the thickness of the spacer bar is 4.5 mm)

4.9.5 Abrasion resistance

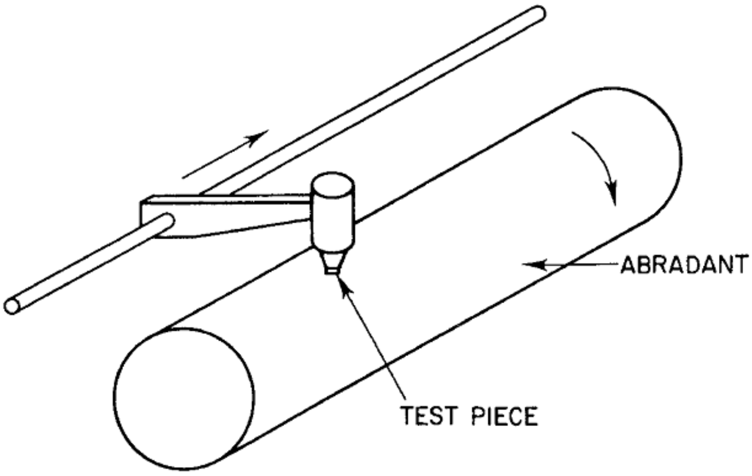

Figure 4.5 Principle of DIN abrader [63]

The DIN abrasion test performed in this work is based on ASTM D5963 and ISO 4649. The principle of the machine is illustrated in Figure 4.5. A disc test piece in a suitable holder is traversed across a rotating drum covered with a sheet of the abradant.

Test pieces are cylindrical in shape with a diameter of 16 ± 0.2 mm (0.630 ± 0.008 in) and a minimum thickness of 6 mm (0.24 in). It is common to convert weight losses to volume. Weight or volume loss can be related to unit distance travelled over the abradant, per 1000 cycles or whatever is convenient.

To calculate the abrasion loss, A_A, the loss in mass, shall be converted into volume loss using the density of the test rubber. Then, the volume loss is corrected by using the "$\frac{S_O}{S}$" ratio where S_O is the "normal abrasiveness" of the abrasive sheet and S is the abrasiveness of the abrasive sheet used for the test. Mathematically, A_A could be calculated as follows:

$$A_A = \frac{\Delta m_t \times S_O}{d_t \times S} \quad \text{.................................[4.5]}$$

where :

A_A = abrasion loss in mm^3,

Δm_t = mass loss of the test piece in mg,

d_t = density of the test rubber in mg/mm^3,

S_o = "normal abrasiveness" (i.e., 200 mg, in this work)

S = abrasiveness in mg.

4.10 Determination of phase morphology

4.10.1 Scanning electron microscopy (SEM)

Phase morphology observation of the sample surfaces is accomplished using scanning electron microscope. For most polymers, fractured surface is required which could be prepared by the cryogenic fracturing technique. Then, the samples were placed on the specimen stub and then sputter coated with gold to prevent electron bombardment on the sample surfaces.

4.10.2 Energy Dispersive X-ray Spectrometer (EDS or EDX)

Energy dispersive X-ray spectroscopy (EDS or EDX) is an analytical technique used for the elemental analysis or chemical characterization of a sample

[64]. EDS could be used in conjunction with scanning electron microscopy (SEM). The EDS technique detects X-rays emitted from the sample during bombardment by an electron beam to characterize the elemental composition of the analyzed volume [65]. The X-ray energy is the characteristics of the element from which it was emitted.

CHAPTER V
RESULTS AND DISCUSSION

5.1 Effect of metal oxide on cure characteristics and mechanical properties

5.1.1 Study of metal oxide effect

As mentioned previously, polychloroprene (CR) rubbers are usually vulcanized by the action of metal oxides. For some engineering products including rubber roll applications, the optimal state-of-cure is desirable in order to achieve good dynamic mechanical properties and chemical resistance. Therefore, suitable types and amounts of curing agent giving good mechanical properties and high state-of-cure are required. In this section, magnesium oxide (MgO), zinc oxide (ZnO) and lead oxide (PbO) were chosen as curing agents. The effects of each metal oxide on properties of CR compounds and vulcanizates are investigated in order to select a suitable type and ratio of curing agent to be used for developing the CR industrial rolls.

5.1.1.1 Crosslink density

Figure 5.1 shows torque difference of CR compounds with various types and loadings of metal oxides. It is obvious that state-of-cure increases with increasing MgO or ZnO loading.

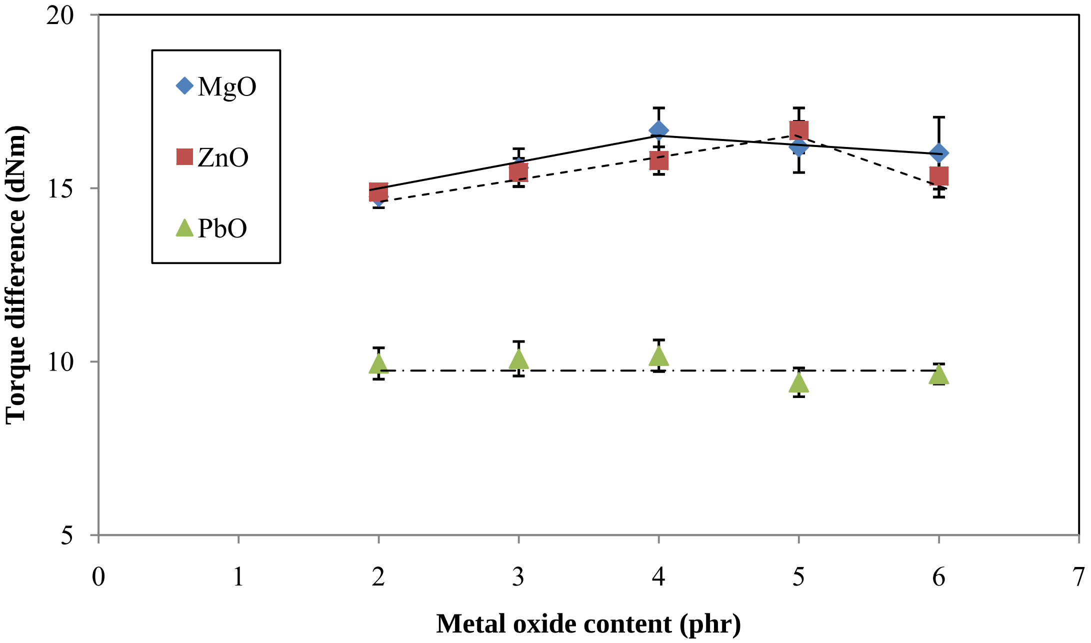

Figure 5.1 Crosslink density of CR vulcanizates with various loadings of metal oxides

The results reveal that, at a given MgO content of 4 phr, the crosslink density increases with increasing ZnO. Likewise, by keeping the ZnO content constant at 5 phr, the density of crosslink appears to increase with increasing MgO content. Additionally, as illustrated in solid and dash lines, the crosslink density will be increased with increasing metal oxide until 4 and 5 phr of MgO and ZnO, respectively. In other words, the maximum crosslink density is observed at the MgO and ZnO contents of 4 and 5 phr, respectively. The results agree with the general formula usually used to vulcanize CR rubber [6, 13, 16, 33].

Furthermore, by replacing MgO with PbO, the magnitude of crosslink density is reduced remarkably. In other words, MgO contributes to the crosslink of CR more effectively than PbO. Also, it appears that the crosslink density is not affected by PbO loading.

5.1.1.2 Scorch time

Figure 5.2 illustrates the scorch time (t_{s2}) of the CR compounds with various loadings of metal oxides. The t_{s2} increases with increasing amount of MgO but decreases with increasing ZnO or PbO loadings.

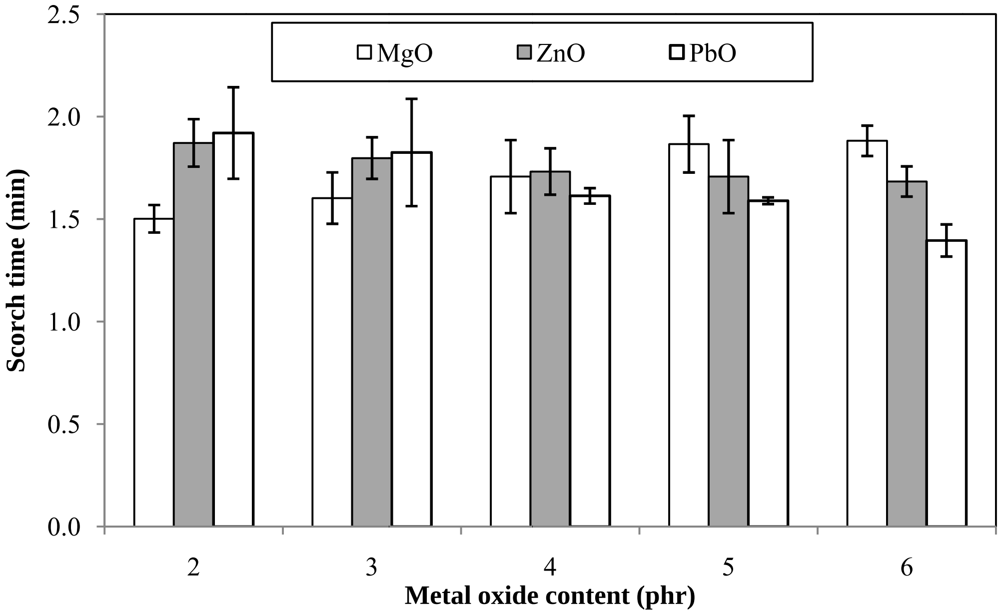

Figure 5.2 Scorch time of CR vulcanizates with various loadings of metal oxides

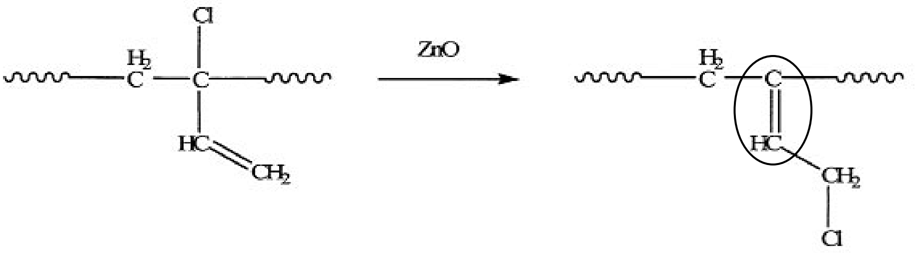

Figure 5.3 Isomerization mechanisms for CR [18]

It was proposed by Mallon et al. that vulcanization for CR compound comprises two competing reaction involving the isomerized and unisomerized species of the 1, 2 – units, which provide the active sites for crosslinking in the CR polymer chain [18, 66]. As illustrated in Figure 5.3, ZnO is the main promoter of the allylic rearrangement of the 1, 2 – units into isomerized species. Thus, the increment of ZnO loading gives the greater amount of isomerized units and thus a shortened t_{s2}.

The exactly mechanism of vulcanizes CR rubber is still unclear. The possible vulcanization mechanisms which have been proposed previously are shown in Figures 3.7 and 3.8 [18, 27]. From the proposed mechanisms, the $ZnCl_2$ which was caused by the accepted Cl atom of ZnO plays significant role in vulcanization process.

Therefore, the CR compounds with ZnO give a greater degree of crosslink and relatively fast onset of vulcanization [6, 16, 23].

It is proposed that MgO scavenges chloride ions produced during mixing, thereby limiting the amount of $ZnCl_2$ that is formed [18]. Furthermore, as suggested by Kuntz et al., the retarding effect of MgO is brought about by the coordination of magnesium (MgO is a Lewis base) to the Lewis acid, thereby deactivating the crosslinking [34]. Thus, the CR compounds with MgO reveal the longer scorch time.

In the case of PbO, the trend of scorch time is similar to ZnO. It should be noted that CR compounds containing lead oxide (PbO) have a much stronger tendency to scorch than ones containing MgO and ZnO which is in line with the previous work [6].

5.1.1.3 Crosslink density as determined from Flory-Rehner equation

The relationship among the crosslink density (as determined from Flory-Rehner equation), metal oxide type, and loading is exhibited in Figure 5.4. It can be observed that the crosslink density increases with increasing metal oxide loading regardless of metal oxides type.

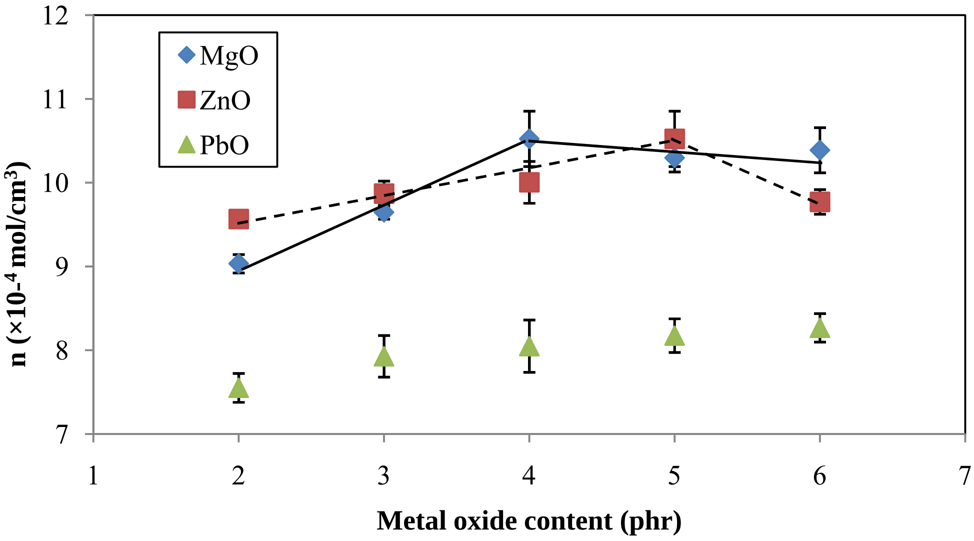

Figure 5.4 Crosslink density of CR vulcanizates at various types and loadings of metal oxides

Additionally, the crosslink density of CR vulcanizates increases with increasing metal oxide up to 4 and 5 phr of MgO and ZnO, respectively (as shown in solid and dash lines, respectively). In other words, the maximum crosslink density is observed at the MgO and ZnO contents of 4 and 5 phr, respectively. Furthermore, in the case of PbO, the magnitude of crosslink density is relatively low which can be summarized that the MgO contributes to the crosslink of CR more effectively than PbO. The results agree with the crosslink density results that were determined from the cure torque difference of MDR in previous section.

5.1.1.4 Hardness

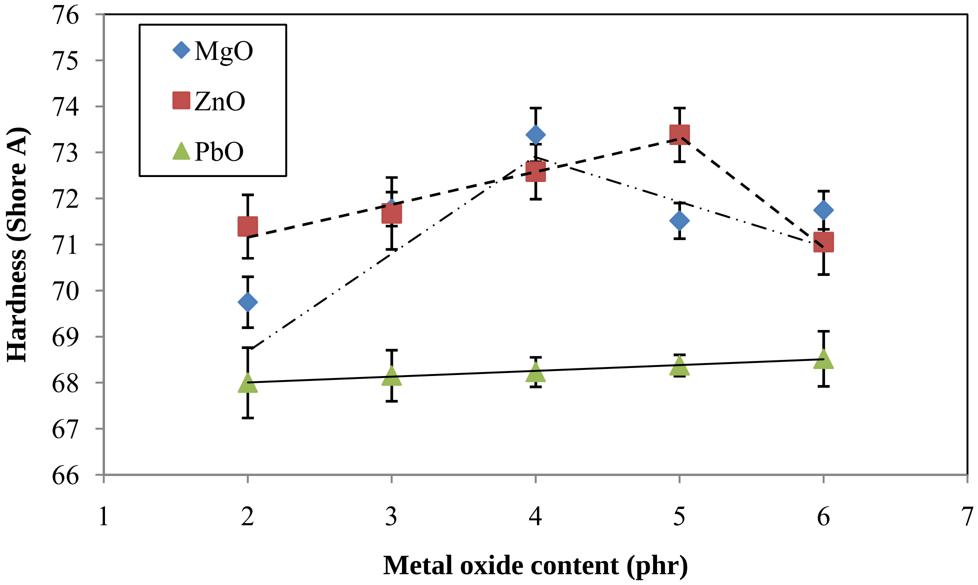

Figure 5.5 Hardness of vulcanizates with various loadings of MgO, ZnO and PbO

Normally, as the magnitude of crosslink density rises, the hardness progressively increases until the steel – elastic state is reached, i.e. until the material becomes ebonite [6]. Figure 5.5 represents the effect of metal oxide curing agents on hardness of rubber vulcanizates. The increases in MgO and ZnO loadings lead to a progressively rise in hardness until 4 and 5 phr, respectively. In the case of PbO, the hardness of vulcanizates is relatively low. The results are in good agreement with the crosslink density results measured from MDR and Flory-Rehner equation in previous sections.

5.1.1.5 Tensile Properties

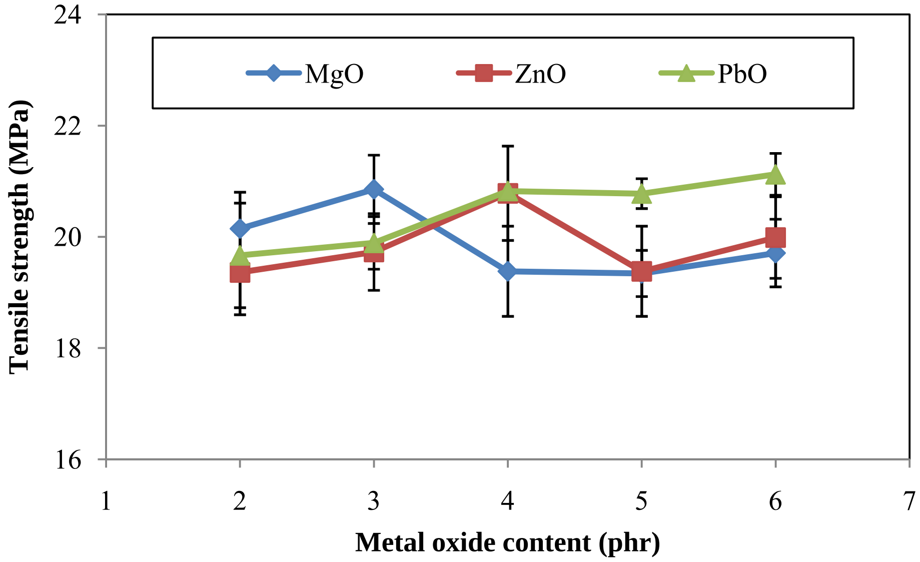

Figure 5.6 Tensile strength of vulcanizates with various loadings of MgO, ZnO and PbO

The results of tensile strength and M100 are exhibited in Figures 5.6 and 5.7, respectively. Tensile strength of vulcanizates increases with increasing metal oxide loading up to 3 and 4 phr of MgO and ZnO respectively. Further loading gives a decrease in tensile strength. It should be noted that, in general, the tensile strength does not rise continuously with the number of crosslinks. Instead the tensile strength rises with the number of crosslinks until an optimum is reached, after which, if the crosslink density is continued, the tensile strength initially falls steeply [6, 28]. Thus, the decrement in tensile strength at high loadings of MgO and ZnO could be explained in terms of excessive crosslink density. In the case of PbO, the tensile strength increases with increasing PbO loading. The results obtained are in good agreement with crosslink density results determined from Flory-Rehner equation (see Figure 5.4).

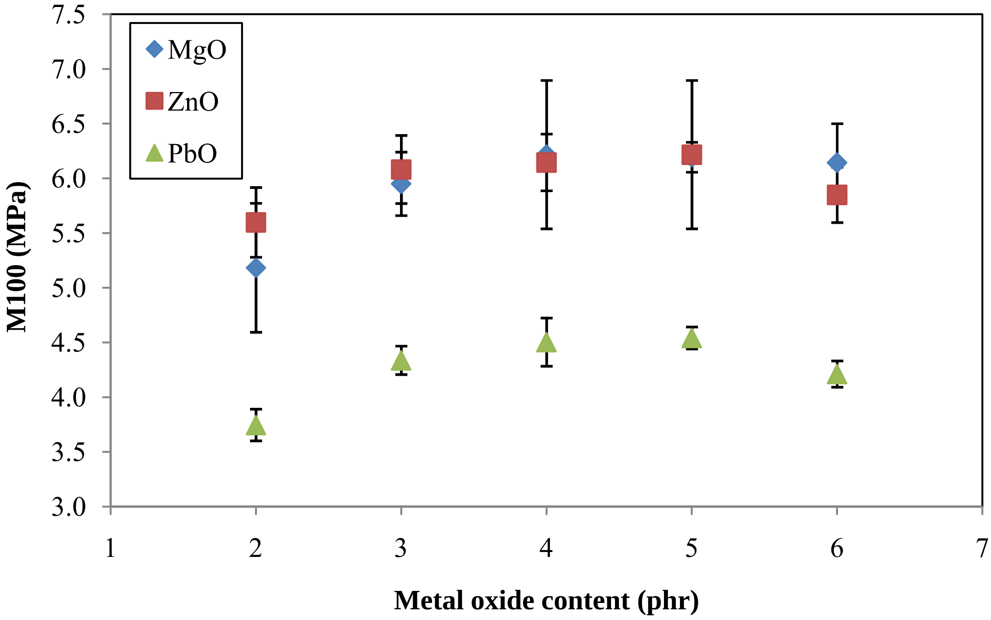

Figure 5.7 Modulus at 100% strain (M100) of vulcanizates with various loadings of MgO, ZnO and PbO

Figure 5.7 reveals M100 defined as the resistance to deformation of the materials at 100% strain. From the cure results as shown previously in Figures 5.1 and 5.4, the crosslink density increases with increasing loading of metal oxides. Thus, an improvement in M100 with increasing metal oxide loading is due partly to the increase in crosslink density. Additionally, a decrease of modulus at high ZnO and MgO contents agrees well with the reduction in crosslink density. In the case of PbO, the relatively low magnitude of M100 is caused by the relatively low crosslink density (see Figure 5.4).

5.1.1.6 Compression set

Compression set is generally used to reflect the ability of elastomeric materials to maintain elastic properties after prolonged compressive stress at a given test temperature. This means an occurrence in plastic deformation of the specimen after being compressive stressed for a set time period.

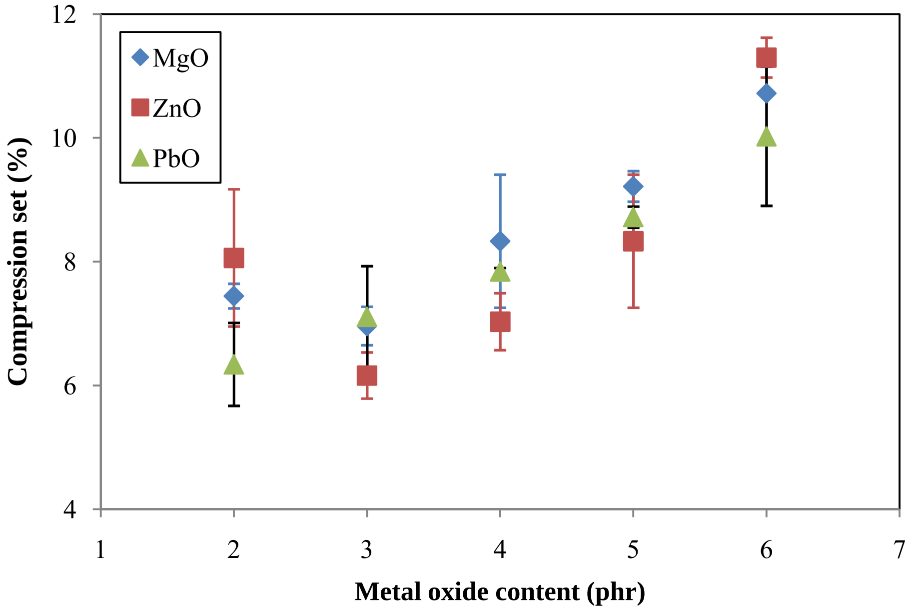

Figure 5.8 Compression set at 70 °C of vulcanizates with various loadings of MgO, ZnO and PbO

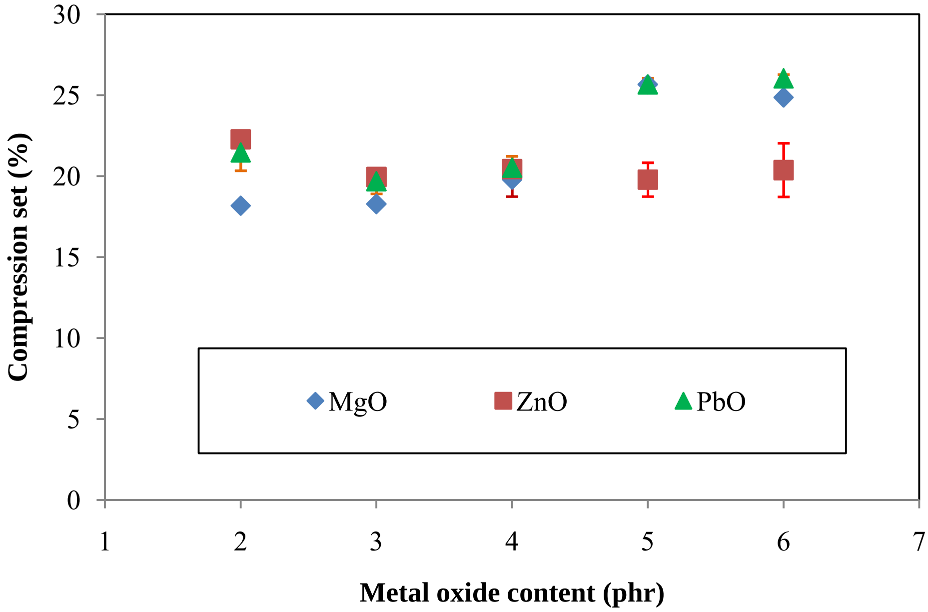

Figure 5.9 Compression set at 100 °C of vulcanizates with various loadings of MgO, ZnO and PbO

As shown in Figures 5.8 and 5.9, it is evident that, except for the vulcanizates with ZnO at 100 °C, compression set of all vulcanizates increases with increasing metal oxide loadings. The results unexpectedly disagree with the crosslink density results. Generally, with increasing crosslink density, the elastic contribution should increase and thus the decrease in compression set. The explanation is proposed in terms of a "post-curing effect". As stated elsewhere, CR could be vulcanized in the absence of curative (as shown in Figure 3.10). Thus, CR is highly subjective to the post-curing phenomenon [38], i.e., the post-curing takes place under compressive strain as shown in Figure 5.10.

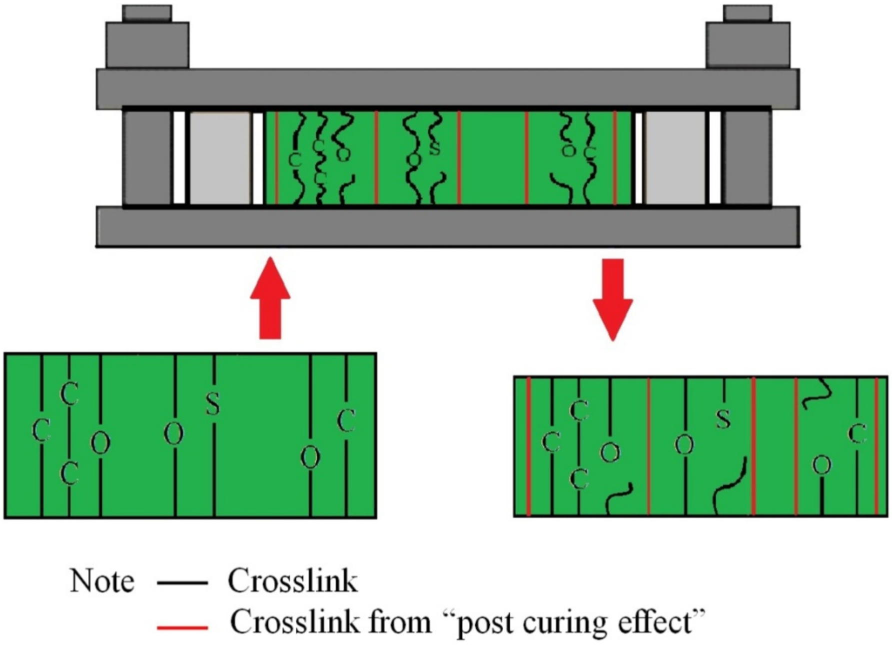

Figure 5.10 Proposed mechanism of post curing effect on increased compression set

Therefore, after load removal, the crosslink formed under compressive strain would restrict the elastic recovery of test specimens. Furthermore, because of the post curing phenomenon of CR, the compression set at 100 °C is much greater than that at 70 °C as shown in Figure 5.11.

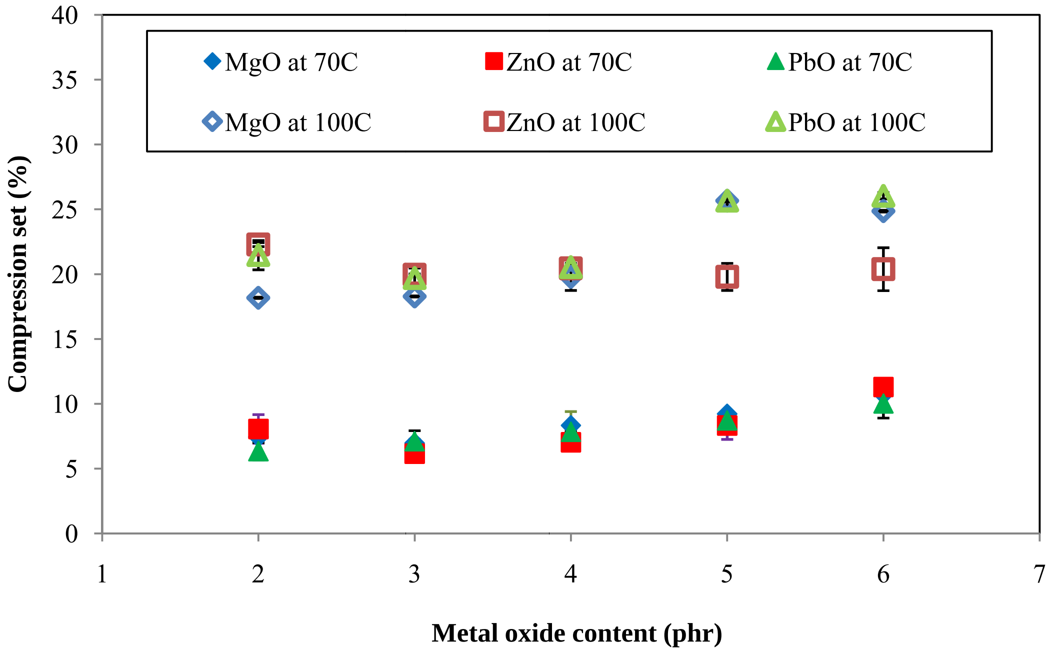

Figure 5.11 Compression set of CR vulcanizates at test temperatures of 70 and 100 °C

5.1.1.7 Heat build - up (HBU)

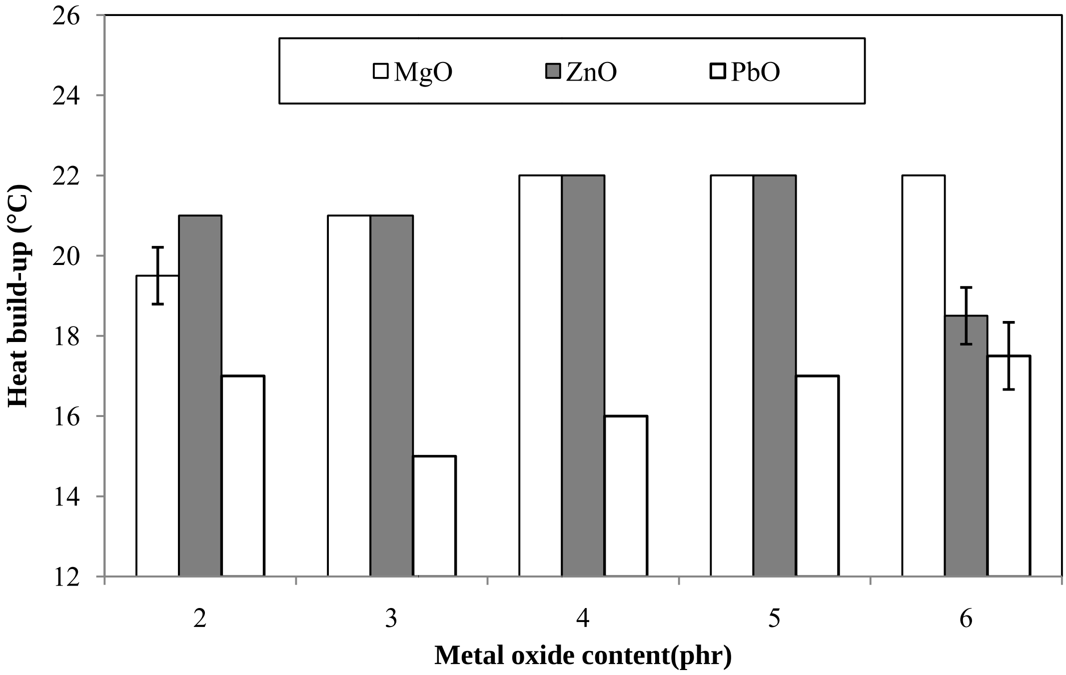

Figure 5.12 Heat build-up (HBU) of vulcanizates with various types and loadings of metal oxides

Results of heat build-up (HBU) are exhibited in Figure 5.12. It is apparent that HBU is dependent on metal oxide loading. The greater the metal oxide loading, the higher the HBU. Such result trend is unexpected. Generally, it is initially anticipated that the rise in crosslink density would reduce the energy dissipation per cyclic and thus the HBU.

The explanation is postulated by the molecular restriction [67]. As the crosslink density increases, as a result of increased metal oxide loading, the molecular mobility is more restricted, resulting in the greater energy required for creating free volume and thus the higher magnitude of hysteresis. The increase in hysteresis with increasing crosslink density is also found in the resin-curing system [68]. (Note: the effect of tanδ on heat build-up is discussed further in appendix E, page)

5.1.1.8 Abrasion resistance

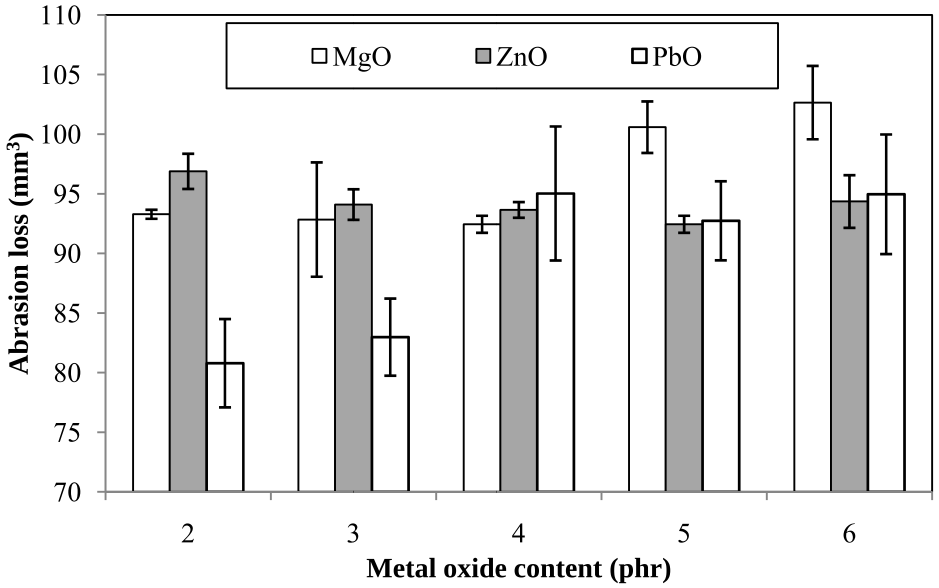

Figure 5.13 Abrasion loss of vulcanizates with various types and loadings of metal oxides

Abrasion resistance is proportional to hardness [69]. Thus, increment of hardness generally leads to the decrease in abrasion loss. From the results obtained, the abrasion resistance is improved by increasing metal oxide loading until the MgO and ZnO loading of 4 and 5 phr, respectively. The results agree with the hardness results as discussed previously.

Unexpectedly, the PbO yields much lower abrasion loss than the MgO at any given loading, despite the relatively low crosslink density and hardness in the case of PbO. The superiority in abrasion resistance provided by PbO could not be explained at present.

However, apart from the hardness, the abrasion resistance could be affected by several factors, such as crosslink density, tensile strength, etc. One of such factors is the dispersion degree of metal oxides. Figure 5.14 reveals the scanning electron microscopy (SEM) images of CR vulcanizates with various amounts of PbO.

It could be observed that the PbO is represented by large bright particles in CR matrix while the fine ones are ZnO particles, as evidenced by results of energy dispersive X-ray spectroscopy (EDS). Figure 5.15a-c reveals the spectrum of element consisting in the CR compound at the specific areas, as circled in SEM images (Figure 5.15). The greater the PbO loading, the higher the tendency of agglomerate formation. The results agree well with the abrasion loss results.

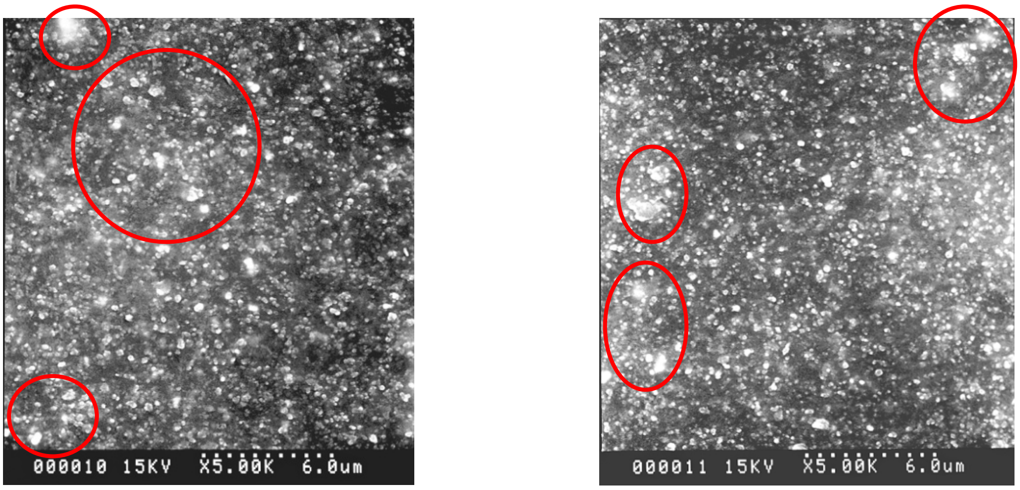

(a) (b)

Figure 5.14 Scanning electron micrographs (×5000) of CR vulcanizates with various PbO loadings (ZnO loading was kept constant at 5 phr): (a) 2 phr; (b) 3 phr; (c) 4 phr; (d) 5 phr; (e) 6 phr

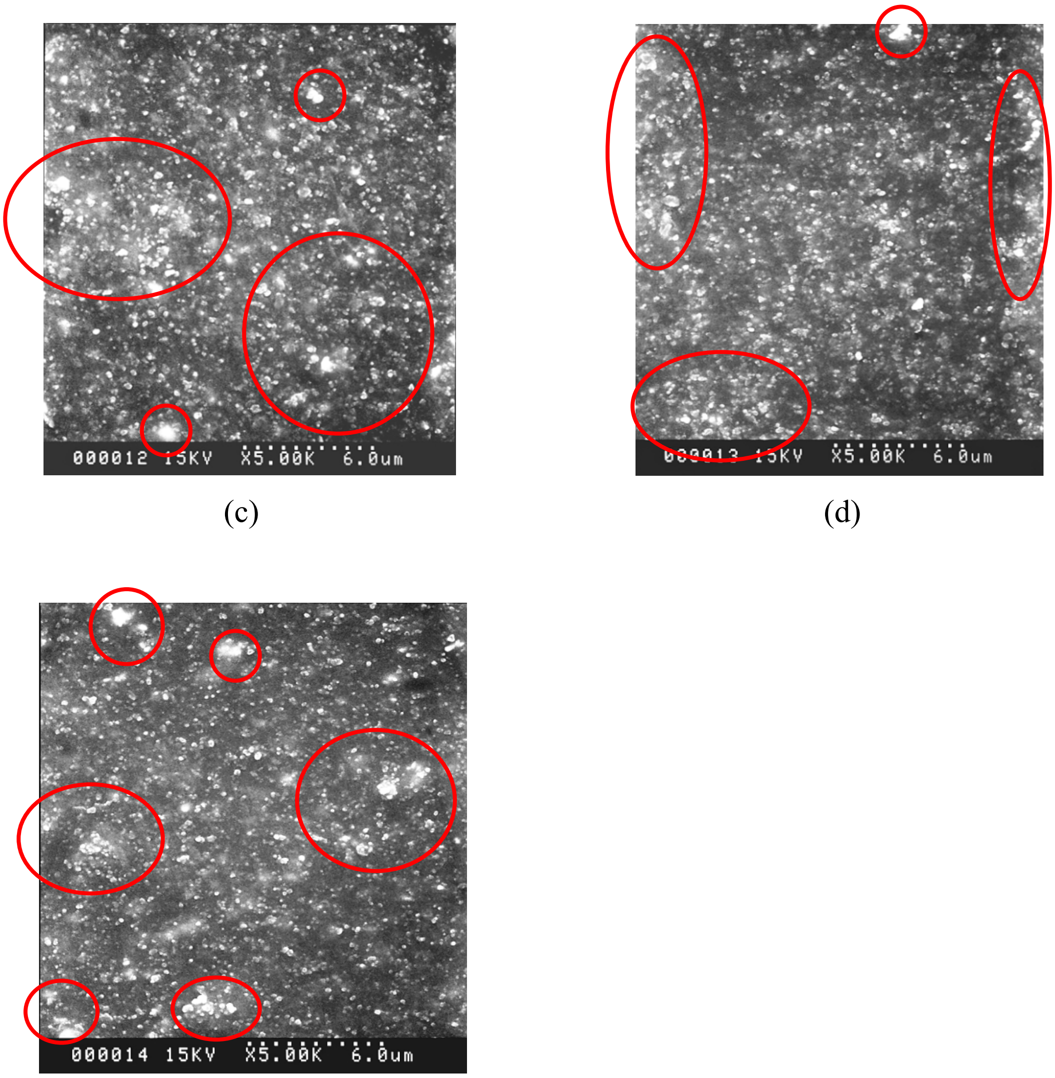

(c)

(d)

(e)

Figure 5.14 Scanning electron micrographs (×5000) of CR vulcanizates with various PbO loadings (ZnO loading was kept constant at 5 phr): (a) 2 phr; (b) 3 phr; (c) 4 phr; (d) 5 phr; (e) 6 phr (cont.)

.

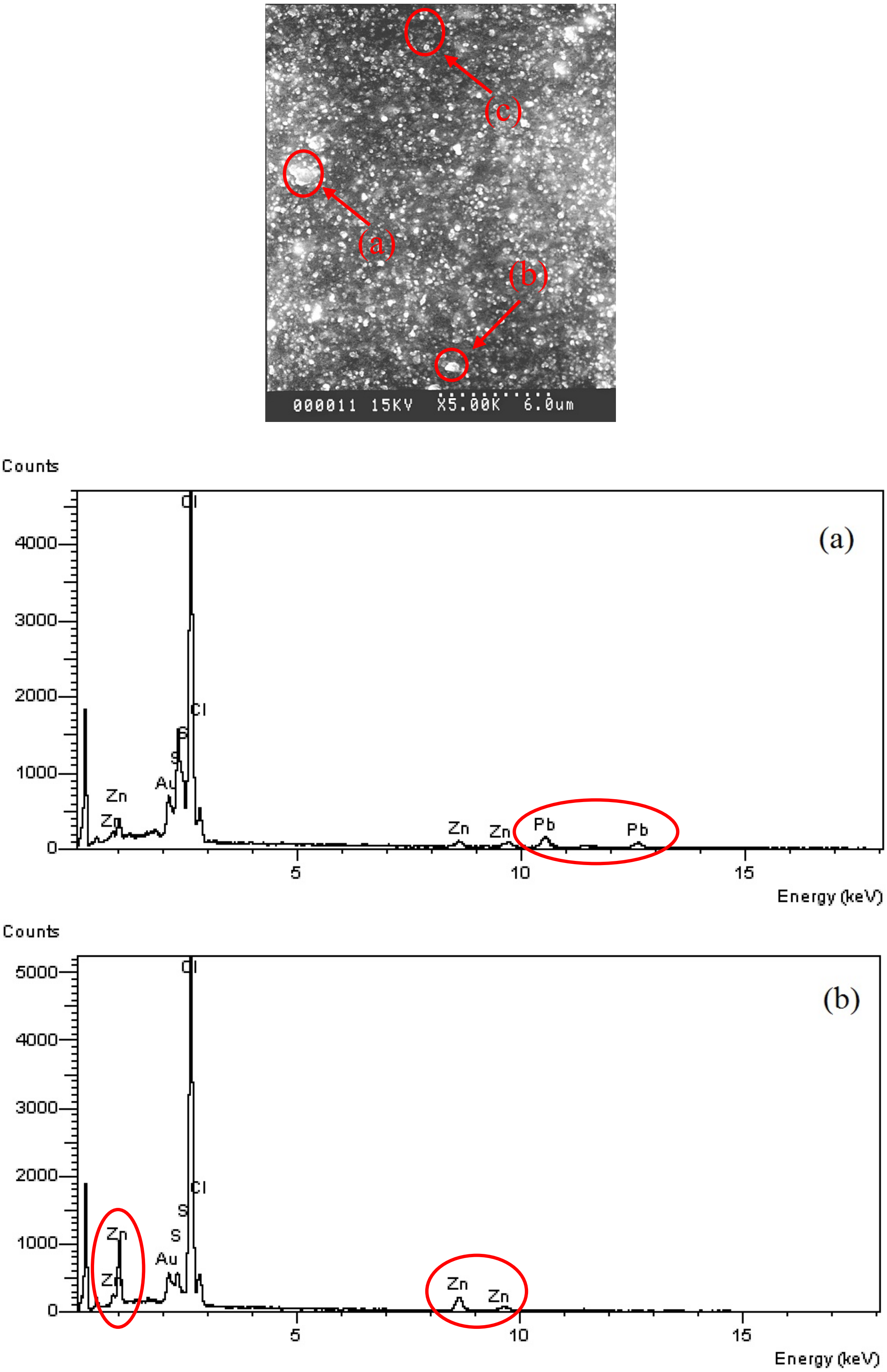

Figure 5.15 SEM image and EDS spectra of CR vulcanizates at the given areas of a, b and c, as circled in SEM image

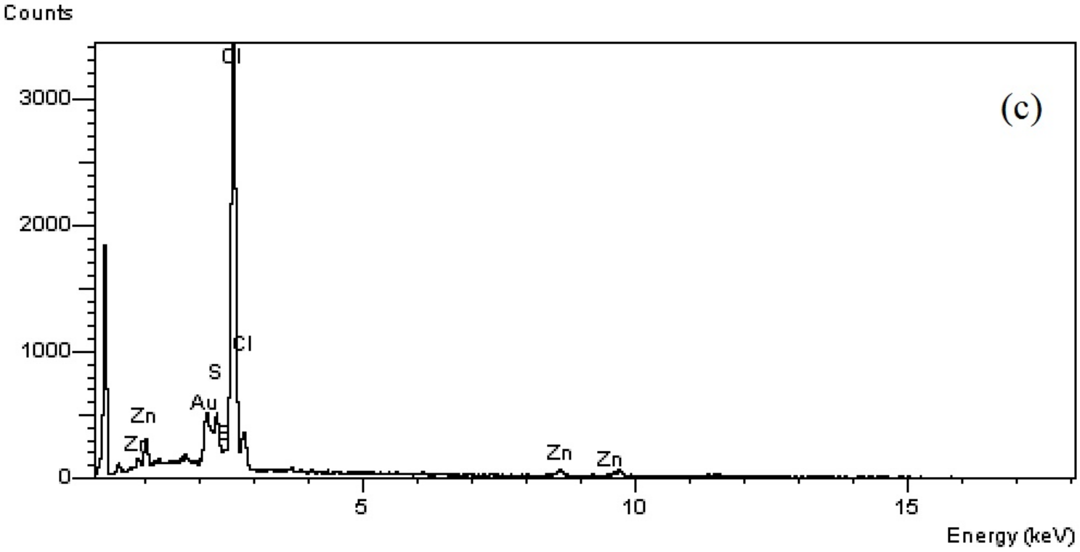

Figure 5.15 SEM image and EDS spectra of CR vulcanizates at the given areas of a, b and c, as circled in SEM image (cont.)

5.1.2 Cure characteristics and properties of CR vulcanizates with MgO and ZnO as a combined curing system

As revealed in previous part, the suitable MgO and ZnO loadings giving maximum crosslink density are of 4 and 5 phr, respectively. In this part, the MgO: ZnO loading ratio of 4:5 was multiplied, and cure as well as mechanical properties of CR vulcanizate were then monitored.

5.1.2.1 Crosslink density

The relationship between torque difference (or crosslink density) and total metal oxide loading is exhibited in Figure 5.16. The crosslink density linearly increases with increasing total loading of metal oxides.

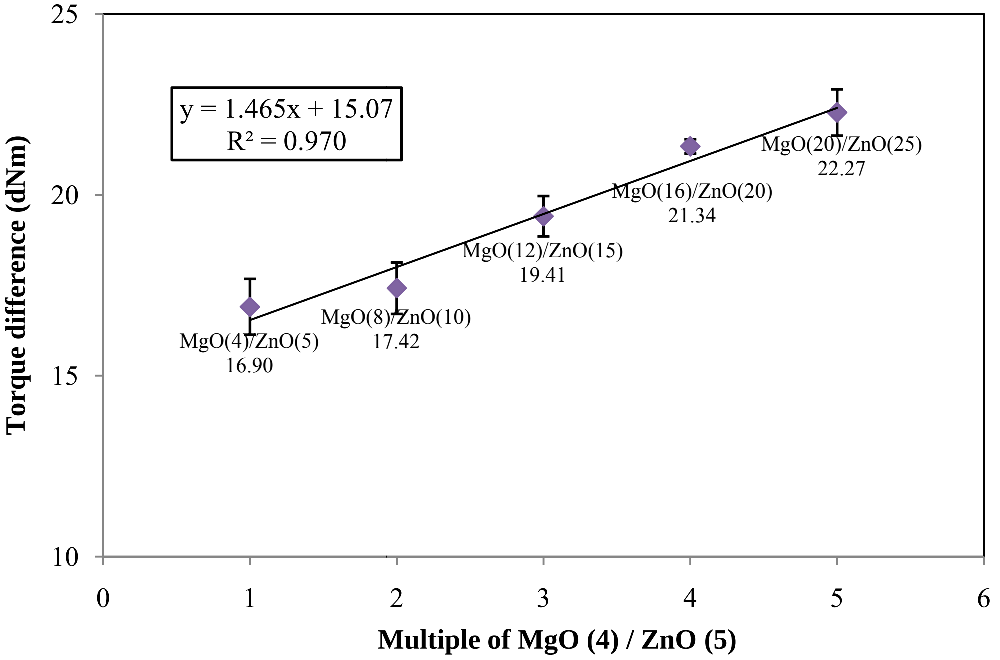

Figure 5.16 Crosslink density as determined from cure torque difference in CR vulcanizates with various total loadings of MgO and ZnO

5.1.2.2 Crosslink density as determined from Flory-Rehner equation

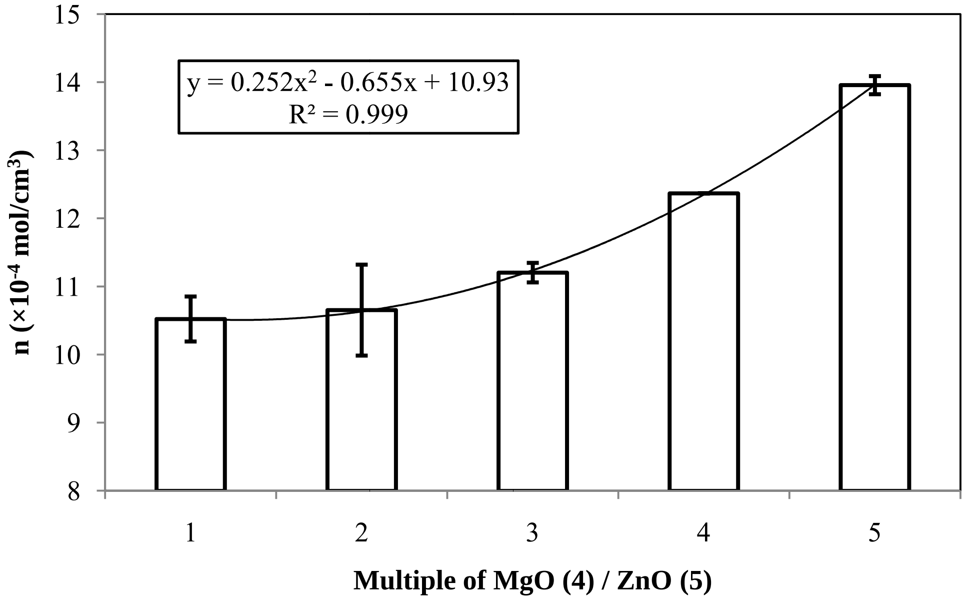

Figure 5.17 Crosslink density of CR vulcanizates with various total loadings of MgO and ZnO

Figure 5.17 exhibits the crosslink density as determined from Flory – Rehner equation of CR vulcanizates with increasing total loading of metal oxides. From the results, the crosslink density polynomially increases with increasing total loading of curing agent (while MgO and ZnO loading ratio is kept constant at 4:5). Also, the Flory – Rehner equation results appear to be in good accordance with cure torque difference as discussed earlier in Figure 5.16. However, the different relationship depends on the different mechanism which unclear at the present.

5.1.2.3 Hardness

The hardness results of CR vulcanizates with various totals loading of MgO and ZnO are illustrated in Figure 5.18. The higher total loading of metal oxides leads to the greater hardness. The results obtained are in good agreement with the crosslink density.

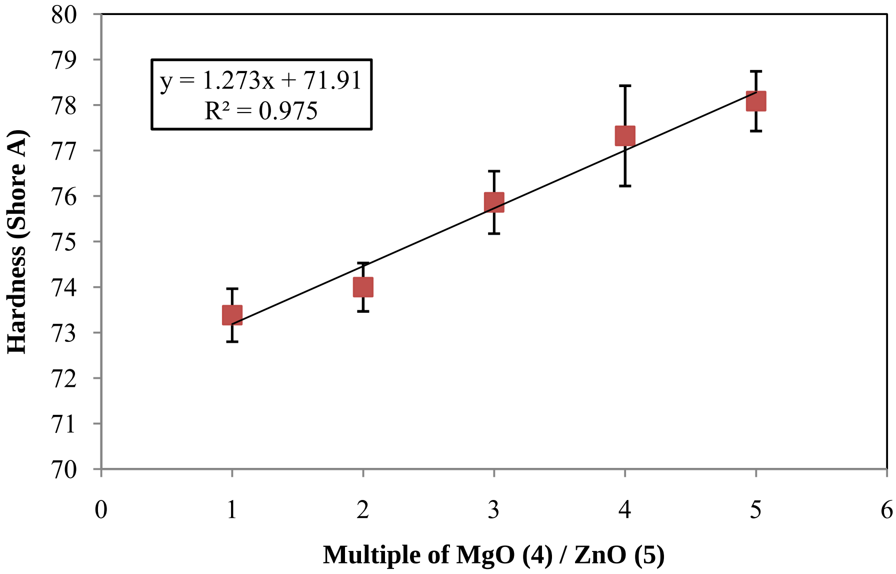

Figure 5.18 Hardness of vulcanizates increases with increasing total loadings of MgO and ZnO

5.1.2.4 Morphology of CR vulcanizates as determined by scanning electron microscopy (SEM) and energy dispersive X-ray spectroscopy (EDS)

In order to investigate the morphology and elemental composition of CR vulcanizates, the scanning electron microscope (SEM) coupled to an energy-dispersive X-ray spectrometer (EDS) is used. SEM image and EDS spectrum of CB-filled CR vulcanizates are shown in Figure 5.19.

There are irregular white particles dispersed in the CR matrix. To identify the elements consisting in these particles, the applicability of EDS as an analytical method is used, and the spectrum results are shown in Figures 5.19a, b and c.

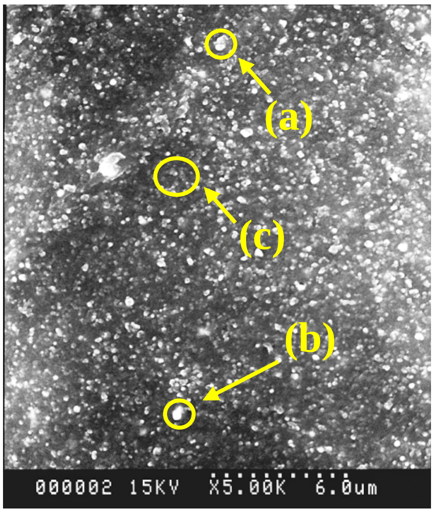

Figure 5.19 SEM micrograph and EDS spectra of CB 50 phr-filled CR (with MgO 4 phr and ZnO 5 phr) at the particular area: irregular white particle (a, b) and no metal oxide area (c)

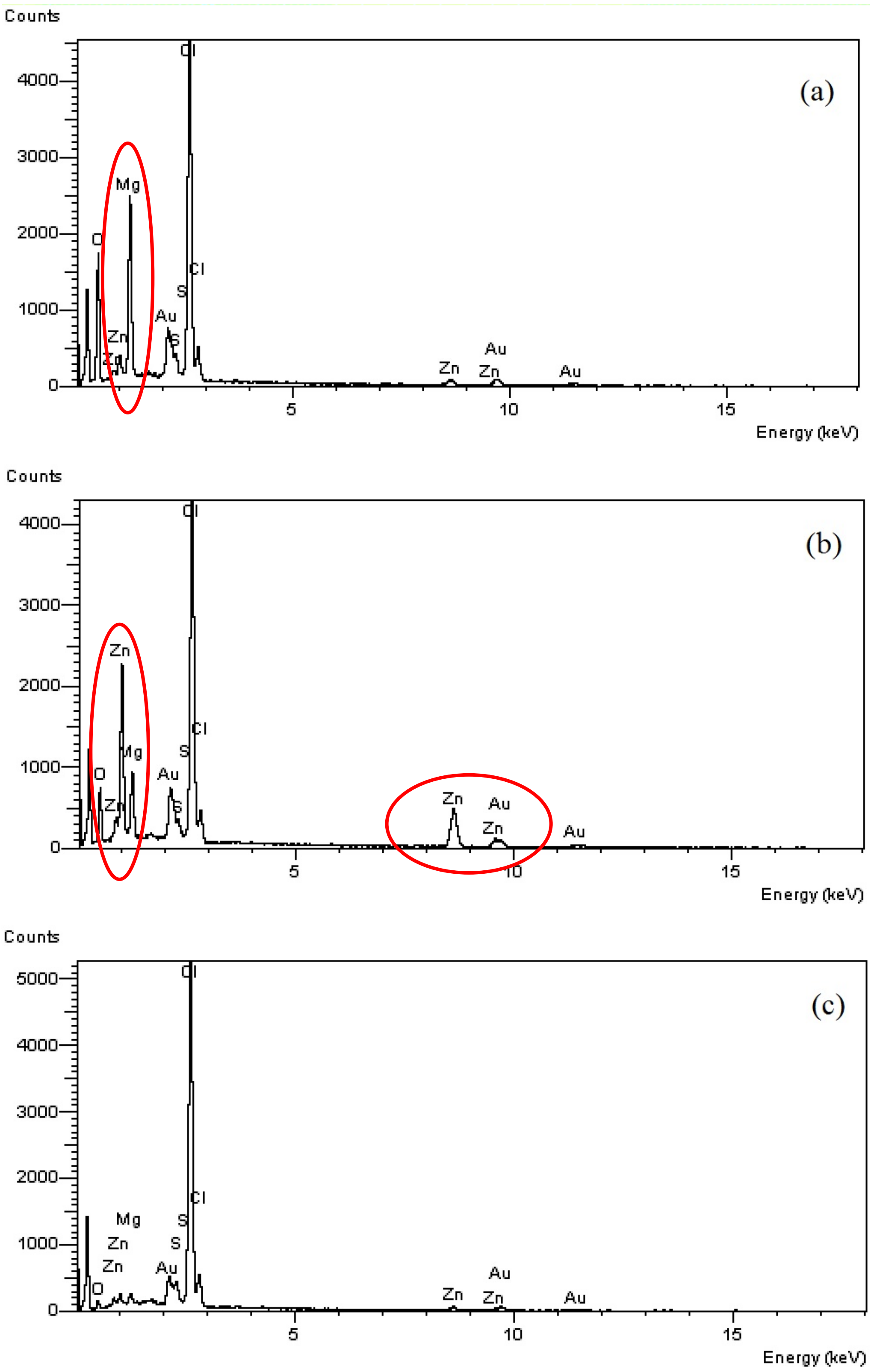

Figure 5.19 SEM micrograph and EDS spectra of CB 50 phr-filled CR (with MgO 4 phr and ZnO 5 phr) at the particular area: irregular white particle (a, b) and no metal oxide area (c) (cont.)

Evidently, the characteristics of either Mg or Zn elements is on the EDS spectrum elucidated from the irregular white particles dispersed in CR matrix.

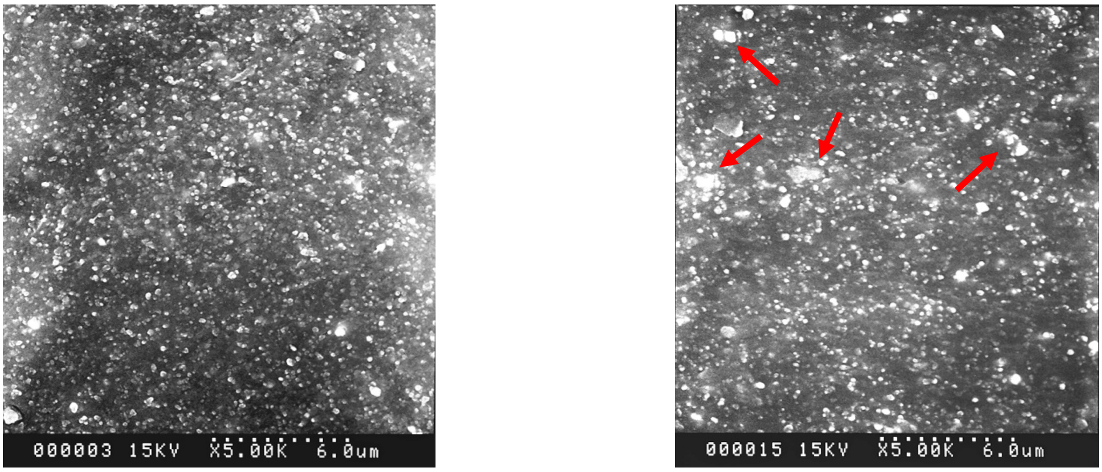

(a) MgO 4 phr/ZnO 5 phr

(b) MgO 8 phr/ZnO 10 phr

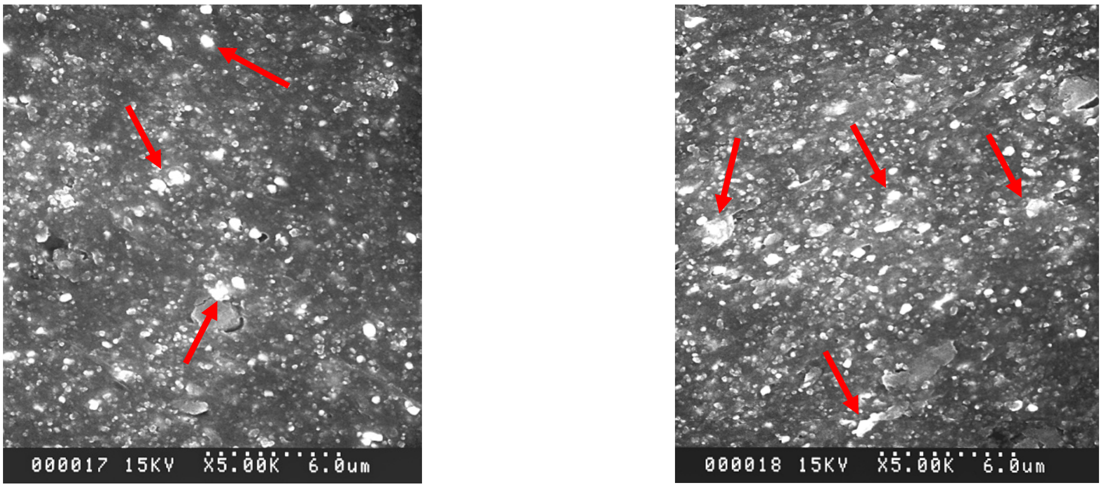

(c) MgO 12 phr/ZnO 15 phr

(d) MgO 16 phr/ZnO 20 phr

Figure 5.20 Morphology of CB-filled CR vulcanizates with various total loadings of MgO and ZnO: (a) MgO 4 phr/ZnO 5 phr; (b) MgO 8 phr/ZnO 10 phr; (c) MgO 12 phr/ZnO 15 phr; (d) MgO 16 phr/ZnO 20 phr; (e) MgO 20 phr/ZnO 25 phr

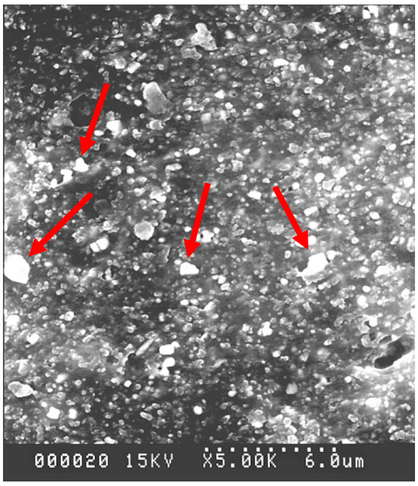

(e) MgO 20 phr/ZnO 25 phr

Figure 5.20 Morphology of CB-filled CR vulcanizates with various total loadings of MgO and ZnO: (a) MgO 4 phr/ZnO 5 phr; (b) MgO 8 phr/ZnO 10 phr; (c) MgO 12 phr/ZnO 15 phr; (d) MgO 16 phr/ZnO 20 phr; (e) MgO 20 phr/ZnO 25 phr (cont.)

SEM images of CR vulcanizates with increasing total loading of metal oxides are illustrated in Figure 5.20. From SEM micrographs, it could be noticed that at higher total loading of MgO and ZnO, the larger white particles (as indicated by the arrows) could be observed.

As evidenced from EDS, results indicate the presence of metal oxides in these particles. Therefore, it might be concluded that at high total loading of MgO and ZnO, the agglomeration of un-dispersed metal oxides could be observed. In order to prove this statement, the strain sweep test was performed, and the results are compared with the Guth-Gold results as shown in Figure 5.21.

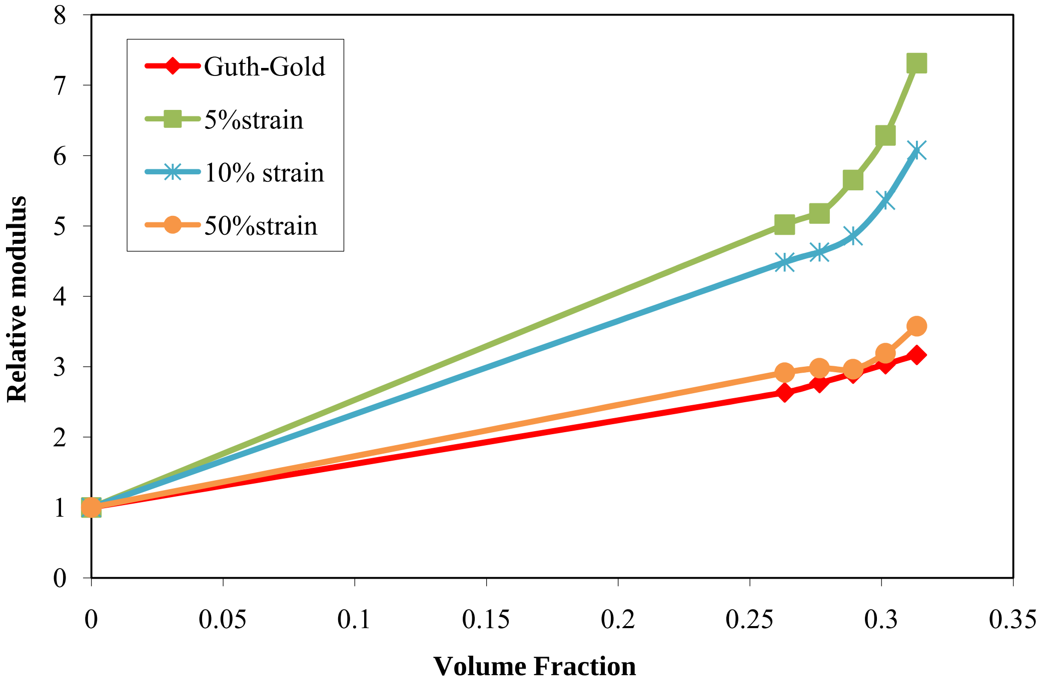

Figure 5.21 Relative elastic modulus (relative G′) at 5, 10, and 50 % strain of CR vulcanizates as a function of metal oxide volume fraction

The positive deviation (particularly at high metal oxide loading) from the Guth-Gold results implies the poor dispersion of filler (or metal oxides in this case) in CR matrix. With increasing strain, the transient network caused by the un-dispersed metal oxides is disrupted. The results support the poor state-of-mix of metal oxides at high loading in CR matrix.

5.1.2.5 Tensile properties

The results of tensile strength and M100 of CR vulcanizates with total amount of MgO and ZnO (at a fixed MgO and ZnO loading ratio of 4:5) are exhibited in Figures 5.22 and 5.23, respectively.

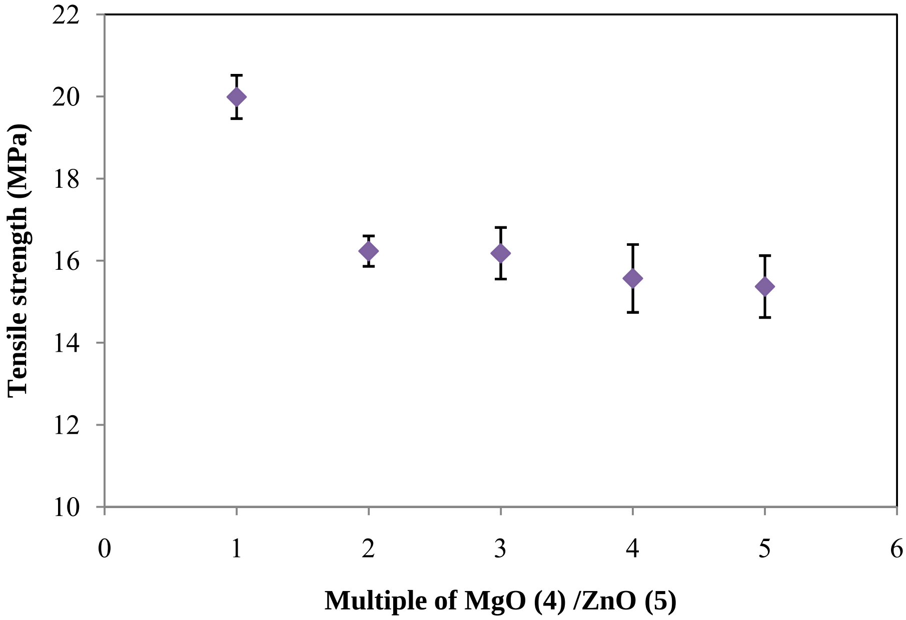

Figure 5.22 Tensile strength of CR vulcanizates with various MgO: ZnO total loadings

As discussed earlier, increases in total amounts of metal oxides in CR vulcanizates result in an increase of crosslink density (see Figures 5.16 and 5.17). The decrease in tensile strength with increasing metal oxide loading is therefore explained by the excessive crosslink density above the optimal point [6, 28]. Apart from the excessive crosslink density, the poor dispersion and distribution of metal oxides could affect the tensile properties. As evidenced in Figure 5.20, the high total loading of metal oxides leads to the poor dispersion of metal oxides in CR compounds. Thus, the reduction in tensile strength with increasing total metal oxide loading could be explained in terms of poor dispersion of metal oxide associated with the excessive crosslink density. The tensile stress at 100% strain or M100 increases with the increment of metal oxide loadings. The results are due partly to (i) the increase in crosslink density as evidence in Sections 5.1.2.1 and 5.1.2.2 and (ii) the hydrodynamic effect (or the dilution of deformable rubber phase by the rigid particles of metal oxides).

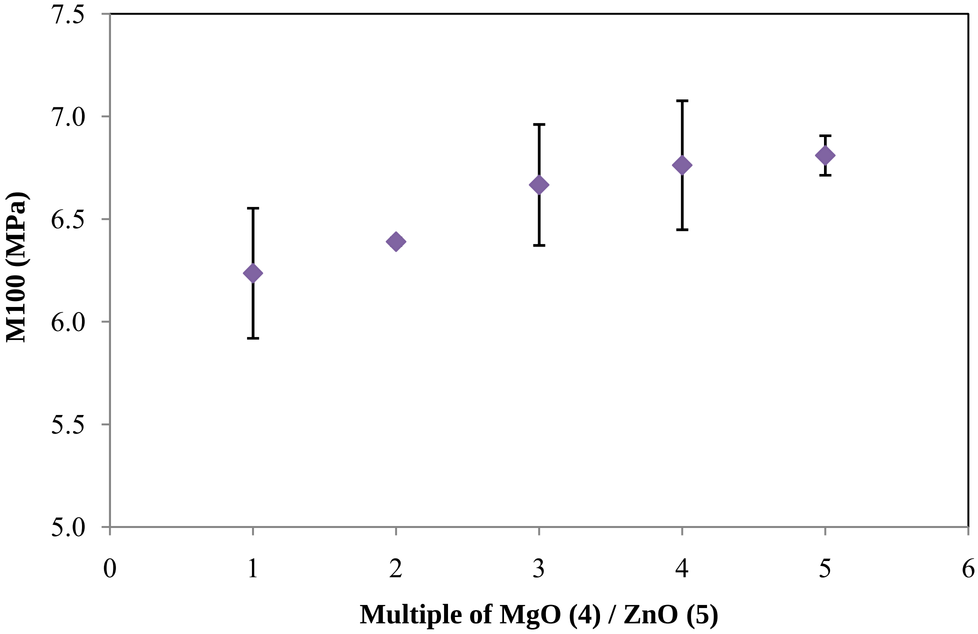

Figure 5.23 Modulus at 100% elongation (M100) of CR vulcanizates with various ZnO: MgO total loadings

5.1.2.6 Compression set

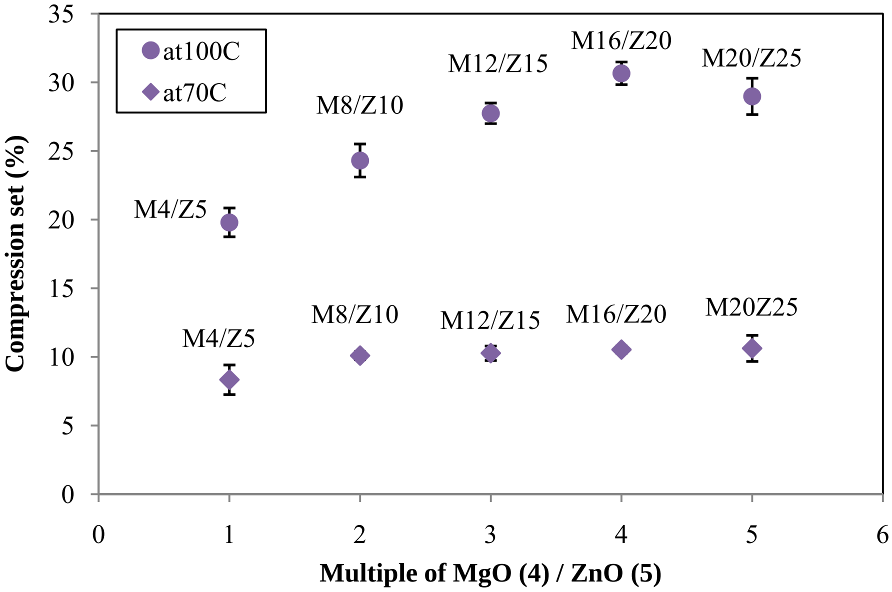

Figure 5.24 Compression set at 70 and 100°C of CR vulcanizates with various total loadings of MgO and ZnO

The dependence of compression set at 70°C and 100°C on total loading of curing agents is illustrated in Figure 5.24. The results reveal that the compression set appears to increase with increasing curing agent loading. However, after MgO to ZnO ratio of 12:15, the increase in compression set is insignificant. As discussed previously, it is believed that the post curing effect is responsible for such unexpected increase in compression set as a function of crosslink density. Additionally, the dilution effect, i.e., the reduction in elastic phase of CR by undeformable metal oxides, could give such increase in compression set.

5.1.2.7 Heat build-up (HBU)

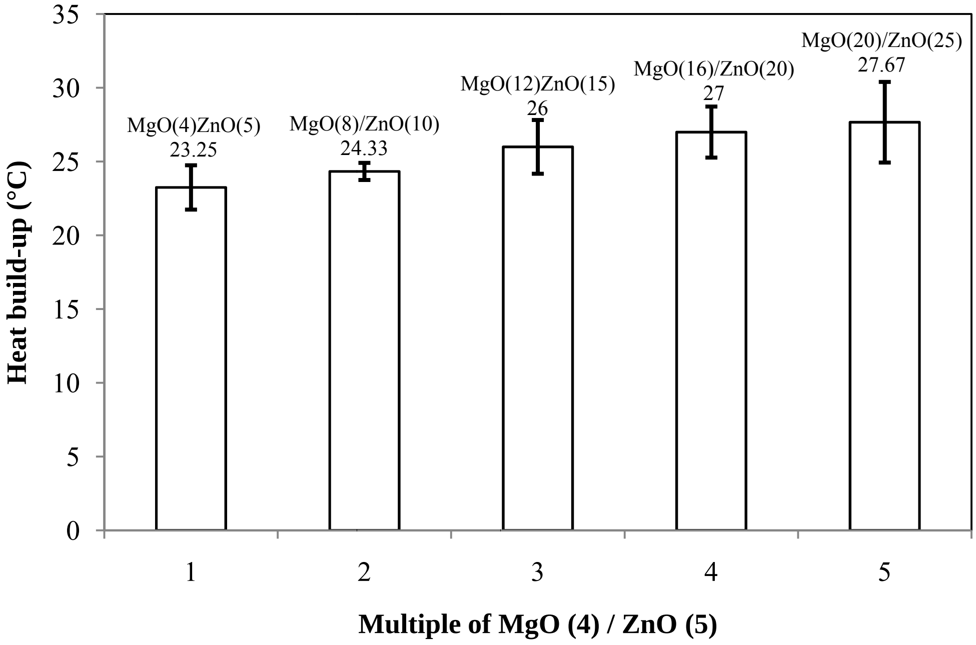

Figure 5.25 Heat build-up (HBU) of CR vulcanizates with various total loadings of MgO and ZnO

As shown in Figure 5.25, the heat build-up (HBU) tends to increase with increasing total loading of metal oxides i.e., with an increase in crosslink density. The unexpected rise in HBU could probably be attributed to the molecular restriction as discussed previously in section 5.1.1.7 [67].

5.1.2.8 Abrasion resistance

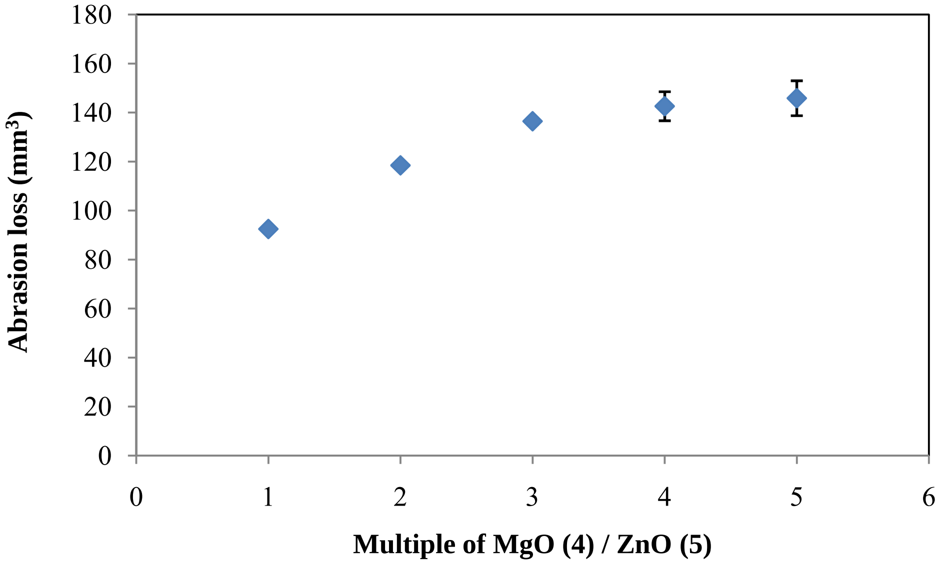

Figure 5.26 Abrasion loss of CR vulcanizates with various total loadings of MgO and ZnO

In general, the abrasion resistance is found to be low if the crosslinking is rather insufficient or excessive [6]. Therefore, the increment in abrasion loss with increasing metal oxide loading could be attributed to the excessive crosslink density. Apart from the excessive crosslink density, the poor dispersion of metal oxides could cause the decrease in abrasion resistance.

5.2 Effect of sulfur

5.2.1 Crosslink density

Figures 5.27-5.28 represent the influence of sulfur on cure characteristics of the CR compounds. Despite the absence of sulfur, the crosslink density increases continuously with increasing metal oxide loading. Apparently, the presence of sulfur gives greater magnitude of crosslink density which is more pronounced in the case of MgO. The results imply that sulfur could enhance the state-of-cure in CR vulcanizates.

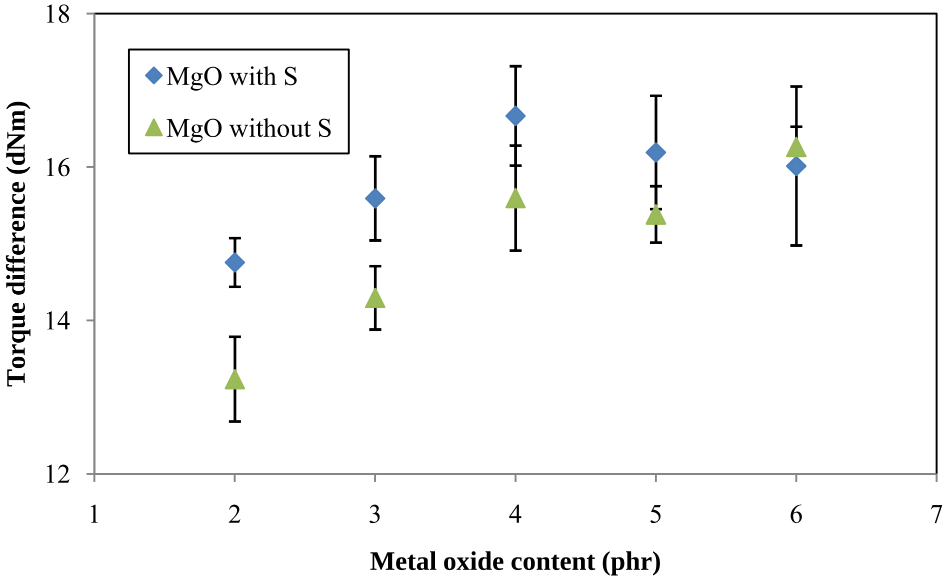

Figure 5.27 Crosslink density as determined from torque difference of vulcanizates with various loadings of MgO with and without sulfur

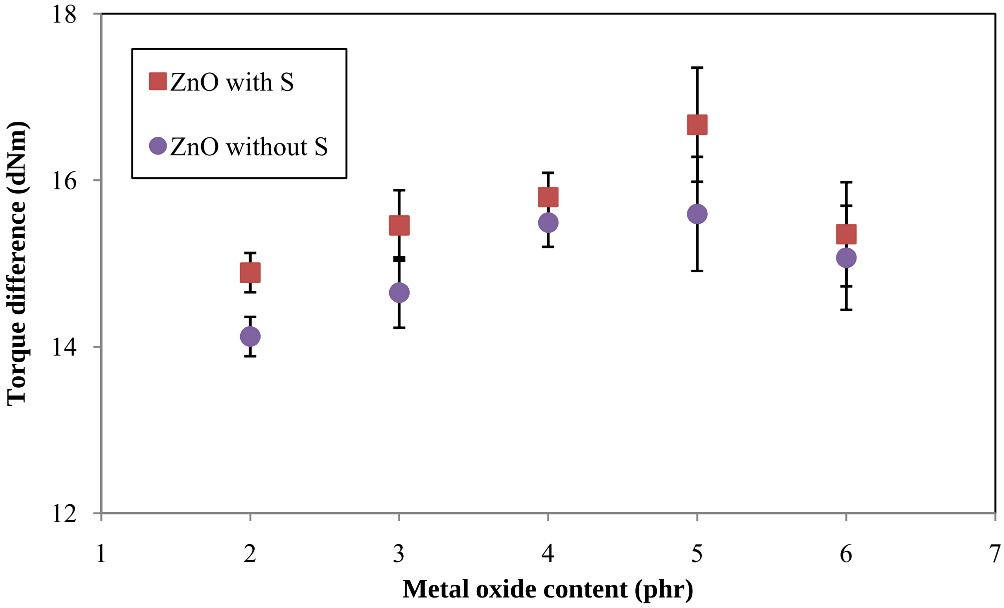

Figure 5.28 Crosslink density as determined from torque difference of vulcanizates with various loadings of ZnO with and without sulfur

When CR compound is vulcanized with metallic oxides in the usual way, the rearrangement of double bonds in CR provides greater opportunity to react with sulfur, as shown in Figure 5.3. Thus, sulfur can be added to increase the crosslink density of CR [16, 29].

5.2.2 Scorch time

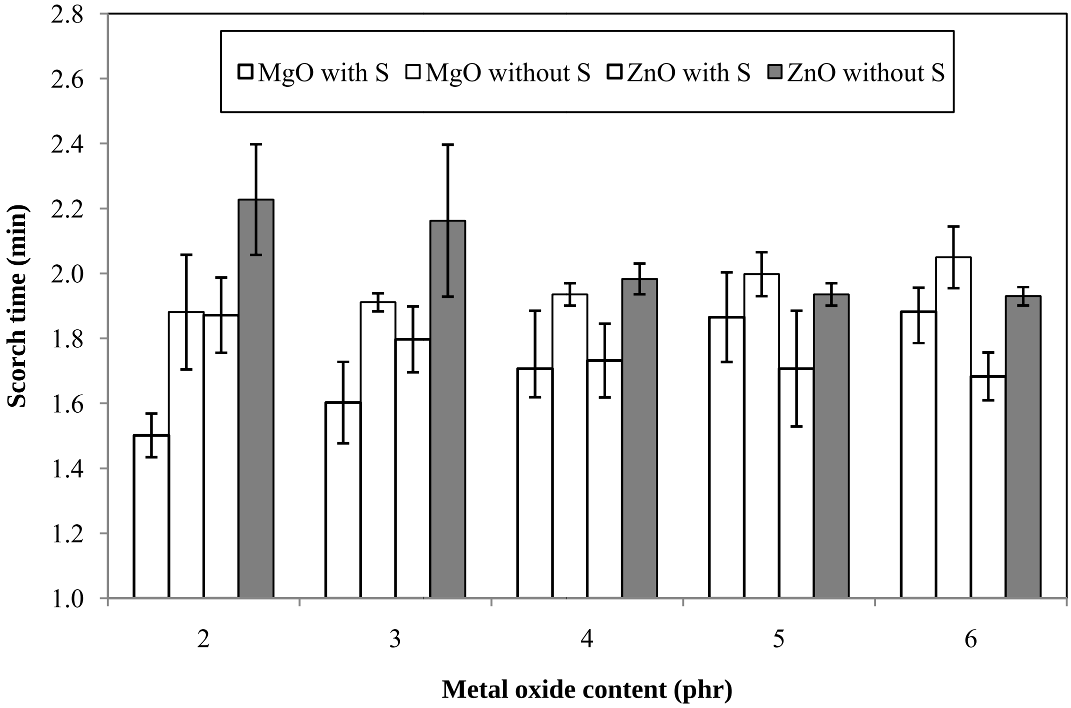

Figure 5.29 Scorch time of CR vulcanizates with various loadings of metal oxides with and without sulfur

The relationship between scorch time (t_{s2}) and metal oxide loading in CR vulcanizates is illustrated in Figure 5.29. The trend of t_{s2} of the system without sulfur is in good agreement with that in sulfur system. In other words, t_{s2} increases with increasing MgO loading, but decreases with increasing ZnO loading. By comparing the t_{s2} of two systems, it is apparent that the CR vulcanizates in non-sulfur system have longer scorch time than those in sulfur system. This supports that the sulfur provides cure promotion of CR vulcanizates.

5.2.3 Crosslink density as determined from Flory-Rehner equation

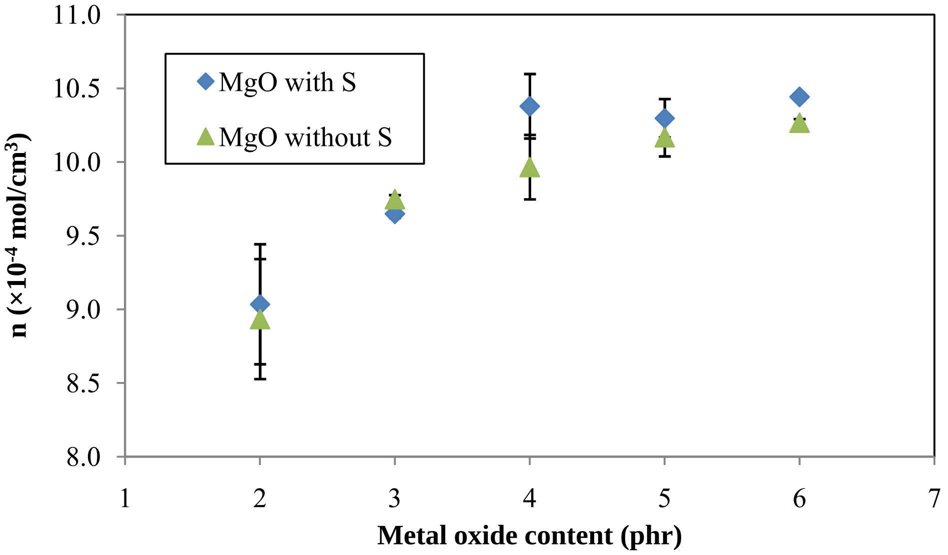

Figure 5.30 Crosslink density of CR vulcanizates as a function of MgO loadings with and without sulfur

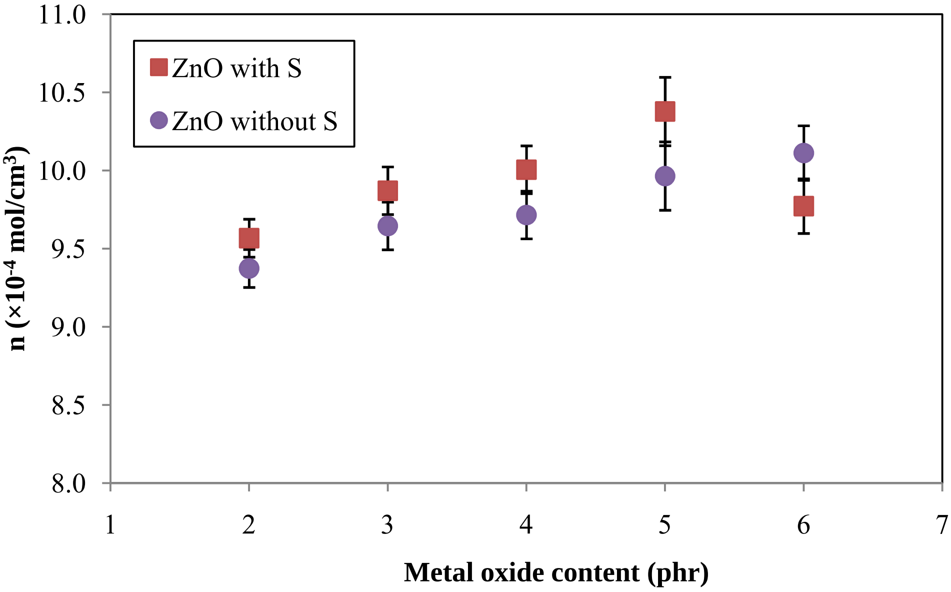

Figure 5.31 Crosslink density of CR vulcanizates as a function of ZnO with and without sulfur

Results of crosslink density of CR vulcanizates as measured by swelling technique via Flory-Rehner equation are shown in Figures 5.30-5.31. The crosslink density increases with increasing MgO and/or ZnO loadings. Furthermore, the vulcanizates with the presence of sulfur have slightly greater crosslink density than those without sulfur. Thus, it could be summarized that sulfur gives the improvement in state-of-cure of CR vulcanizates to some extent. The results are in good agreement with the crosslink density as determined from torque difference discussed previously.

5.2.4 Hardness

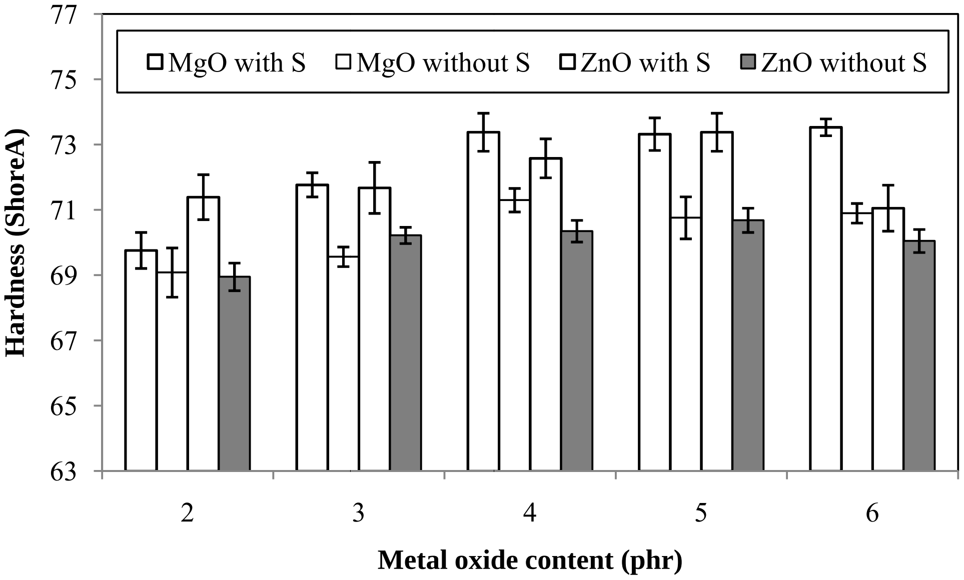

Figure 5.32 Hardness of vulcanizates with various loadings of MgO and ZnO with and without sulfur

Figure 5.32 shows hardness results of CR vulcanizates in non-sulfur and sulfur systems against metal oxide loading. The results are in good accordance with the results of crosslink density in a way that the change in hardness via metal oxide loading is caused by crosslink density, and the addition of sulfur could enhance further the hardness.

5.2.5 Tensile properties

Results of tensile strength and M100 of CR vulcanizates in non-sulfur and sulfur systems against metal oxide loading are illustrated in Figures 5.33 and 5.34, respectively. It could be observed that the tensile strength increases with increasing metal oxide loading up to 4 phr, regardless of metal oxides type. Beyond this loading, tensile strength decreases. As mentioned earlier, the tensile strength rises with the magnitude of crosslink density until reach the maxima. The decrement in tensile strength of high metal oxide loading is due probably to the excessive crosslink density [6, 28].

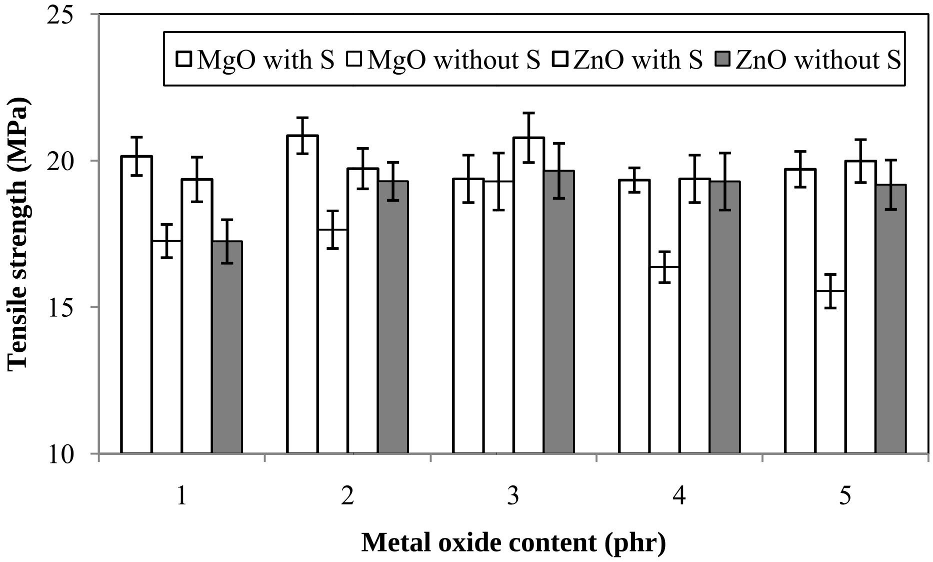

Figure 5.33 Tensile strength of vulcanizates with various loadings of MgO and ZnO in sulfur and non-sulfur system

Additionally, it is apparent that CR vulcanizates in sulfur system give the greater magnitude of tensile strength than those in non-sulfur system. This could be attributed to the presence of labile crosslink characteristics of polysulfidic linkage presented in the vulcanizates with sulfur. Likewise, the M100 results of CR vulcanizates in sulfur system are little higher than that in non sulfur system which could be explained in terms of greater crosslink density in CR vulcanizates with sulfur.

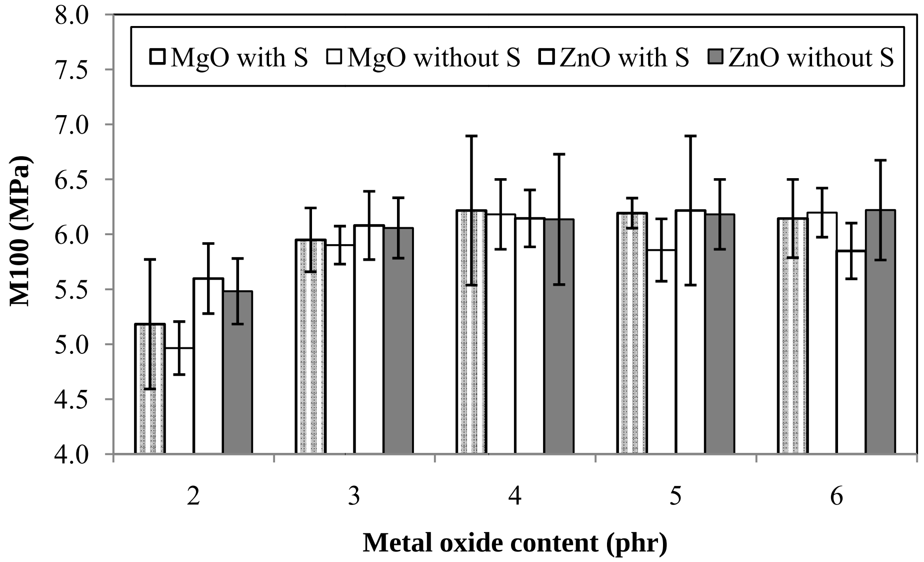

Figure 5.34 Modulus at 100% elongation (M100) of vulcanizates with various loadings of MgO and ZnO with and without sulfur

5.2.6 Compression set

Figure 5.35 exhibits the compression set results of the CR vulcanizates studied. Similar compression set behavior is found in CR vulcanizates with and without sulfur. The compression set appears to increase slightly with increasing metal oxide loadings. As stated previously, CR is highly subjective to the post-curing phenomenon [12, 14, 69]. When the specimens were subjected to high temperature during the test, the post curing could take place under compression stage leading to the reduction in elastic recovery of specimens after load removal. Thus, regardless of sulfur, the CR vulcanizates exhibit an increase in compression set with increasing metal oxide loading (i.e., with an increase in crosslink density via post-curing phenomenon). The proposed explanation of post curing effect on compression set is supported by the compression set results at 100°C (as shown in Figure 5.36) where the post curing phenomena could occur substantially. The compression set appears to be much higher than that tested at 70°C.

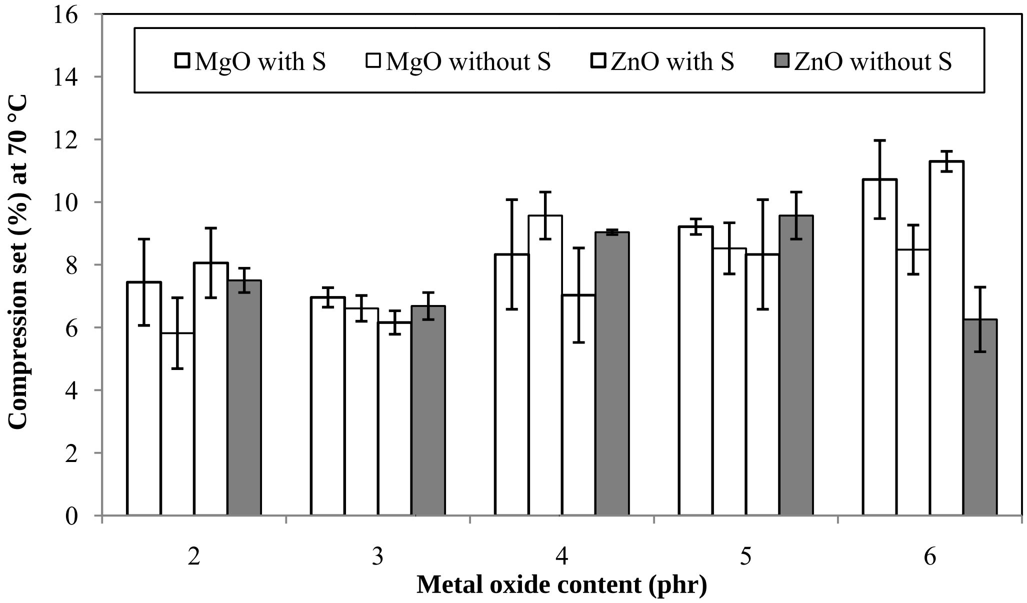

Figure 5.35 Compression set of CR vulcanizates with various amounts of MgO and ZnO in non – sulfur and sulfur system at 70 °C

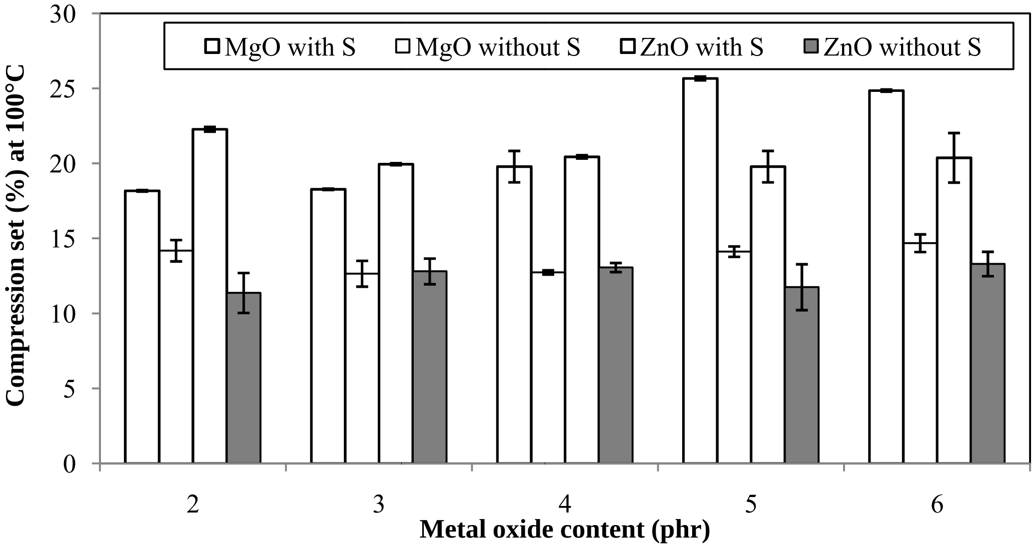

Figure 5.36 Compression set at 100 °C of CR vulcanizates with various loadings of MgO and ZnO with and without sulfur

Additionally, compared with the non-sulfur system, the vulcanizates with sulfur reveal greater compression set, especially at high test temperature of 100 °C (as shown in Figure 5.36). This could be attributed to the breakdown of sulfidic linkages in vulcanizates. Upon heating, the sulfidic linkages caused by sulfur added could be splited off under the test [19, 69-70]. This phenomenon is sometimes knows as the "de-sulfuration".

5.2.7 Heat build - up (HBU)

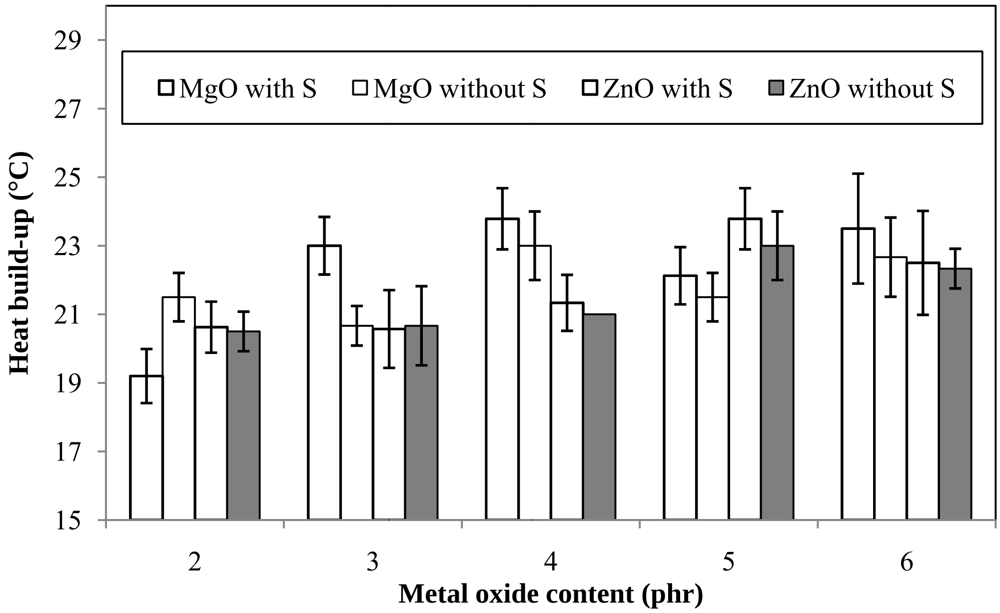

Figure 5.37 Heat build-up (HBU) of CR vulcanizates with various types and loadings of metal oxides

Since rubber compounds are viscoelastic, they return part of the energy of deformation and absorb a relatively a small fraction of the energy input, converting it to heat [16]. Such heat measured from a cyclic deformation is usually known as heat build-up (HBU).

Results of the HBU of the vulcanizates with and without the presence of sulfur are illustrated in Figure 5.37. The HBU slightly increases with increasing loading of metal oxide. This could be ascribed to the molecular restriction as discussed earlier in section 5.1.1.7. Moreover, comparing between two systems, it could be observed that the vulcanizates with the presence of sulfur gives greater HBU value than those without sulfur added. This might be the results of the de-sulfuration of sulfidic linkages as discussed previously [19, 69-70].

5.2.8 Abrasion resistance

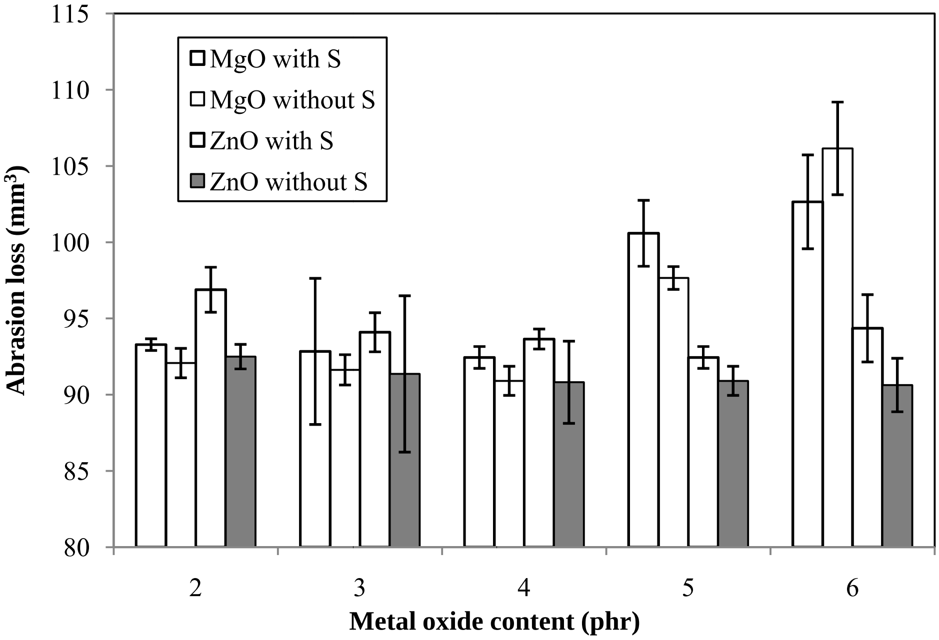

Figure 5.38 Abrasion loss of CR vulcanizates with various loadings of MgO and ZnO with and without sulfur

Figure 5.38 reveals the plot of abrasion loss against metal oxide loading in non-sulfur system. From the results obtained, the abrasion loss is not influenced by metal oxide loading, up to 4 phr regardless of types of metal oxide. Beyond 4 phr of MgO, the abrasion loss significantly increases with increasing MgO content. It must be noted that the abrasion resistance of rubber is influenced by several factors, including tensile strength, hardness, and dynamic properties of vulcanizates. Referred to Figure 5.33, the tensile strength increases with increasing amount of MgO, and then decreases at 5 and 6 phr of MgO. Thus, such reduction in tensile strength might partly be responsible for the decrease in abrasion resistance. Additionally, the CR vulcanizates without sulfur added offer the greater abrasion resistance than those with the presence of sulfur. The results obtained are in contradiction with the crosslink density and tensile strength results. This means the explanation of the superiority in abrasion resistance found in the system without sulfur is still unclear.

Apart from hardness and tensile properties, the dynamic properties could govern the abrasion resistance. In theory, the system with higher elasticity (lower tanδ)

would exhibit greater resistance to abrasion due to the ability to contract the abraded surface and return to its original after being stressed [71-72].

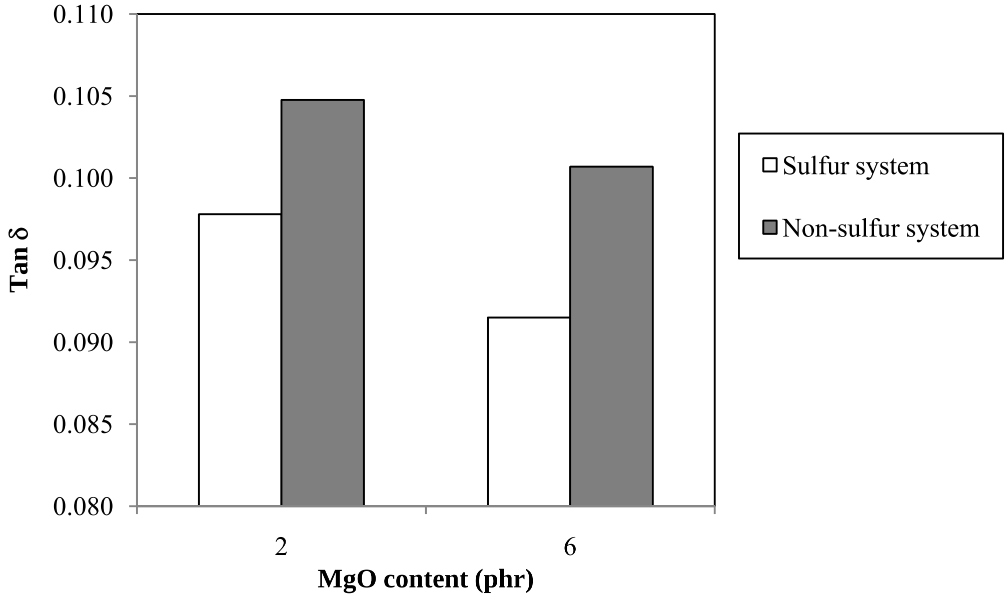

Figure 5.39 Tan δ at 30°C of CR vulcanizates with and without sulfur (ZnO is kept constant at 5 phr)

From the tan δ results, as illustrated in Figure 5.39, it could be noticed that the CR vulcanizates with the presence of sulfur reveal the lower in tanδ value and should theoretically give greater abrasion resistance. However, the experimental results as illustrated in Figure 5.38 reveal greater resistance to abrasion in the case of CR vulcanizates without sulfur. The explanation is not known at present.

5.3 Effect of reinforcing filler

5.3.1 Crosslink density

Effects of filler (i.e., carbon black (CB) and precipitated silica (PSi)) loading on torque difference as the indication of crosslink density are illustrated in Figure 5.40 [32, 35-36]. The crosslink density increases continuously with increasing filler loading which could be attributed to the development of interaction between the CR and filler. Similar finding has been reported elsewhere [14].

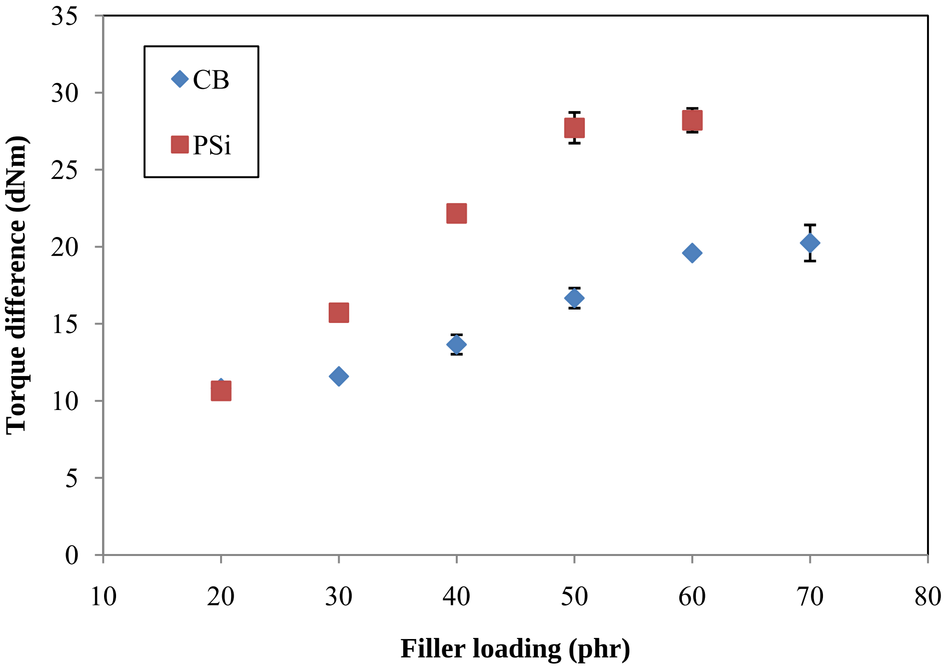

Figure 5.40 Crosslink density as determined from cure torque difference in CR vulcanizates with various loadings of precipitated silica (PSi) and carbon black (CB)

Moreover, by comparing between PSi and CB, the crosslink density of CR filled with PSi is much higher than that with CB implying a superior cure promotion taking place in PSi-filled system. This might be due to the strong interaction between silanol groups of PSi surfaces and chlorine atoms of CR [20]. In other words, the PSi might act as multi-crosslink site or crosslinker for CR. The pseudo-crosslink is finally resulted [14].

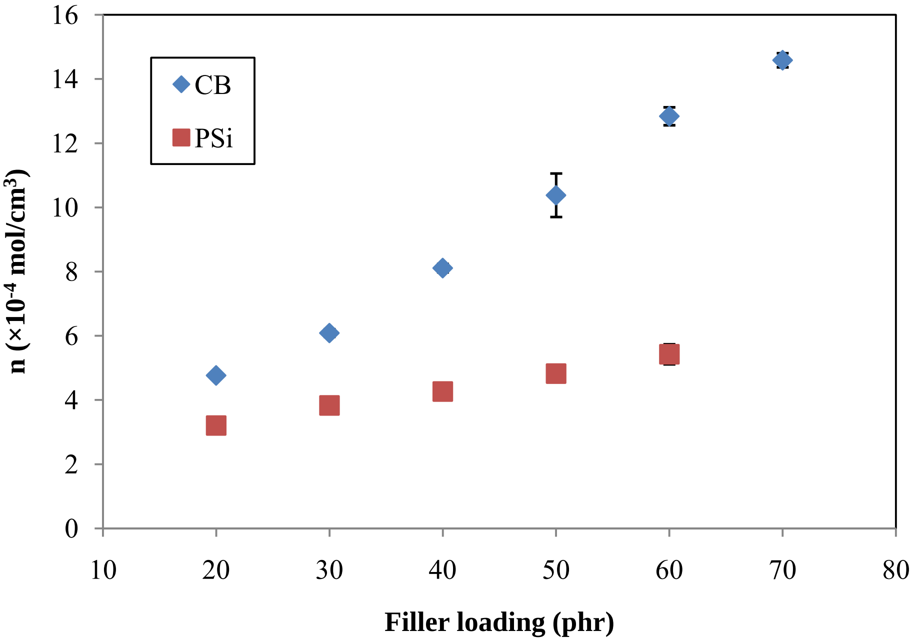

Figure 5.41 Crosslink density of vulcanizates with various loadings of PSi and CB which determined from Flory-Rehner concept

In order to support the findings in Figure 5.40, the crosslink density is measured by swelling technique based on the Flory-Rehner concept. Results obtained are given in Figure 5.41. It could be observed that, by this means, the crosslink density of CR vulcanizates increases with increasing filler loading which is in good agreement with that determined from cure torque difference. However, there is the result contradiction in which the crosslink density in vulcanizates filled with PSi appears to be lower when measured from the swelling technique, and is found to be in the other way round when measured from cure torque difference (Figure 5.41). This is a believed that the high magnitude of torque difference as illustrated in Figure 5.41 is dominated by the development of filler transient network (or the pseudo-crosslink [73]) under low strain of deformation during the measurement (as shown in Figures 5.42 and 5.43). By contrast, the vulcanizates used for swelling technique was prepared from compression molding process in which the large deformation takes place during the mold filling step. Such large deformation might disrupt the filler transient network or pseudo-crosslink as shown in Figure 5.43 [73].

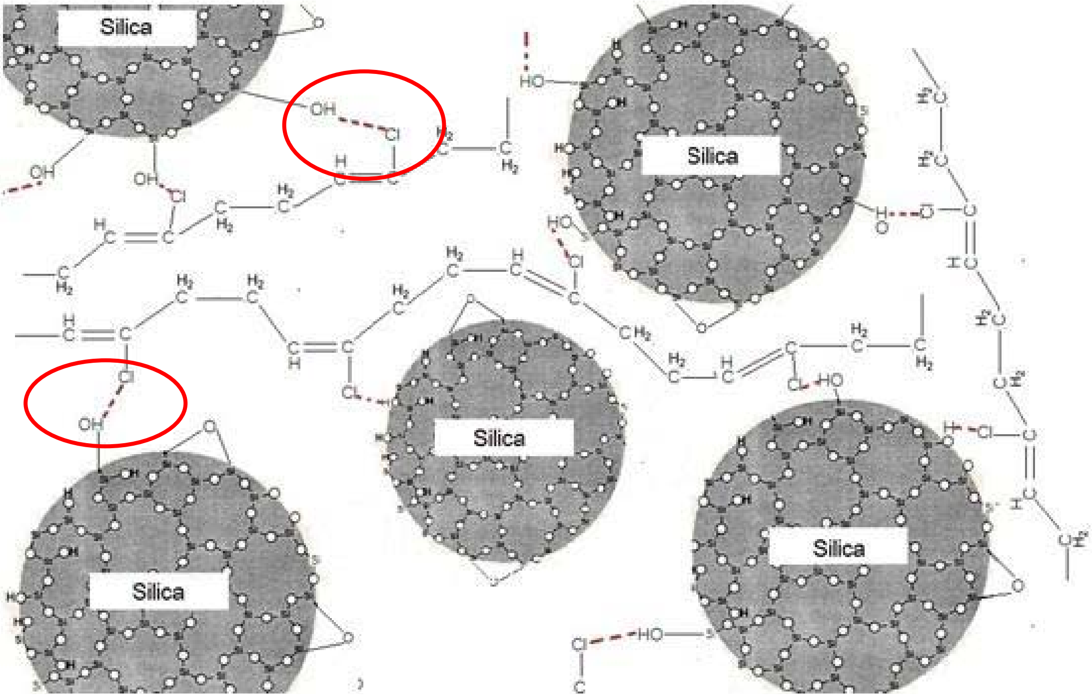

Figure 5.42 Schematic model of a pseudo-crosslink formation caused by CR-silica and silica–silica interactions

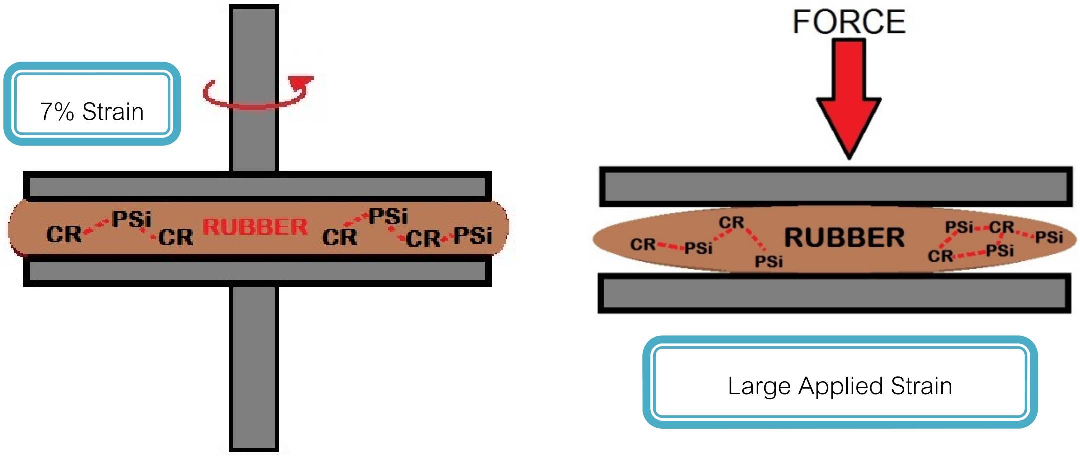

(a) (b)

Figure 5.43 Proposed models of pseudo-crosslink formation taking place in RPA test (a); and mold cavity (b)

In order to prove the proposed explanation, the swelling test of the vulcanizates molded from RPA under low strain is performed. Surprisingly, the result trend obtained is in line with that from the hot press. This means the proposed explanation on difference in magnitude of pseudo-crosslink is not valid. Another proposed explanation is based on the disruption of transient network by the penetration of solvent into the pseudo-crosslink network. The hydrostatic pressure caused by swelling might overcome the interaction within the pseudo-crosslink, leading to the filler network disruption.

The small amount of crosslink density which determined by Flory-Rehner equation in PSi-filled CR could be due to the presence of silanol group in PSi surface. As known well, silanols are responsible for the hydrophilic nature of silica and its unique (versus carbon black) reactivity with water and/or soluble zinc which is the major influence on the low cure states (reduced crosslinking) [35].

5.3.2 Strain sweep test

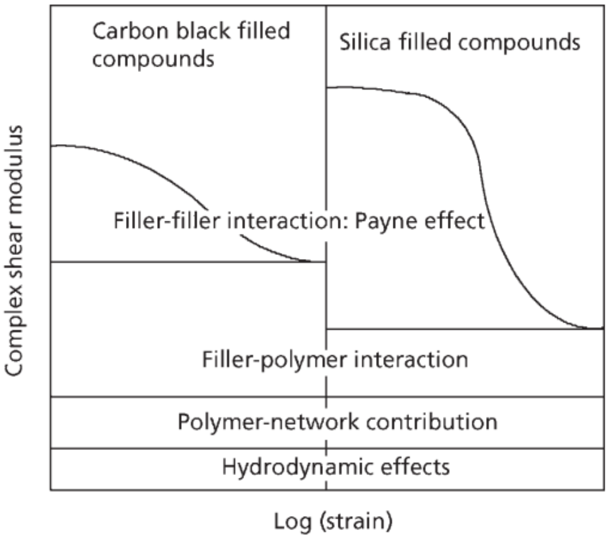

Figure 5.44 Effects contributing to the complex shear modulus [74]

In the aspect of reinforcement mechanism, it is known that the reinforcement of filled vulcanizates is affected by (i) hydrodynamic effect, (ii) chemical crosslink, (iii) polymer-filler interaction, and (iv) filler-filler interaction, as shown in Figure 5.44 [49, 74]. In the case of polar rubber, (such as chlorinated polyethylene (CPE) and CR) filled with PSi, the occurrence of filler-filler and rubber-filler interactions is possible as shown in Figure 5.42. As mentioned elsewhere, the Guth-Gold equation is applicable for describing the state-of-mix of compound [49, 72]. Thus, to investigate the state-of-mix of CR vulcanizates, the Guth-Gold equation is applied.

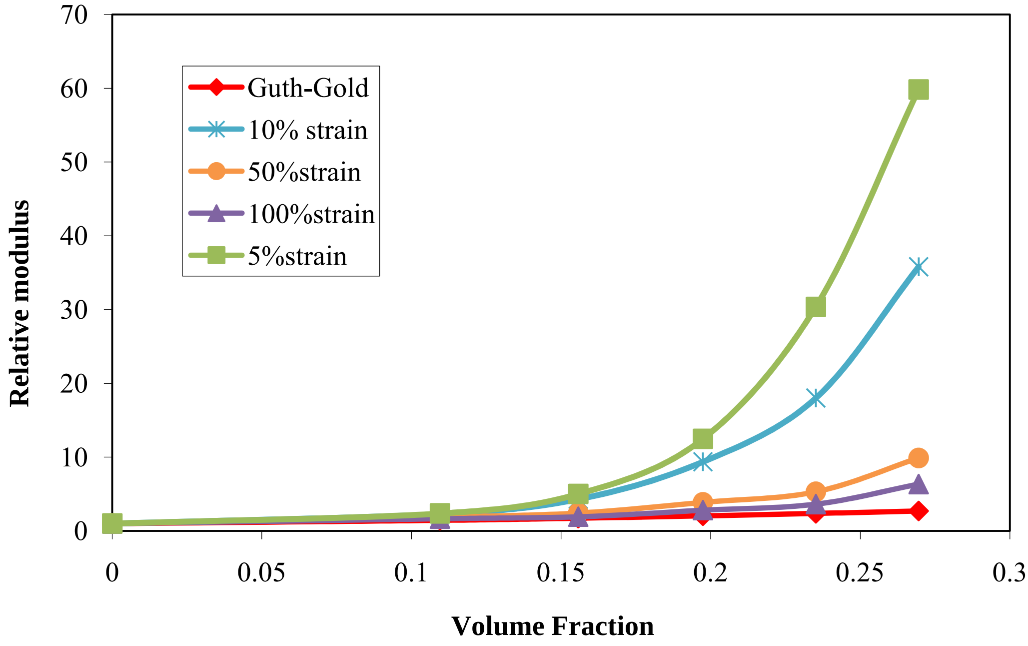

Figure 5.45 Relative elastic modulus (relative G′) at 5, 10, 50 and 100 % strain of PSi-filled CR as a function of silica volume fraction

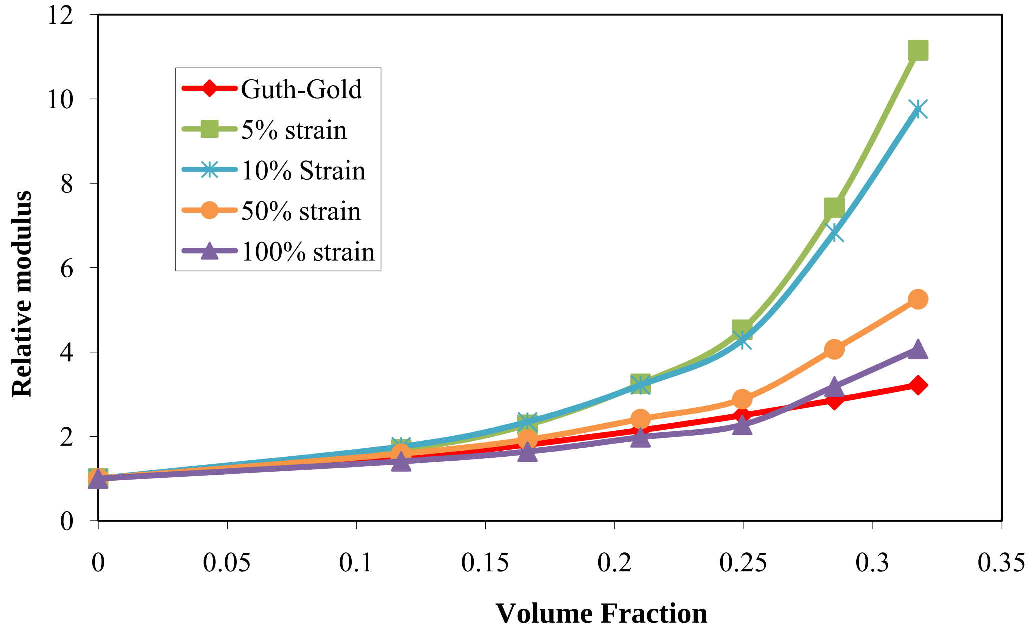

Figure 5.46 Relative elastic modulus (relative G′) at 5, 10, 50 and 100 % strain of CB-filled CR as a function of carbon black volume fraction

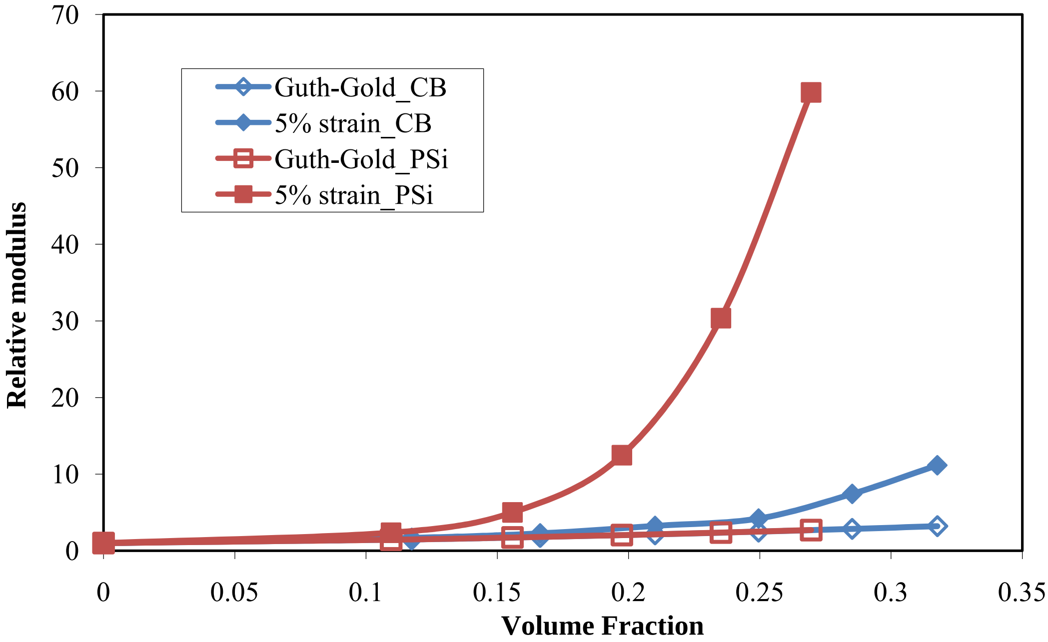

Figure 5.47 Guth-Gold equation and relative elastic modulus (relative G′) at 5% strain of CB and PSi-filled CR as a function of filler volume fraction

Figures 5.45-5.47 show the relative modulus results as calculated from the Guth-Gold equation which excludes the filler network and filler-rubber effects [75]. It is evident that the experimental results of relative modulus (relative G′) at low strain is much higher than the calculated results, especially in the case of PSi-filled CR. Results indicate the presence of filler network and/or filler-rubber interaction. However, filler network and most of physical interaction are transient which could be destroyed by a large applied strain as revealed in Figures 5.45 and 5.46. Undoubtedly, at high strain of 100%, the relative G′ falls to the calculated G′ based on the Guth-Gold equation.

As shown in Figure 5.47, the relative G′ at low strain of CR filled with PSi is much higher than that with CB implying a superior filler-filler and/or filler-rubber interactions taking place in the PSi-filled system.

5.3.3 Hardness

The relationship of hardness of CR vulcanizates and filler loading is revealed in Figure 5.48. As expected, the hardness of CR vulcanizates increases with filler loading due to the reinforcement effect [38]. The effect of filler types on hardness is not significantly different.

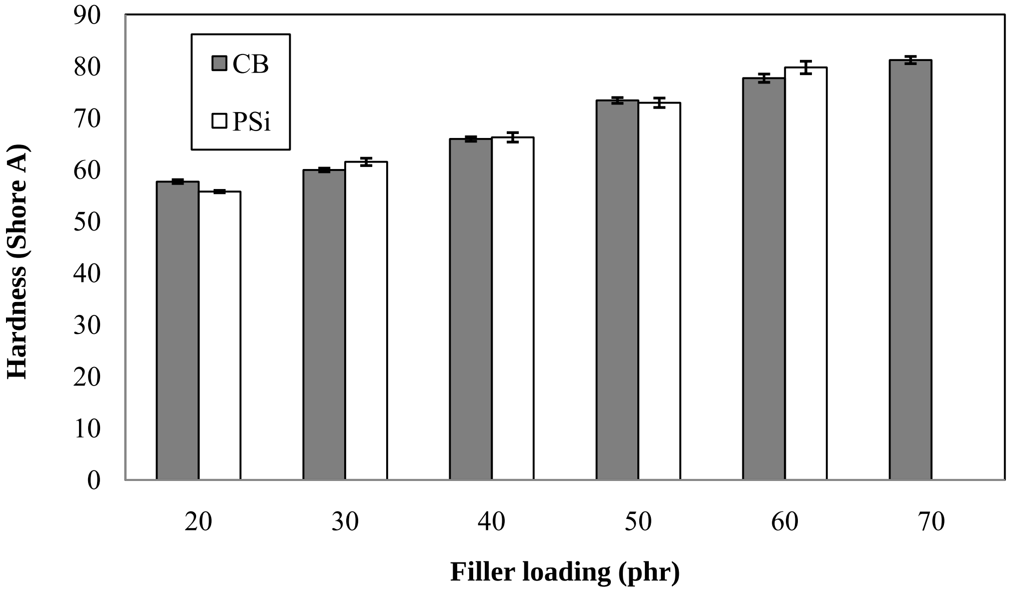

Figure 5.48 Hardness of vulcanizates with various loadings of filler

5.3.4 Tensile properties

Plots of tensile strength and M100 against filler loading are revealed in Figures 5.49 and 5.50, respectively. Tensile strength of CR vulcanizates progressively increases with increasing filler loading and then decreases at the loading beyond 50 phr. In general, there are two main factors thought to be responsible for the results, namely, crosslink density and state-of-mix. The increase in tensile strength is due to the reinforcement effect associated with the increase in crosslink density. At loading beyond 50 phr, the decrease in tensile strength could be due to the excessive crosslink density and/or incomplete filler dispersion leading to the presence of flaws in vulcanizates [6, 16, 28].

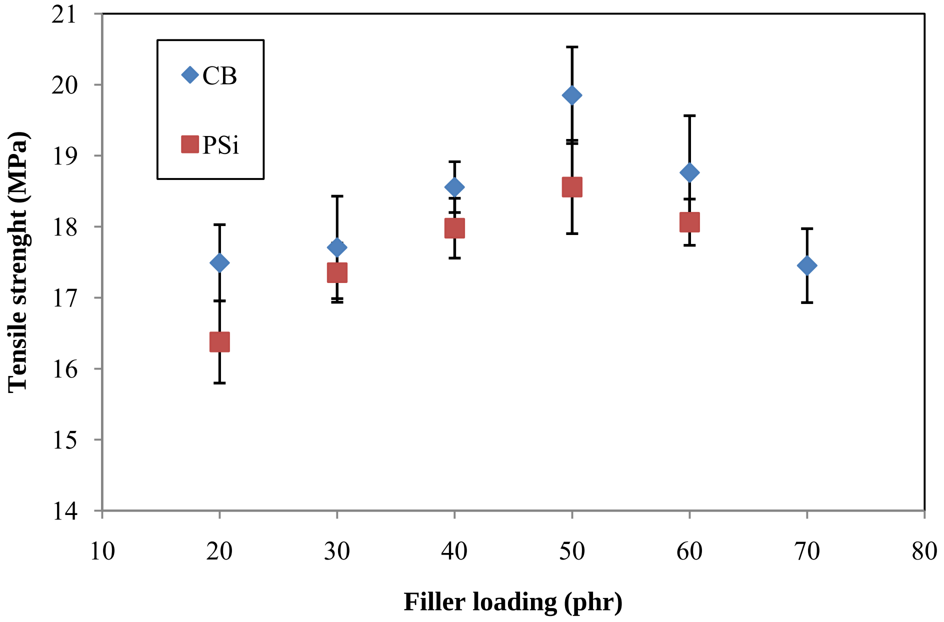

Figure 5.49 Tensile strength of vulcanizates with various loadings of CB and PSi

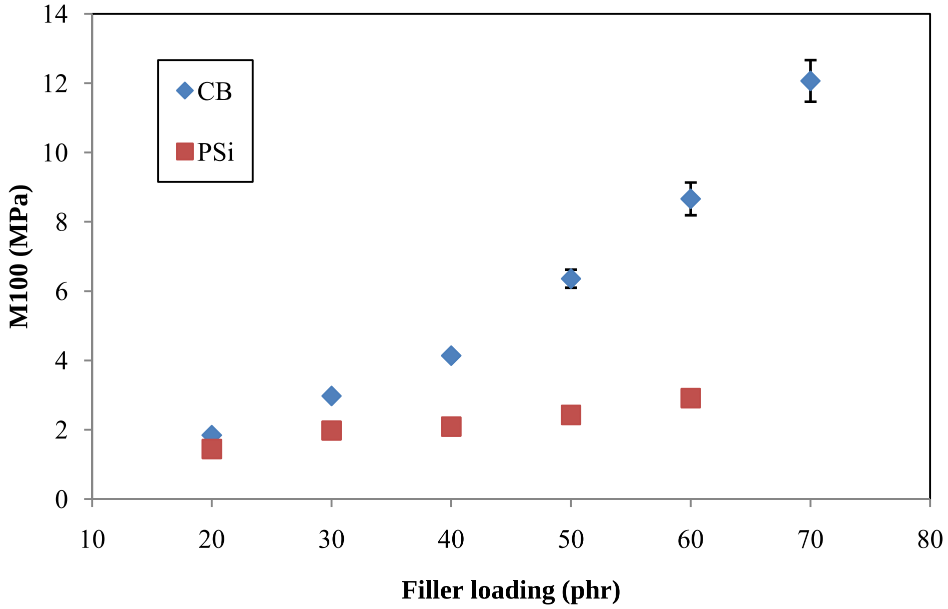

Figure 5.50 Modulus at 100% elongation (M100) of vulcanizates with various filler loadings

The influence of filler loading on the modulus at 100% elongation (M100) is illustrated in Figure 5.50. The magnitude of M100 improvement increases with filler loading, which is more pronounced in the case of CB. Since M100 is measured at large strain of 100%, the effect of pseudo-network (filler transient network) could be disregarded. Thus, the high M100 found in CB-filled CR vulcanizates is probably dominated by the crosslink density as illustrated in the results of swelling test (as shown in Figure 5.41).

5.3.5 Compression set

The dependence of compression set at elevated temperatures of 70 and 100 °C on filler loading is illustrated in Figures 5.51 and 5.52, respectively. The results of crosslink density and compression set of filled CR vulcanizates are not in good agreement. As filler loading increases, both crosslink density and compression set increase. The increment in compression set at high filler loading is believed to be the result of: (i) dilution effect (i.e., the elastic phase of CR is diluted by the undeformable PSi aggregates), (ii) the post-curing effect as discussed previously and (iii) the energy dissipation via molecular relaxation at the rubber-filler interfaces via molecular slippage [76-78].

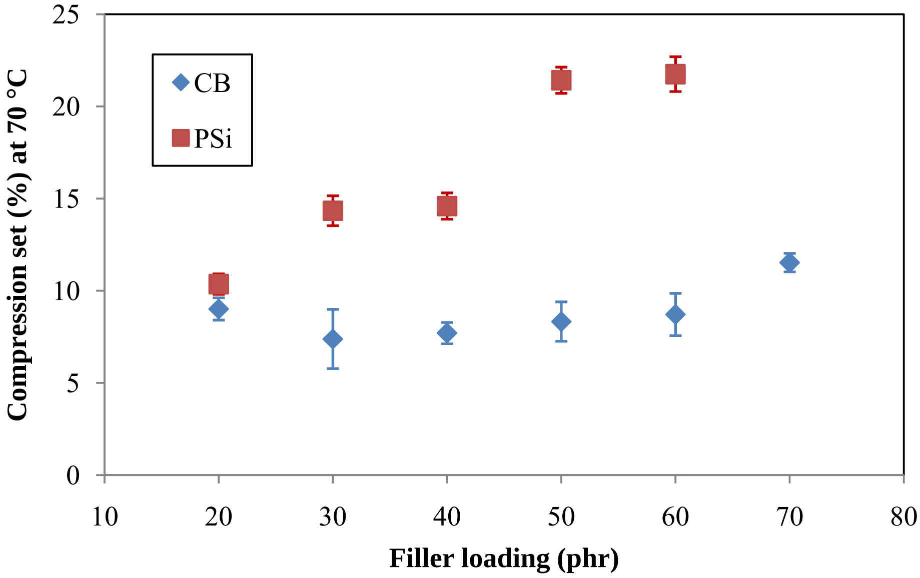

Figure 5.51 Compression set at 70° C of CR vulcanizates with various filler loadings

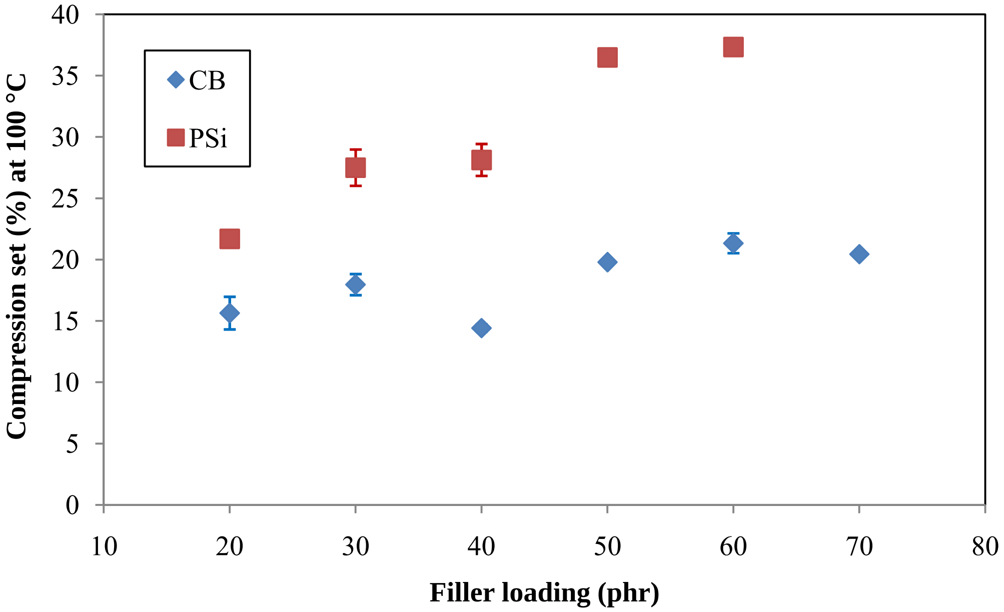

Figure 5.52 Compression set at 100° C of CR vulcanizates with various filler loadings

Furthermore, CR vulcanizates reinforced by PSi possess greater magnitude of compression set than those with CB. Such greater compression set could be attributed to the greater magnitude of post-curing via the development of filler – filler and/or filler – rubber interactions, as shown in Figures 5.53.

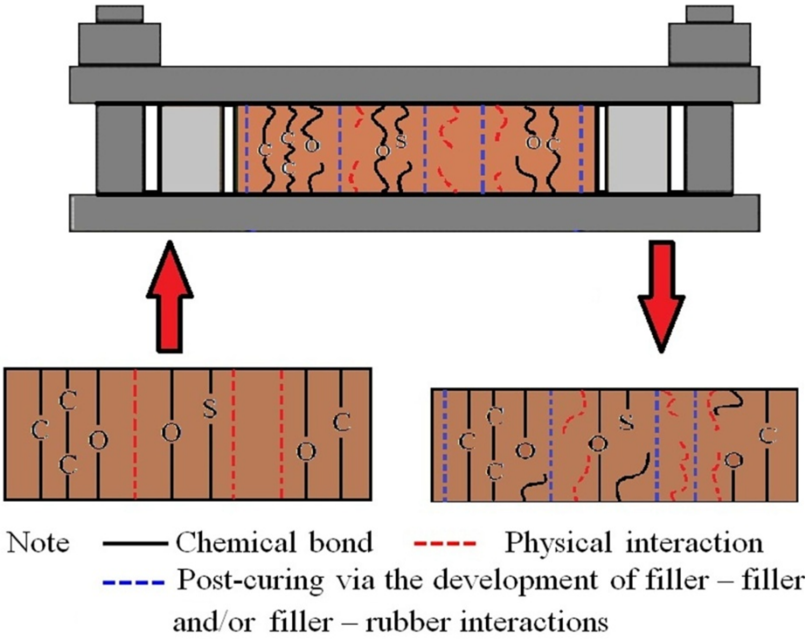

Figure 5.53 Proposed mechanism of post curing effect via the development of filler – filler and/or filler – rubber interactions

5.3.6 Heat build - up (HBU)

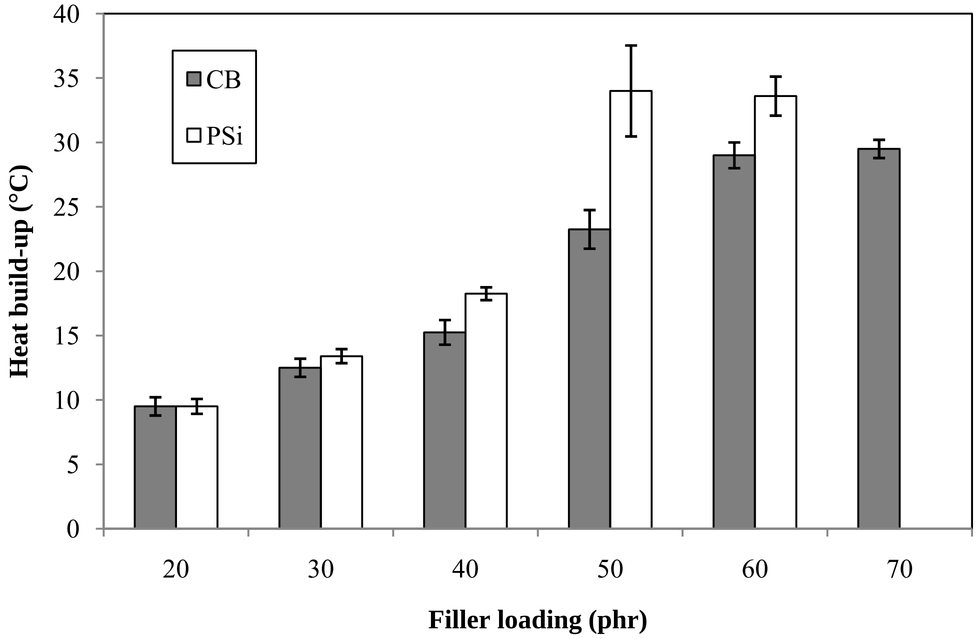

Figure 5.54 Heat build-up (HBU) of CR vulcanizates with various filler loadings

Figure 5.54 represents the effect of filler loading on hysteresis loss of the rubber vulcanizates. Obviously, the HBU is increased by an increase in filler loading. This result could be attributed to the molecular slippage, particularly at rubber-filler interfaces, as discussed previously. Typically, the particles of filler act as centers of energy dissipation [79]. Also, it has been reported that the hysteresis in filled-rubbers is due mainly to the energy dissipation during repeated destruction and reconstruction of the filler network. Upon straining, the filler network is disrupted, and thereafter the polymer molecules rearrange themselves along with the filler particles. These combined processes release energy in the form of heat [73].

5.3.7 Abrasion resistance

Abrasion resistance of CR vulcanizates, expressed as abrasion loss, is presented in Figure 5.55. The abrasion volume loss decreases with increasing filler loading up to 40 and 60 phr of PSi and CB, respectively. Further loading of fillers leads to a reduction of abrasion resistance (or the increment in abrasion loss).

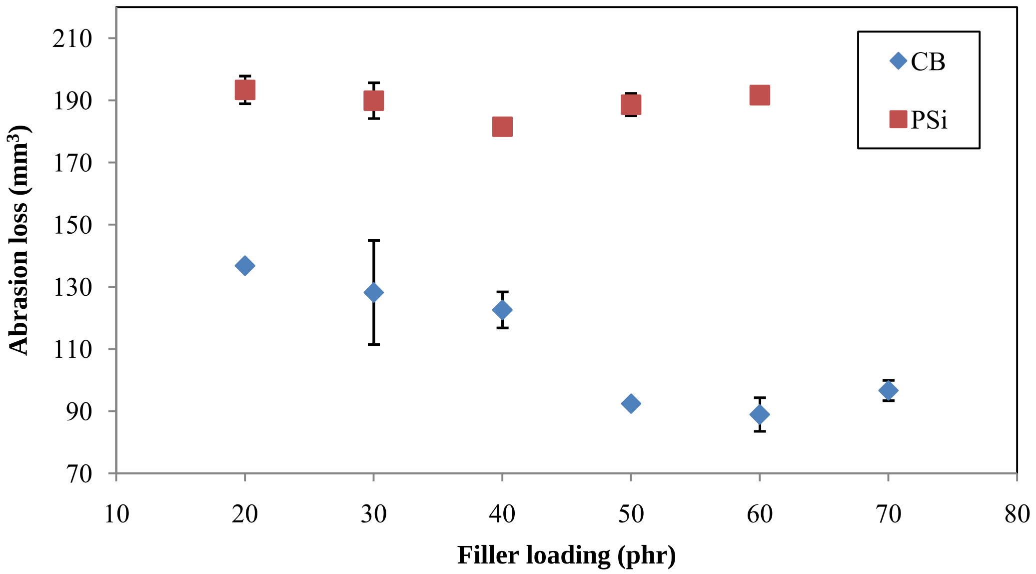

Figure 5.55 Abrasion loss of CR vulcanizates with various filler loadings

The increment of abrasion resistance with increasing filler loading is attributed to the filler reinforcement effect. The reduction of abrasion resistance at high filler loading could be due to the poor filler dispersion or strong filler–filler interaction, especially in the case of PSi [79-80]. Additionally, the decrease in tensile strength at high filler loading (see in Figure 5.49), might be responsible for a local failure and thus a decrease in abrasion resistance.

Compared with PSi at the same loading, CB gives the rubber vulcanizates with higher abrasion resistance. As known well, PSi surface silanols produce a low degree of silica-elastomer bonding, which leads to low abrasion resistance [35]. Moreover, at the same filler loading, the relatively small particle size of PSi might reduce abrasion resistance which is attributed to the increased surfaces available for molecular slippage at PSi surfaces.

5.3.8 Morphology of CR vulcanizates

Figure 5.56 shows the SEM micrographs of unfilled CR vulcanizates with MgO and ZnO at loadings of 4 and 5phr, respectively. It could be observed that the metal oxides are represented by the bright particles (as circled) in the CR matrix.

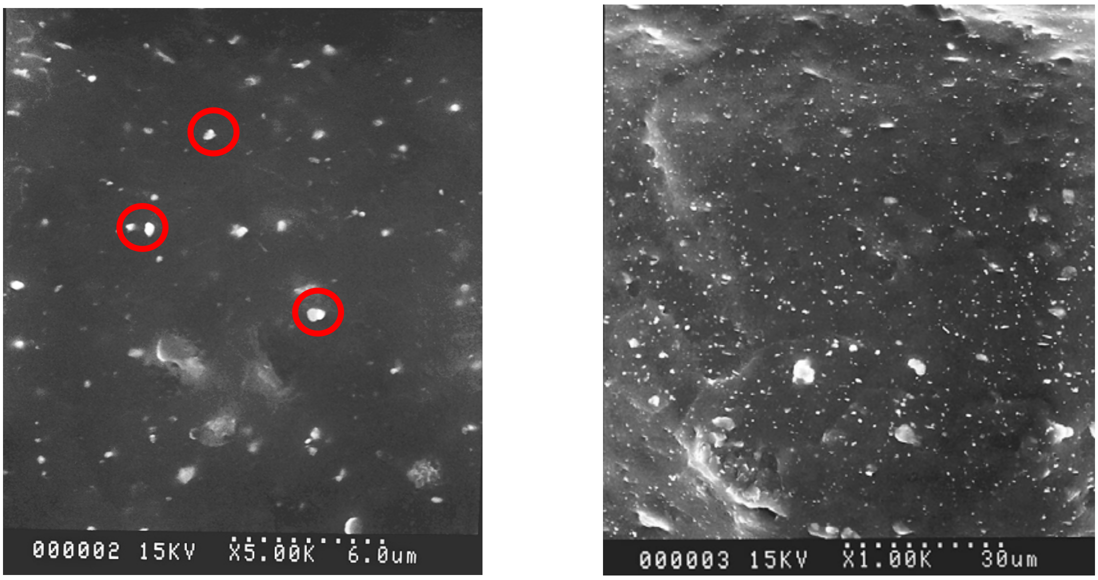

(a) (b)

Figure 5.56 SEM micrographs of the unfilled-filled CR vulcanizates with magnification power of: (a) 5000× and (b) 1000×

SEM micrographs of CR vulcanizates with various loadings of PSi and CB are illustrated in Figures 5.57 and 5.58, respectively. Referred to the unfilled CR vulcanizates (Figure 5.56), the large white particles could be the metal oxides in CR compound while fine particles are believed to be PSi particles. A number of fine particles increase with increasing PSi loading. Furthermore, the degree of PSi dispersion of all specimens is not significantly different.

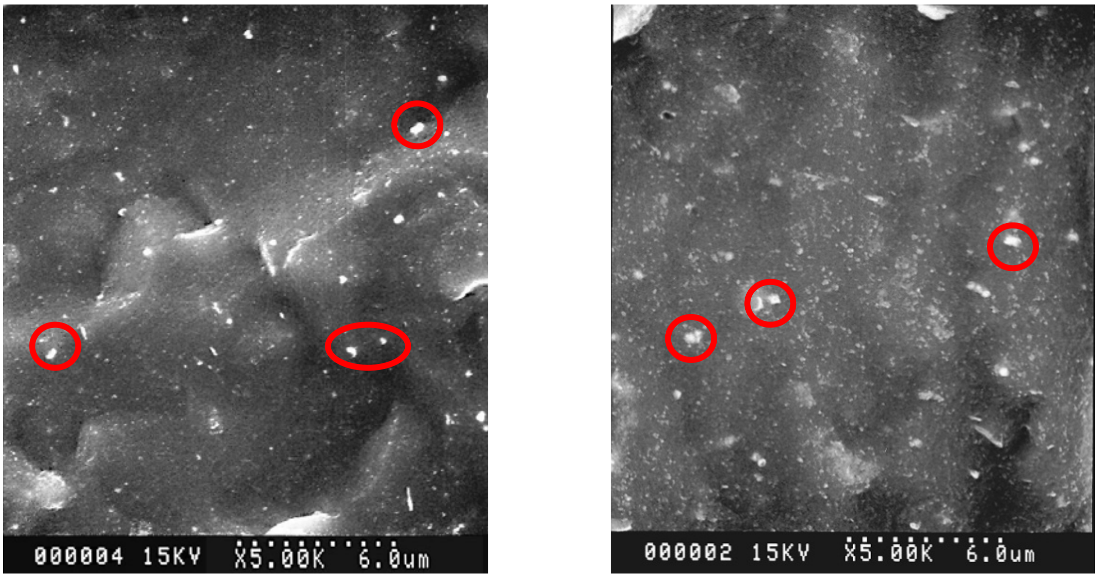

(a) PSi 20 phr (b) PSi 30 phr

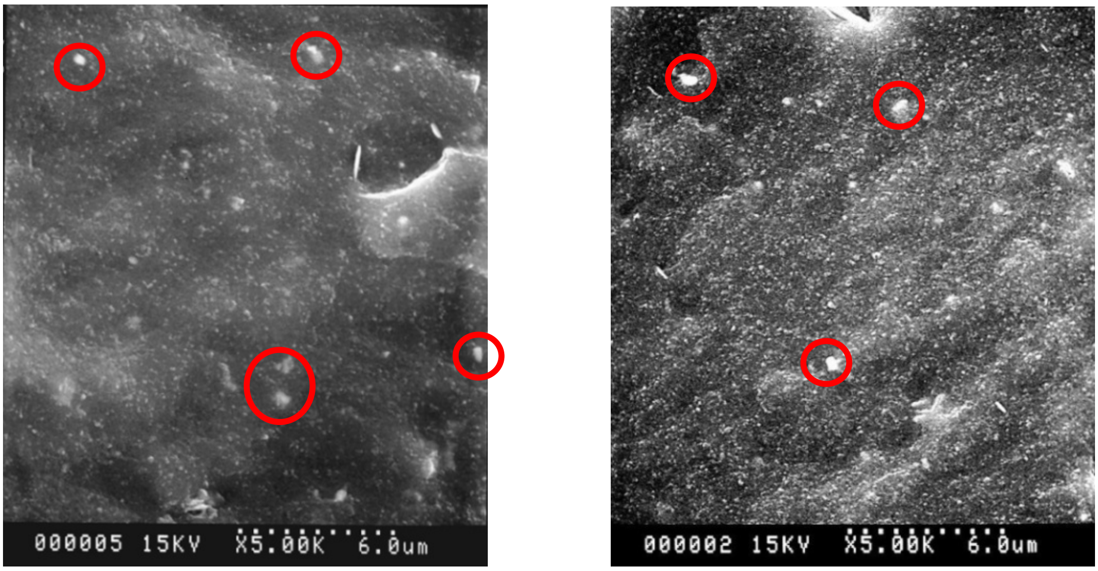

(c) PSi 40 phr (d) PSi 50 phr

Figure 5.57 Morphology of PSi-filled CR vulcanizates with various loadings of PSi

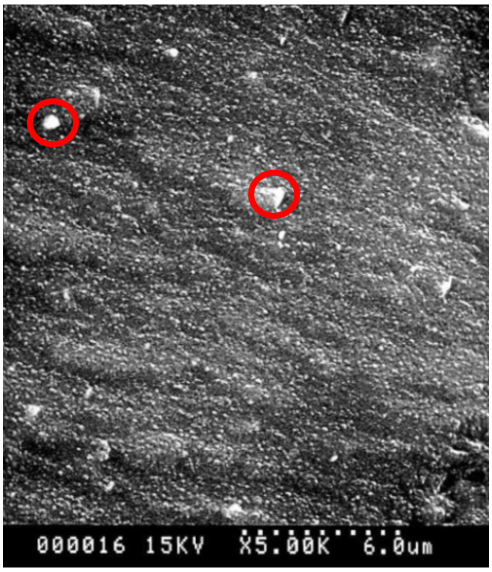

(e) PSi 60 phr

Figure 5.57 Morphology of PSi-filled CR vulcanizates with various loadings of PSi (cont.)

Figure 5.58 illustrates SEM images of CB-filled CR with various loadings of CB. Similar to the case of PSi, large white particles could be the metal oxides, while the fine particles are CB. Also, the degree of CB dispersion of all specimens is not significantly different. Notably, the CB particles dispersed in CR matrix are apparently larger than PSi particles.

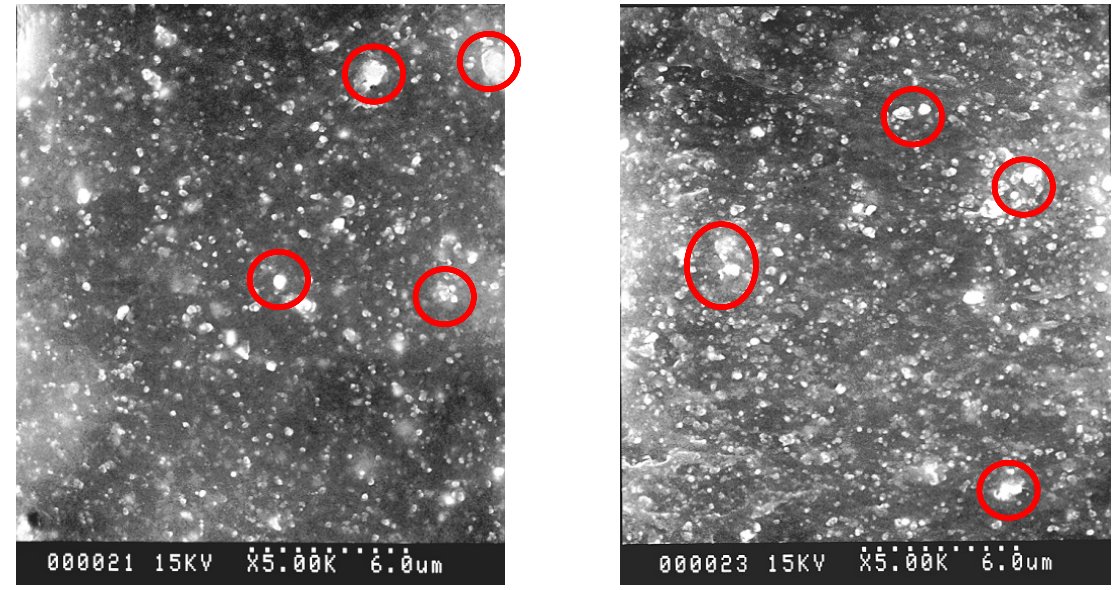

(a) CB 20 phr (b) CB 40 phr

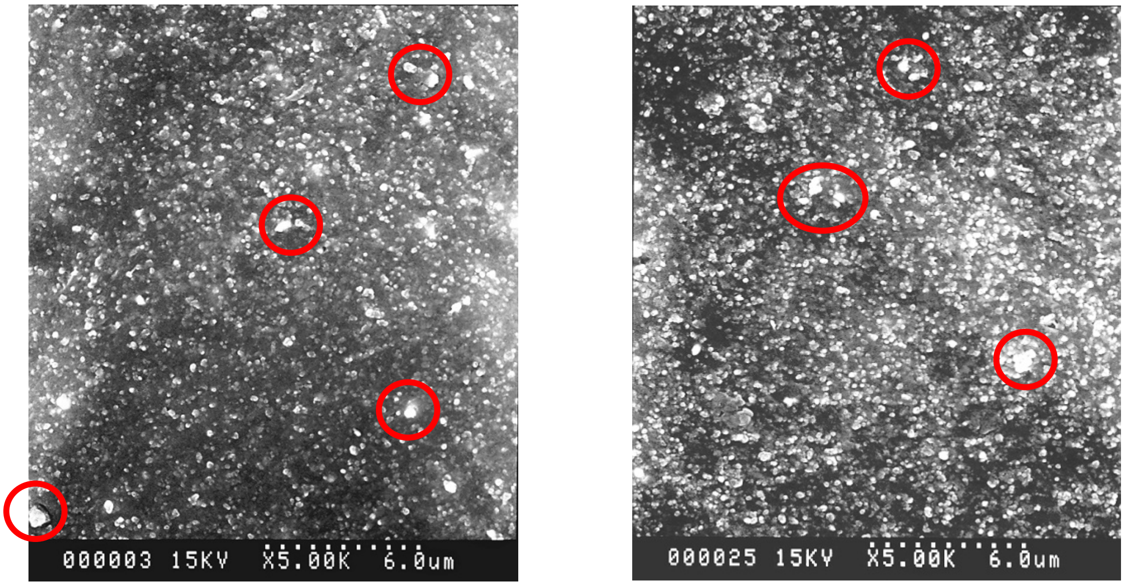

(c) CB 50 phr (d) CB 70 phr

Figure 5.58 Morphology of CB-filled CR vulcanizates with various loadings of CB

5.3.9 Energy dispersive X-ray spectroscopy (EDS)

In order to verify the explanation of metal oxide agglomeration in SEM micrographs, EDS technique is used to determined the elemental composition at the circled area, i.e., the large white particles and the fine spots. The EDS spectrum is revealed in the Figure 5.59.

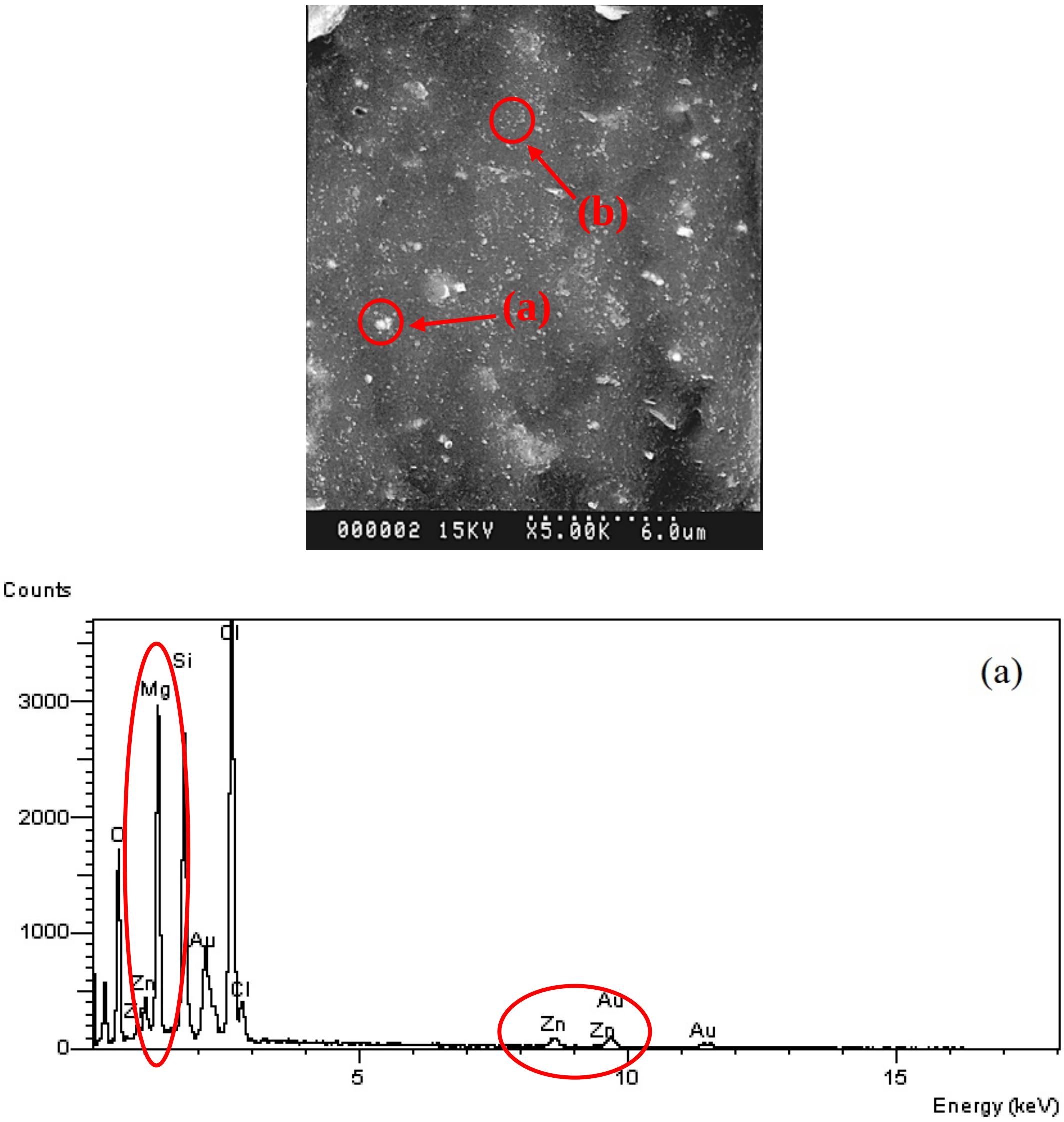

Figure 5.59 SEM micrographs and EDS spectra of PSi-filled CR at the particular area: irregular white particle (a) and no metal oxide area (b)

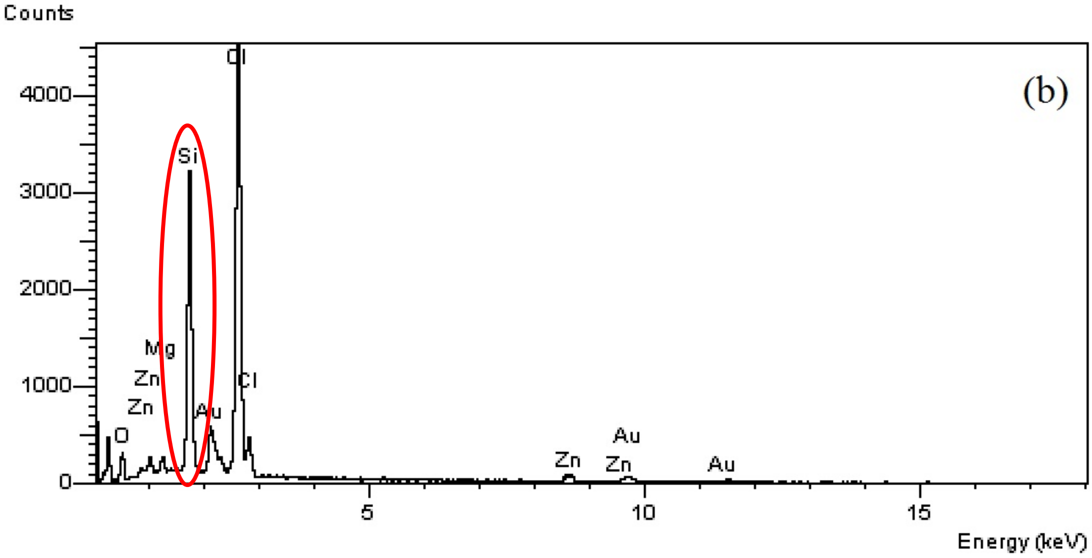

Figure 5.59 SEM micrographs and EDS spectra of PSi-filled CR at the particular area: irregular white particle (a) and no metal oxide area (b) (continued)

Evidently, the EDS spectrum (a) reveals the presence of Mg and Zn in large white particle, especially for MgO. Meanwhile, the EDS spectrum (b) as measured at the area of fine particles shows the high Si peak. This finding supports the SEM results in the previous section. In the case of CB, EDS spectra of CB-filled CR vulcanizates as shown previously (see Figure 5.19) are in good agreement with the SEM images.

5.4 Effect of silane coupling agent (SCA)

As stated elsewhere, the principal functional group found on the polar PSi is silanol (Si-OH) group. The Si-OH is responsible for hydrophilic nature of PSi and thus its unique (versus carbon black) reactivity with water, soluble zinc and other compounding ingredients as well as elastomers [35]. A very important surface modification for PSi has been the treatment by organic silanes to enhance filler-polymer bonding and, thereby, reinforcement.

Although it has been reported that PSi and CR could form strong pseudo-crosslink, i.e., CR could self-crosslink in the sole presence of PSi through the chemical interaction between allylic chlorine atoms and silanol groups [20]. It is therefore interesting to investigate the role of silane coupling agent (SCA) in silica-filled CR compounds. For this purpose, two types of organosilanes with different functional groups are used, bis-(3-triethoxysilylpropyl)tetrasulfane (Si-69,TESPT) and 3-thiocyanatopropyl triethoxy silane (Si-264, TCPTS).

5.4.1 Crosslink density

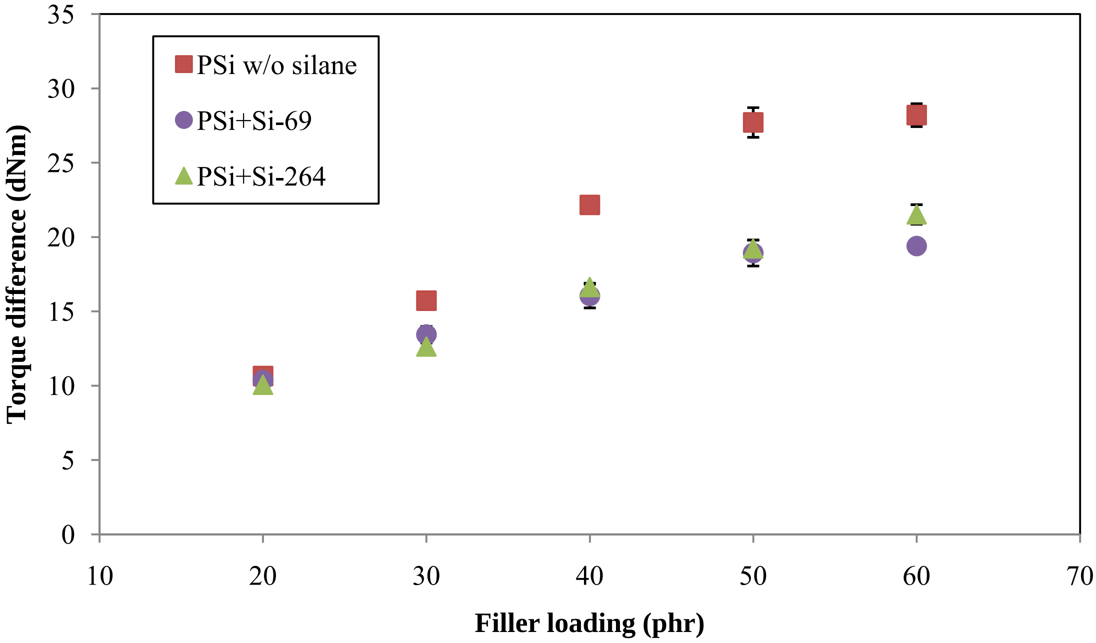

Figure 5.60 Crosslink density as determined from cure torque difference in vulcanizates with various loadings of PSi

The relationship between cure torque difference and amount of PSi loading is illustrated in Figure 5.60. The crosslink density significantly increases with increasing PSi loading, regardless the presence of SCA. The rise of crosslink density could be attributed to the greater of filler-rubber and/or filler-filler interaction. Likewise, compared with the crosslink density in non-silane system, PSi-filled CR vulcanizates which treated with SCA have lower degree of crosslink density. The decrement in crosslink density might be due to the reduction in availability of silanol group required for the formation of pseudo-crosslink [73].

In order to support the findings in Figure 5.60, the crosslink density is measured by swelling technique based on the Flory-Rehner concept. The results obtained are shown in Figure 5.61.

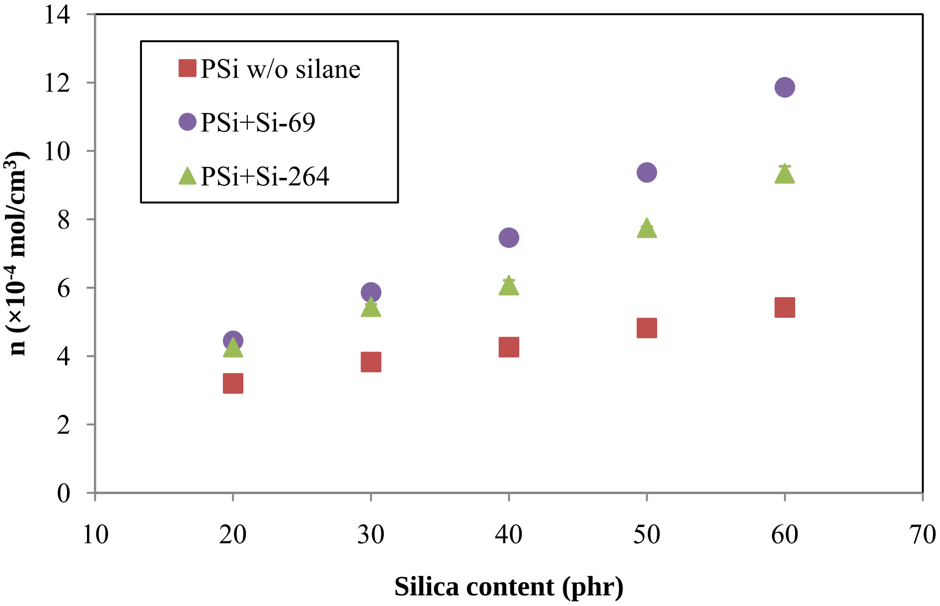

Figure 5.61 Crosslink density as determined from Flory – Rehner equation in vulcanizates with various loadings of PSi

It could be noticed that the crosslink density of CR vulcanizates increases with increasing PSi loading, regardless of the presence of SCA. The results are in good agreement with that determined from cure torque difference. On the other hand, there is the result contradiction in which the crosslink density in vulcanizates with SCA treatment appears to be greater when measured from the swelling technique. The explanation of such disagreement is proposed as follows:

Under the swelling test, the penetration of solvent might inhibit the pseudo-crosslink formation, and therefore only the chemically linkage is responsible for the swelling behavior of CR vulcanizates. The vulcanizates with SCA treatment would reveal lower magnitude of cure retardation usually found in PSi-filled rubber system [81]. Furthermore, it is known well that the polar surface of PSi could interact with soluble zinc and curatives which are the major influence on the low cure states (reduced crosslinking) [35]. The presence of SCA reduces the polar surface interacting with soluble zinc. Thus, CR vulcanizates with SCA have the greater amount of crosslink density than that without SCZ.

Also, the Si-69 silane reveals greater crosslink density due to the release of free sulfur during the vulcanization process [69-70]. This phenomenon is sometimes known as the “sulfur contribution effect” [48, 69-70]. Such effect is not found in the case of Si-264 silane.

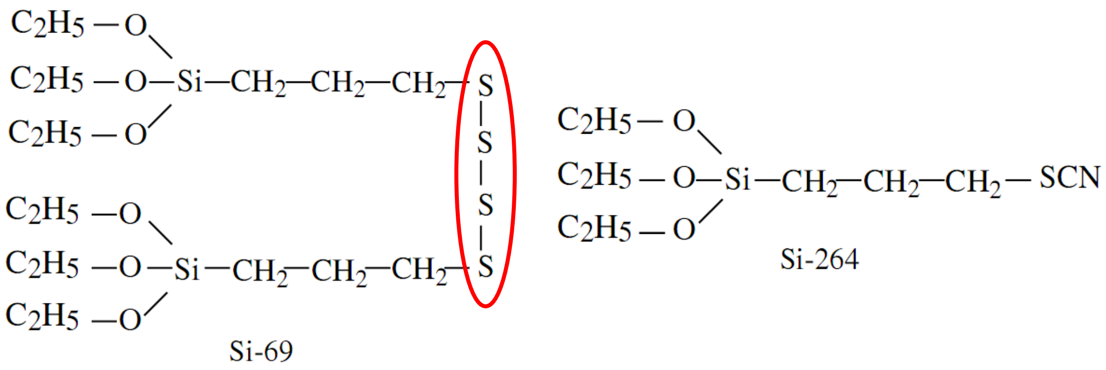

Figure 5.62 Chemical structures of Si-69 and Si-264

5.4.2 Strain sweep test

It is well known that the Payne effect can be used to explain the reinforcement mechanism of filled rubber. As mentioned previously, factors affecting dynamic modulus of filled blends include polymer network properties, hydrodynamic effect, filler-rubber structure and filler-filler interaction. From the previous section, it is evident that the experimental results of relative modulus (relative G′) at low strain are much higher than the calculated results, especially in the case of PSi-filled CR. Results indicate that PSi-filled CR compound provides a superior filler-filler interaction and/or filler-rubber interaction. Thus, in this present study, the roles of two SCAs, i.e., bis-(3-triethoxysilylpropyl) tetrasulfane (Si-69) and 3- thiocyanatopropyl triethoxy silane (Si-264), commonly used in rubber applications were studied to verify their reinforcing efficiency in CR compounds.

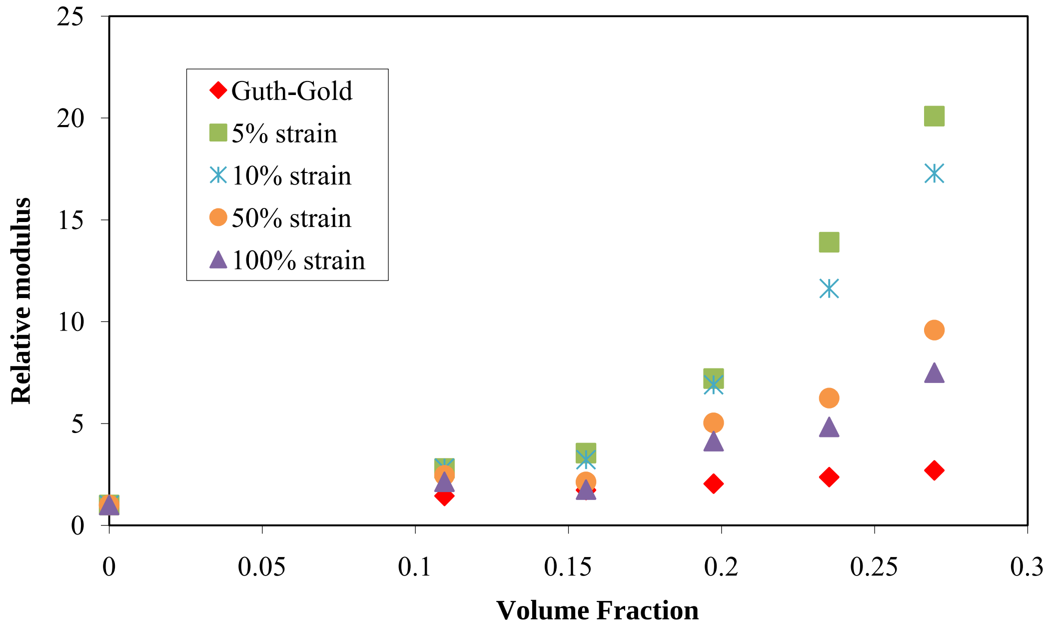

Figure 5.63 Relative elastic modulus (relative G′) at 5, 10, 50 and 100 % strain of PSi-filled CR compounds with Si-69 as a function of PSi volume fraction

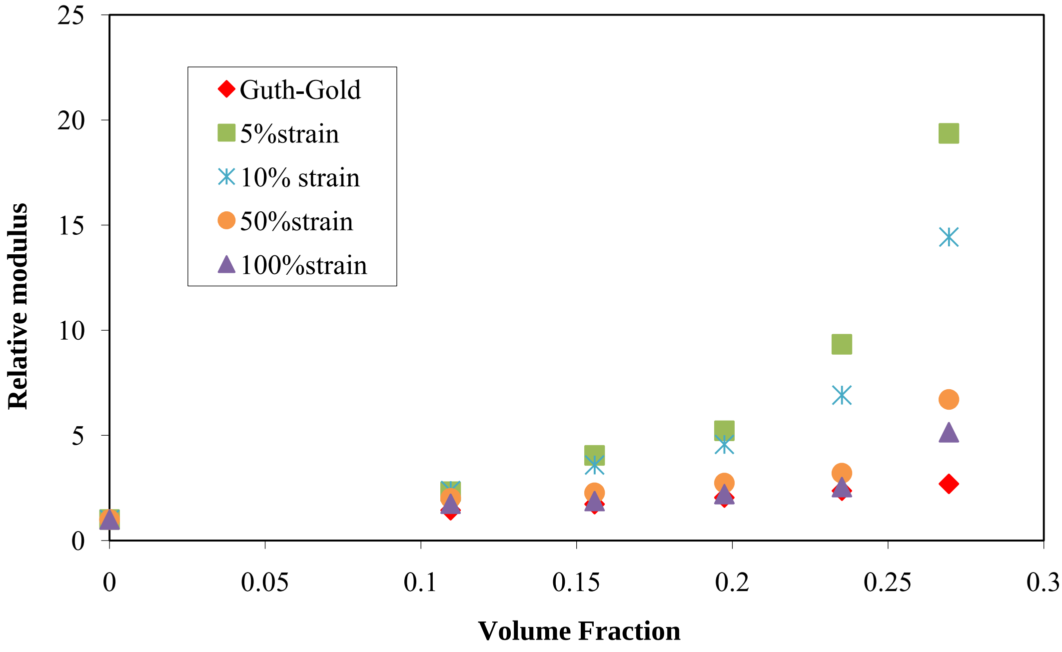

Figure 5.64 Relative elastic modulus (relative G′) at 5, 10, 50 and 100 % strain of PSi-filled CR compounds with Si-264 as a function of PSi volume fraction

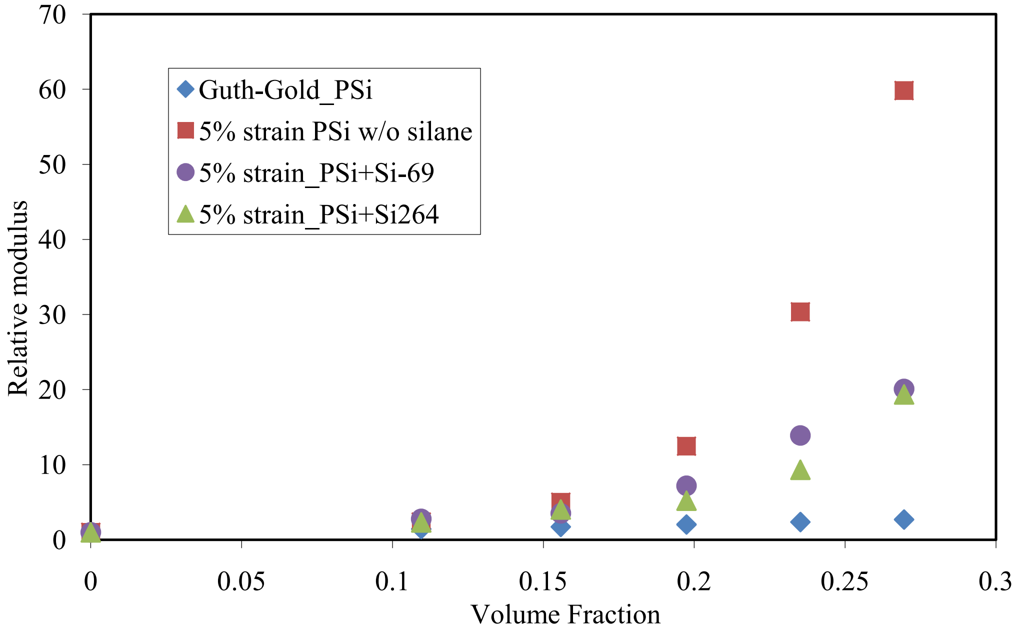

Figure 5.65 Guth-Gold equation and relative elastic modulus (relative G′) at 5% strain of PSi-filled CR compounds with and without SCA as a function of PSi volume fraction

Figures 5.63-5.65 show the relative modulus calculated from the Guth-Gold equation. It is apparent that the experimental results of relative modulus (relative G′) at low strain are much higher than the calculated results, regardless of the presence of SCA. Nevertheless, the presence of SCA leads to the lower magnitude of the relative modulus at low strain of 5% strain (as illustrated in Figure 5.69). Results indicate the reduction of filler network and/or filler-rubber interaction which is caused by the addition of SCA. In order to prove this statement, the SEM micrograph of PSi-CR is carried out.

The SEM micrographs of CR vulcanizates filled with PSi treated with Si-69 and Si-264 are illustrated in Figures 5.66 and 5.67, respectively. The micrograph of unfilled CR vulcanizates as a reference reveals white particles of metal oxide in CR compound (as remarked by the circles). The fine particles are PSi particles with SCA treatment. Evidently, the PSi-filled CR with SCA treatment provides the greater degree of filler dispersion. This implied that the SCA has a significant role in reduction of filler-filler interaction in PSi-filled CR compounds. Furthermore, the degree of PSi dispersion of both silane systems is not significantly different.

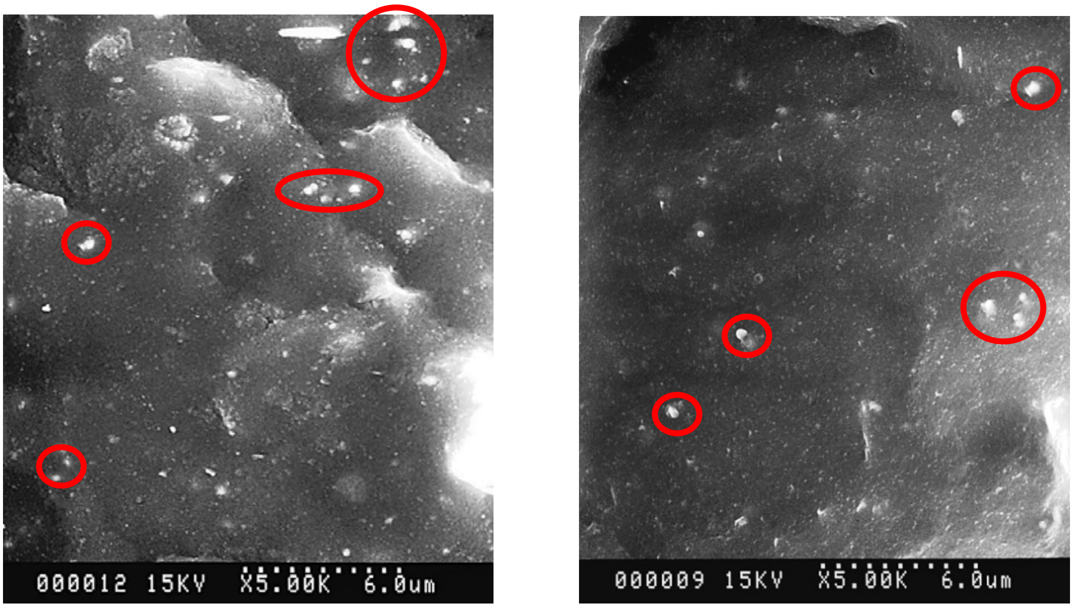

(a) PSi 20 phr with Si-69 (b) PSi 30 phr with Si-69

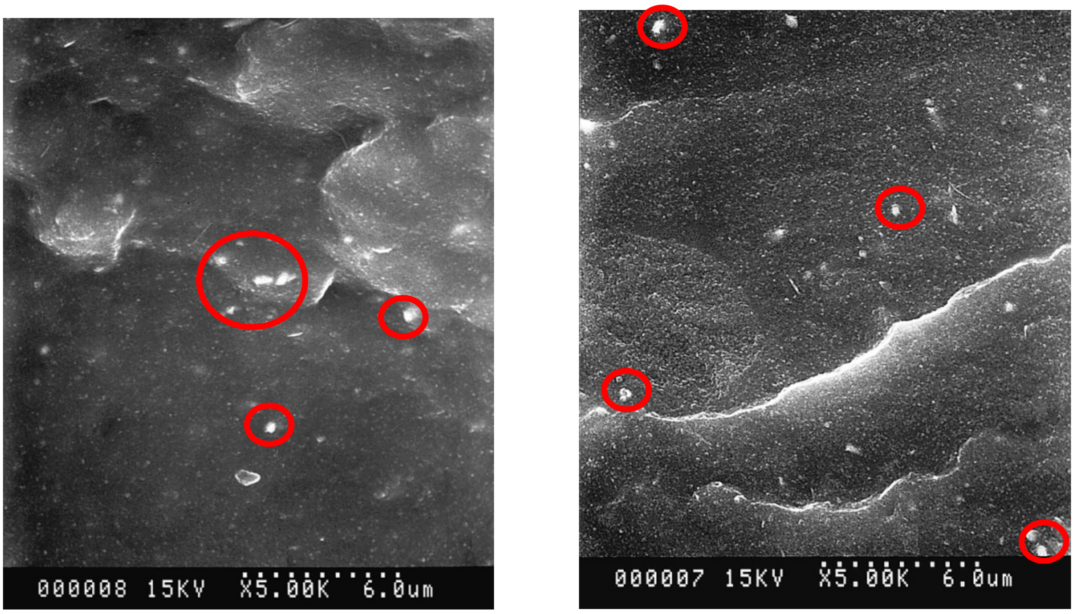

(c) PSi 40 phr with Si-69 (d) PSi 50 phr with Si-69

Figure 5.66 SEM micrographs (×5000) of the PSi-filled CR vulcanizates Si-69

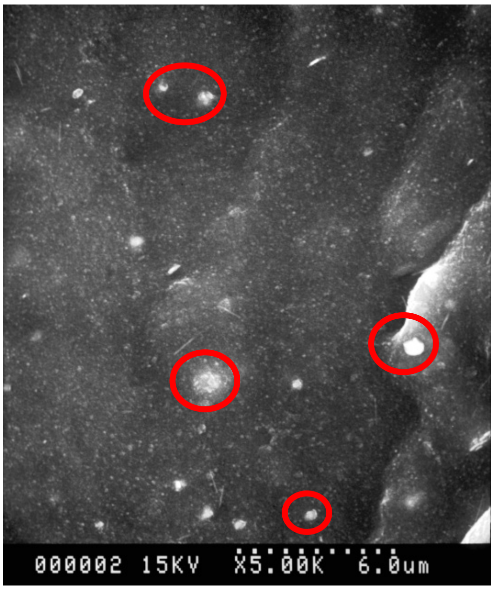

(e) PSi 60 phr with Si-69

Figure 5.66 SEM micrographs (×5000) of the PSi-filled CR vulcanizates Si-69 (cont.)

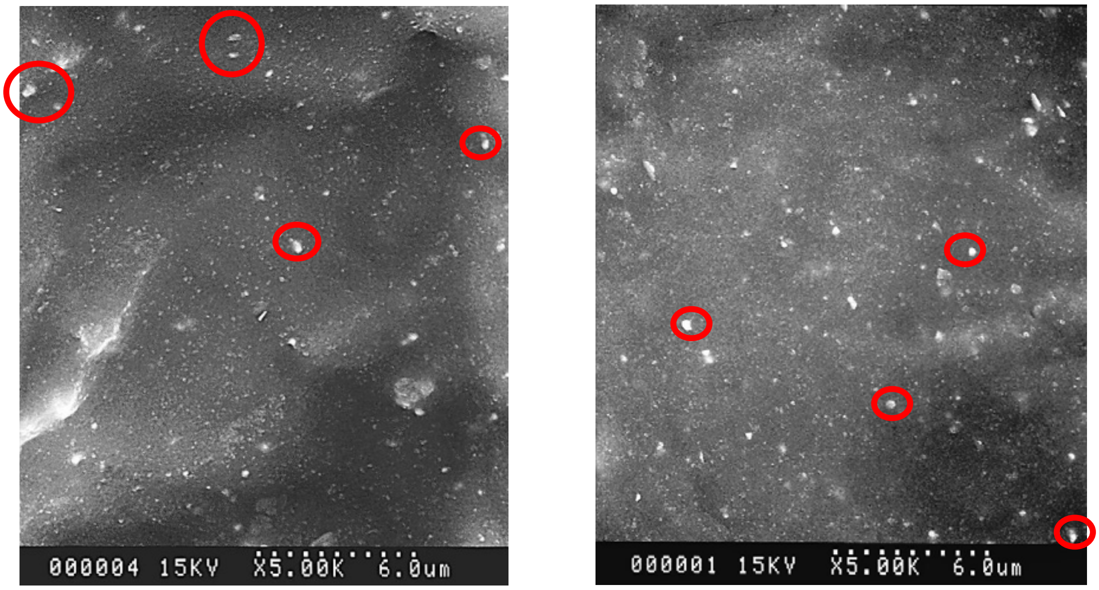

(a) PSi 20 phr with Si-264

(b) PSi 30 phr with Si-264

Figure 5.67 SEM micrographs (×5000) of the PSi-filled CR vulcanizates Si-264

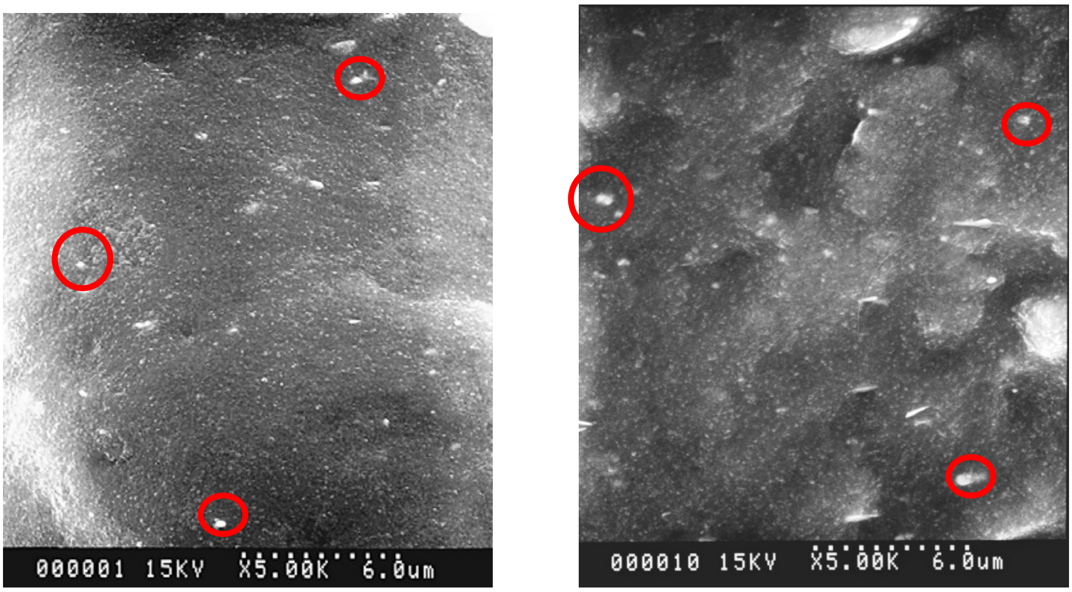

(c) PSi 40 phr with Si-264

(d) PSi 50 phr with Si-264

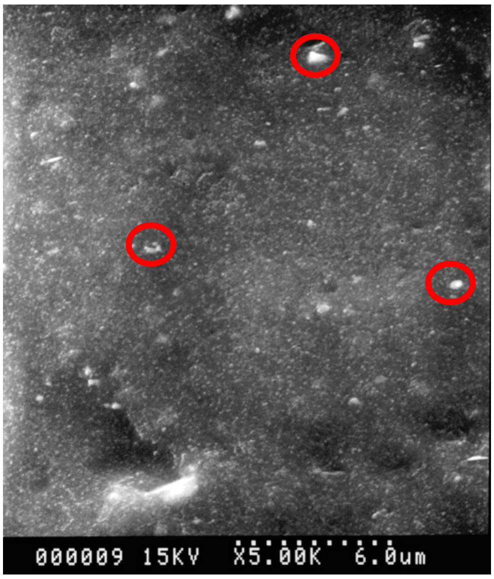

(e) PSi 60 phr with Si-264

Figure 5.67 SEM micrographs (×5000) of the PSi-filled CR vulcanizates Si-264 (cont.)

5.4.3 Energy dispersive X-ray spectroscopy (EDS)

To verify the presumption from SEM images, EDS technique was performed at the circled areas. EDS spectra of PSi-filled CR vulcanizates with Si-69 and Si-264 treatment are shown in Figures 5.68 and 5.69, respectively.

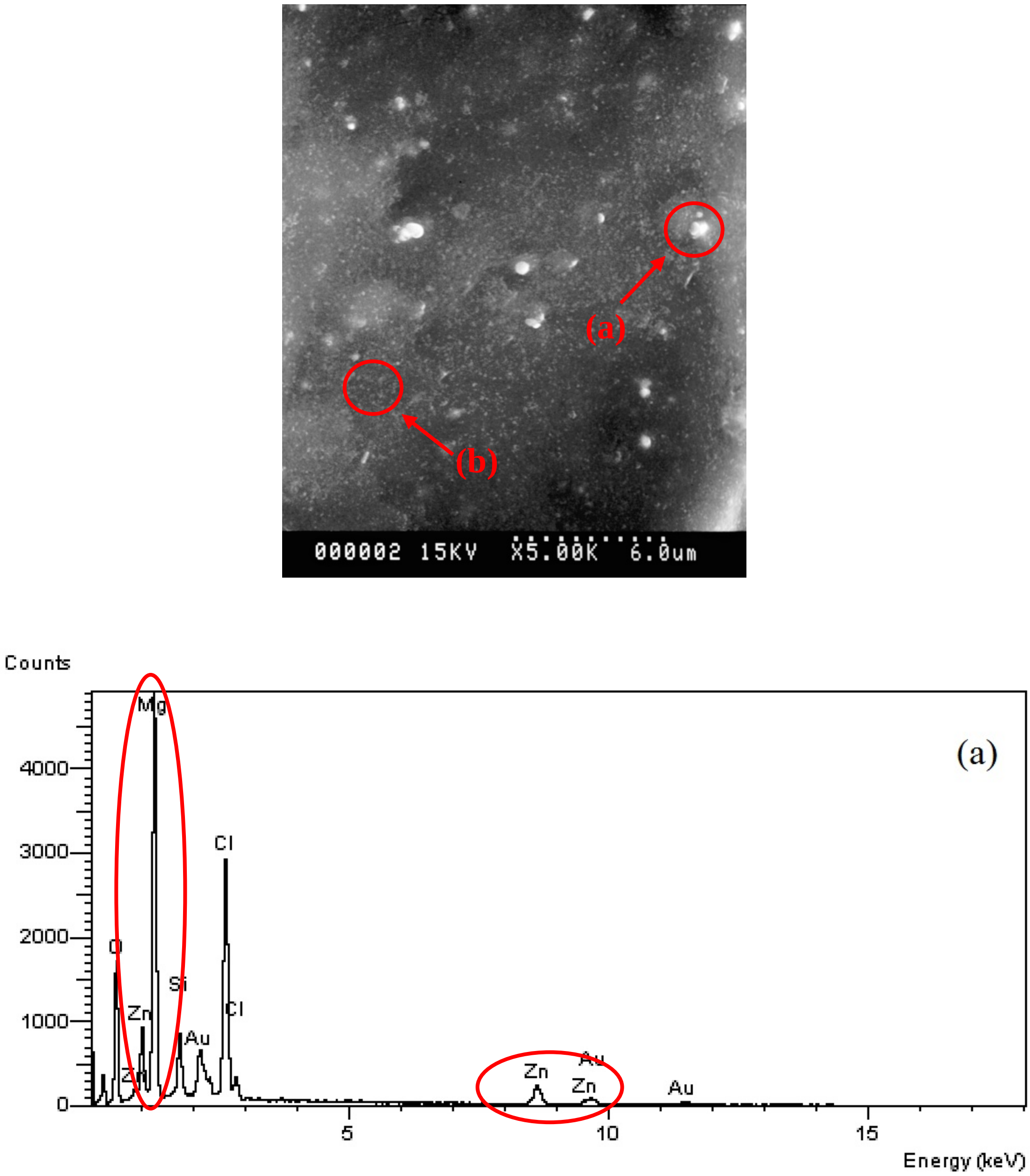

Figure 5.68 SEM images and corresponding EDS spectra of PSi-filled CR vulcanizates with Si-69 treatment at areas "a" and "b" as circled

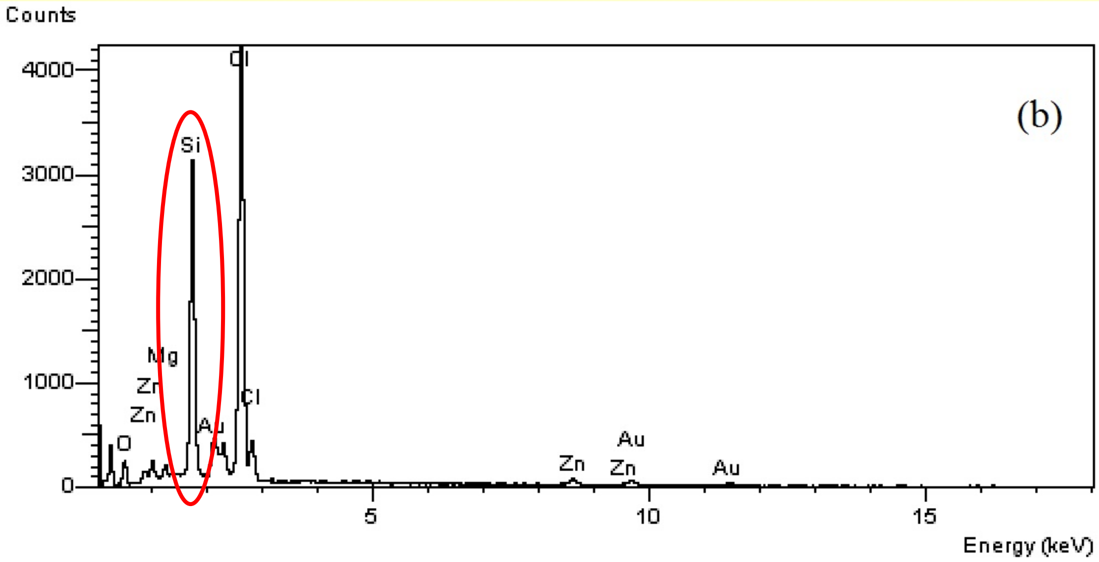

Figure 5.68 SEM images and corresponding EDS spectra of PSi-filled CR vulcanizates with Si-69 treatment at areas "a" and "b" as circled (cont.)

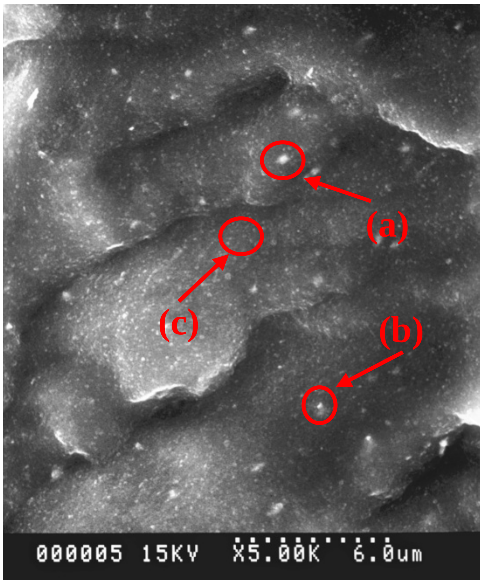

Figure 5.69 SEM images and corresponding EDS spectra of PSi-filled CR vulcanizates with Si-264 treatment at areas "a" and "b" as circled

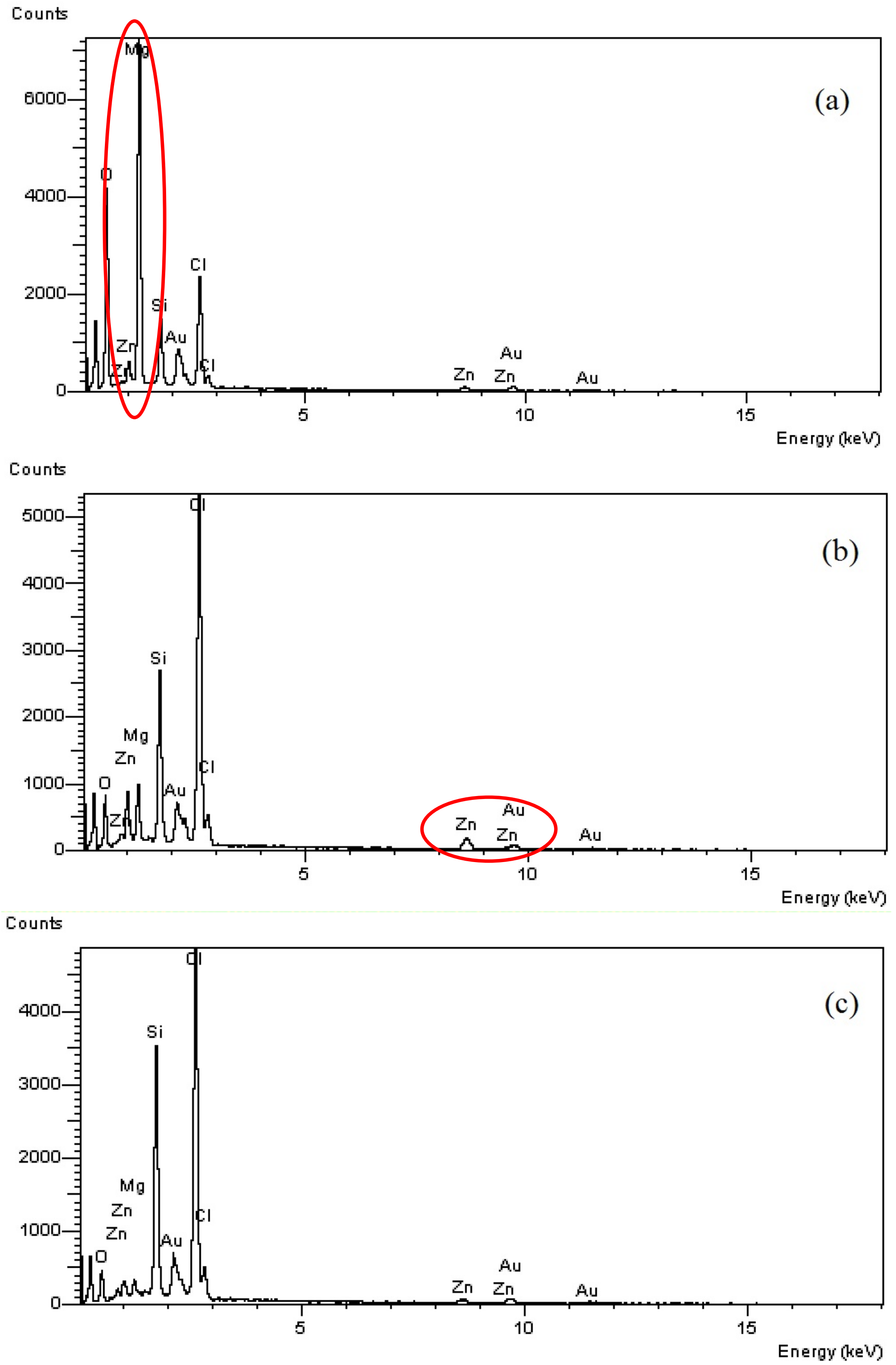

Figure 5.69 SEM images and corresponding EDS spectra of PSi-filled CR vulcanizates with Si-264 treatment at areas “a” and “b” as circled (cont.)

The characteristics of either Mg or Zn elements are shown in Figure 5.68a, 5.69a and 5.69b. Results indicated the accordance between both metal oxide and the big white particles in SEM micrographs. Meanwhile, the fine particles could be the PSi particles which are supported by EDS spectrum as shown in Figure 5.68b and 5.69c. This finding confirms the assumption in SEM micrographs in the previous section.

5.4.4 Hardness

Plots of hardness against filler loading are revealed in Figure 5.70. The results reveal that the hardness of CR vulcanizates is increased by increasing amount of filler due to the pseudo-crosslink formation and/or filler reinforcement effect as discussed previously.

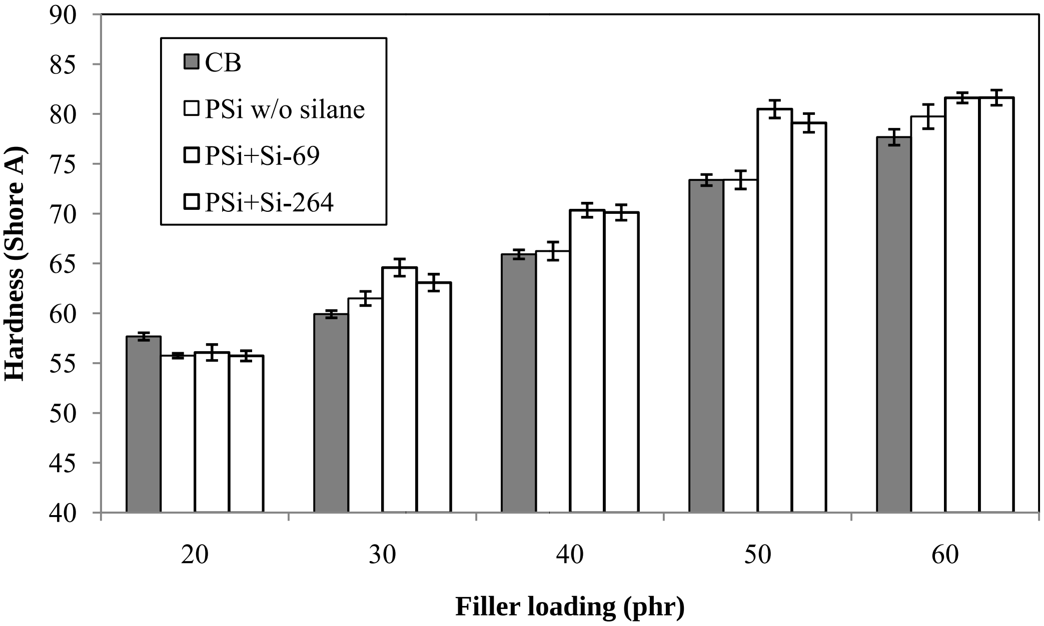

Figure 5.70 Hardness of CR vulcanizates with various loadings of filler

However, the presence of SCA improves significantly the hardness of the CR vulcanizates. The improvement could be explained in terms of the enhancement in rubber-filler interaction. The alkoxy groups in SCA could react chemically with the silanol groups on silica surfaces, giving rise to the reduction of filler-filler interaction

[48]. Apart from the improvement in rubber-filler interaction, the increment in crosslink density (as shown in Figure 5.61) could enhance the mechanical properties of CR vulcanizates. Thus, the improvement in hardness of CR vulcanizates with SCA treatment could be attributed to the combined effect of improved filler dispersion, increased state of cure and enhanced rubber–filler interaction.

5.4.5 Tensile properties

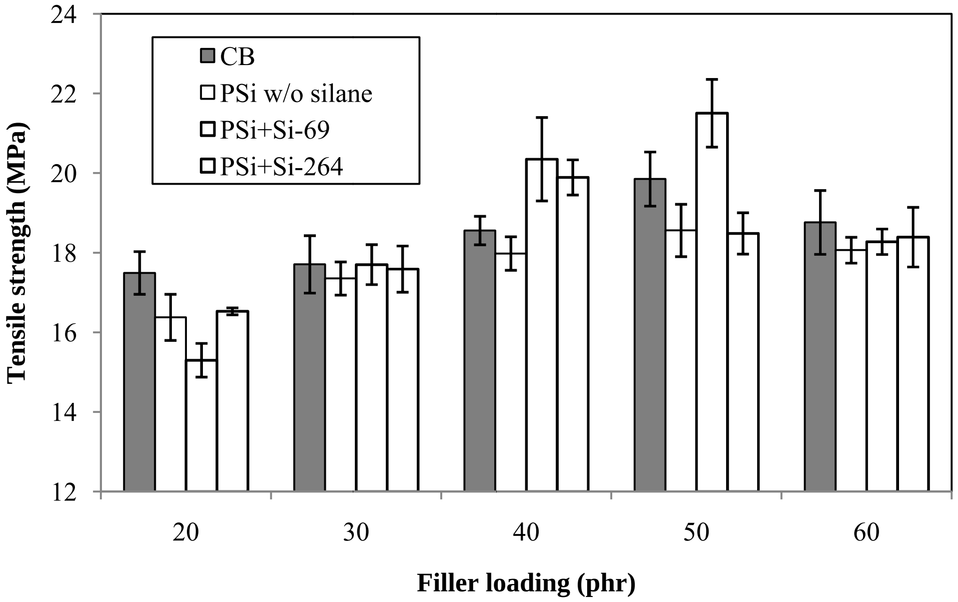

Figure 5.71 Tensile strength of vulcanizates with various loadings of filler

The effect of SCA on tensile properties of the PSi-filled CR vulcanizates was also investigated, and the results are given in Figures 5.71-5.72. The addition of SCA could enhance the tensile strength of PSi-filled CR vulcanizates. The improvement in tensile strength in the presence of SCA is thought to arise mainly from the improved filler dispersion associated with the improved filler-rubber interaction. Furthermore, the decrement of tensile strength at high filler loading, regardless of silanol surface treatment of PSi, could be explained by the excessive crosslink density in conjunction with decreased degree of filler dispersion.

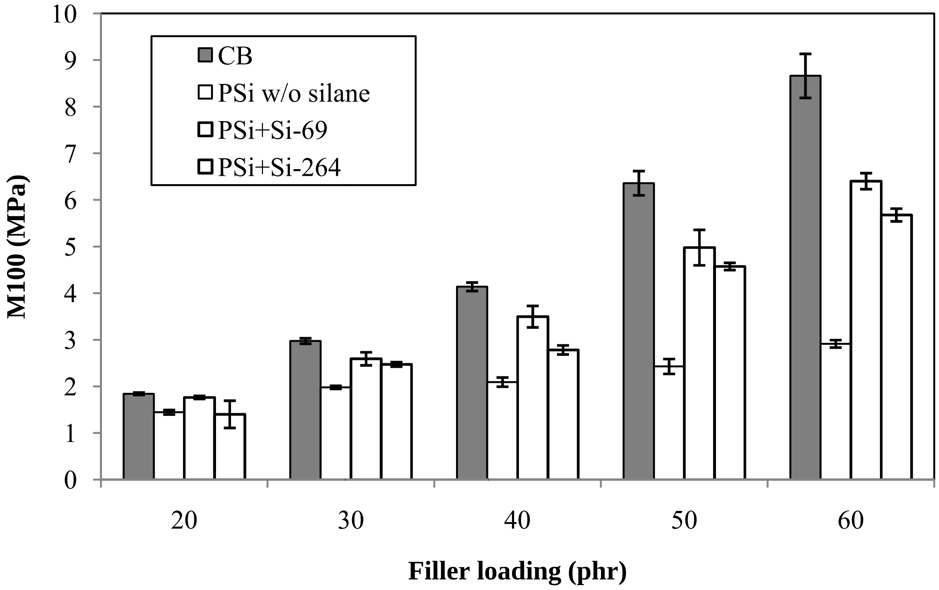

Figure 5.72 Modulus at 100% elongation (M100) of vulcanizates with various filler loadings

The influence of SCA on modulus at 100% elongation (M100) is revealed in Figure 5.72. As it is widely known that the modulus of the rubber vulcanizate is directly proportional to crosslink density, the results of M100 therefore could partly be due to the crosslink density as determined from Flory-Rehner equation, as shown in Figure 5.73. The development of M100 with the presence of SCA could also be attributed to the greater magnitude of filler-rubber interaction. Compared with Si-264 at any given PSi loading, the Si-69 gives the rubber vulcanizates with higher M100 due to the greater crosslink density.

However, compared with PSi system regardless the presences of SCA, CB-filled vulcanizates offer the greater magnitude of M100. This could be attributed to the higher degree of crosslink density in CB-filled CR vulcanizates, as evidenced in Figure 5.73.

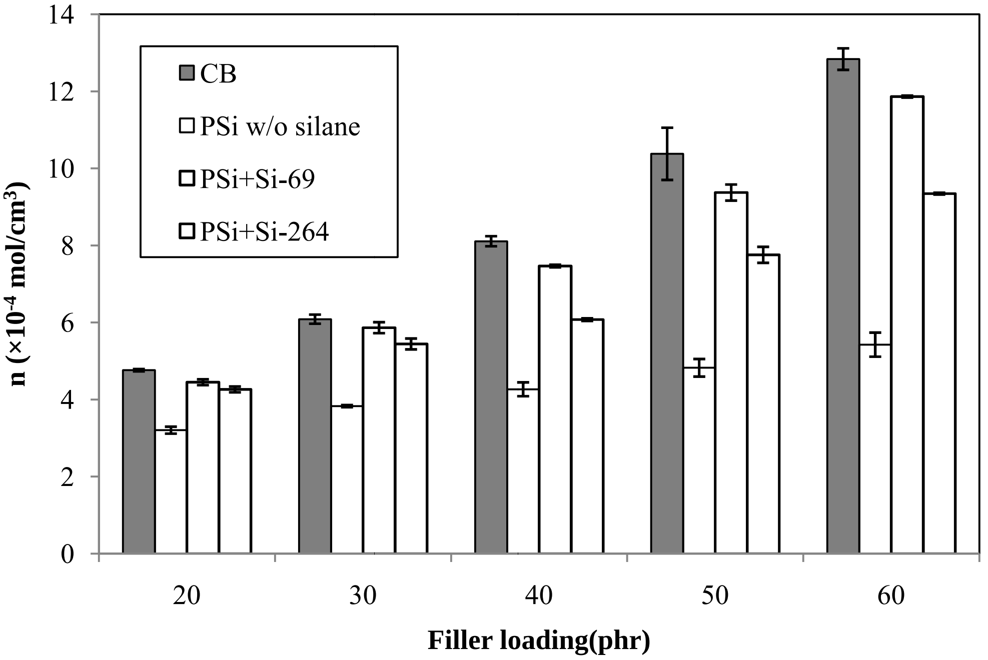

Figure 5.73 Crosslink density which determined from Flory-Rehner equation of CR vulcanizates with various loadings of filler

5.4.6 Compression set

The effect of SCA on compression set at elevated temperature is illustrated in Figures 5.74 and 5.75. Regardless of the SCA type, the compression set is noticeably decreased in both types, compared with the vulcanizates without silane, especially at high test temperature and/or high PSi loading. The improvement in compression set with the presence of SCA is thought to arise mainly from the enchantment in the state-of-mix, state-of-cure, and filler-rubber interaction.

It is noticeable that the Si-69 silane offers vulcanizates with lower compression set at 70°C than that Si-264. At elevated temperature of 100°C, Si-69 demonstrates the similar compression set to Si-264. Again, the explanation mainly goes to the de-sulfuration, as mentioned previously (section 5.2.6). In other words, at elevated temperature, the sulfidic linkage could breakdown, giving the vulcanizates with poorer thermal aging resistance and, thus, poorer compression set at elevated temperature, compared to Si-264.

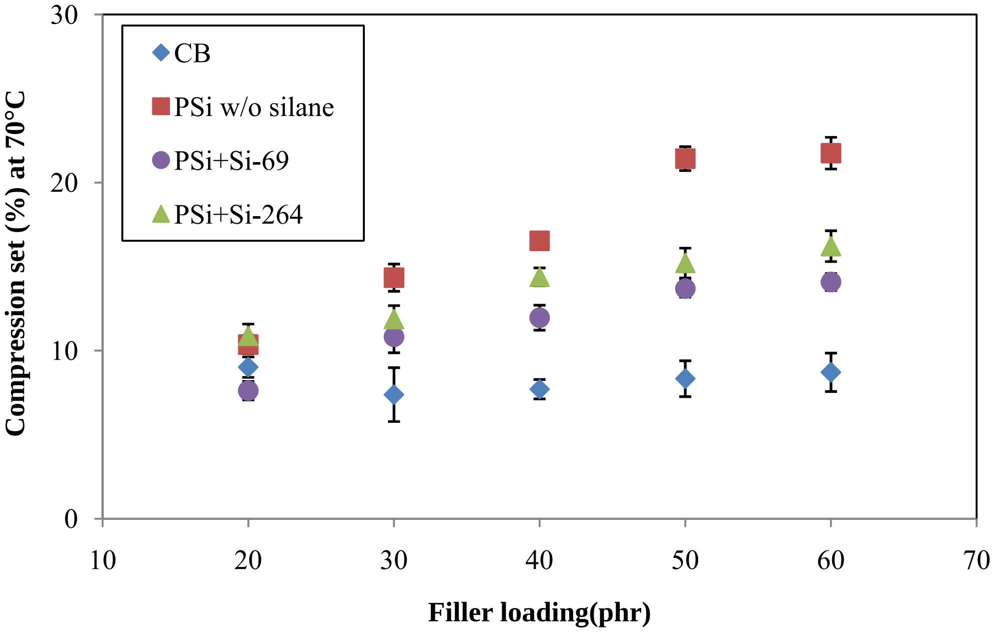

Figure 5.74 %Compression at 70°C of CR vulcanizates with various filler loadings

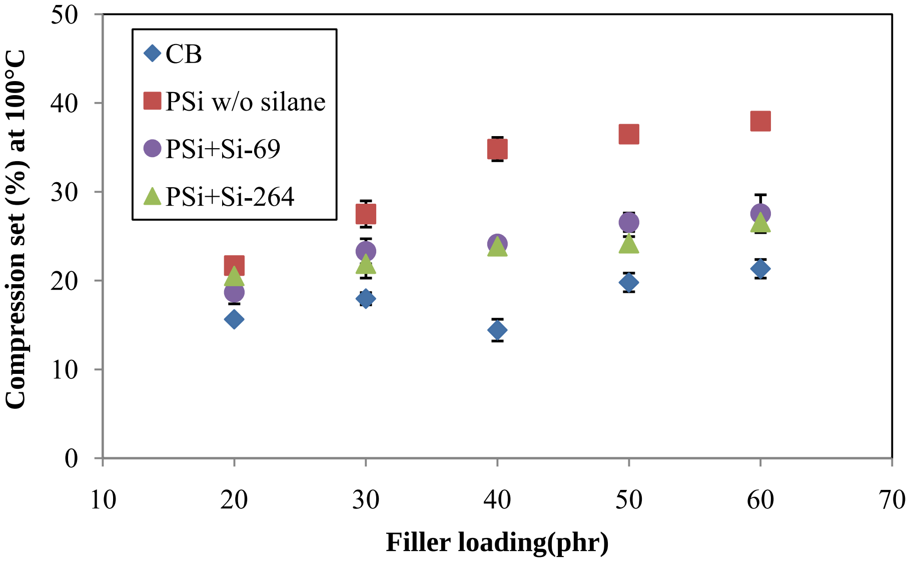

Figure 5.75 %Compression at 100°C of CR vulcanizates with various filler loadings

Likewise, the relatively good compression set found in CB-filled CR vulcanizates could be explained by the greater amount of crosslink density (as revealed in the Figure 5.73). Furthermore, as mentioned previously, the greater magnitude of compression set in PSi-filled CR vulcanizates could be attributed to the greater magnitude of post-curing via the development of filler – filler and/or filler –

rubber interactions, as shown in Figures 5.53. Moreover, the relatively large particle size of CB might enhance compression set which is probably due to the decreased surfaces available for molecular slippage at CB surfaces.

5.4.7 Heat build - up (HBU)

The relationship between HBU and filler loading is revealed in Figure 5.80. The HBU results reveal that the HBU tends to increase with increasing filler loading which is attributed to the molecular slippage particularly at rubber-filler interfaces. As mentioned earlier, the hysteresis in filled-rubber is mainly due to the energy dissipation during repeated destruction and reconstruction of the filler network. Thus, the reduction in HBU with the use of SCA could be due to the combined effects of enhancement in filler dispersion, rubber–filler interaction and crosslink density.

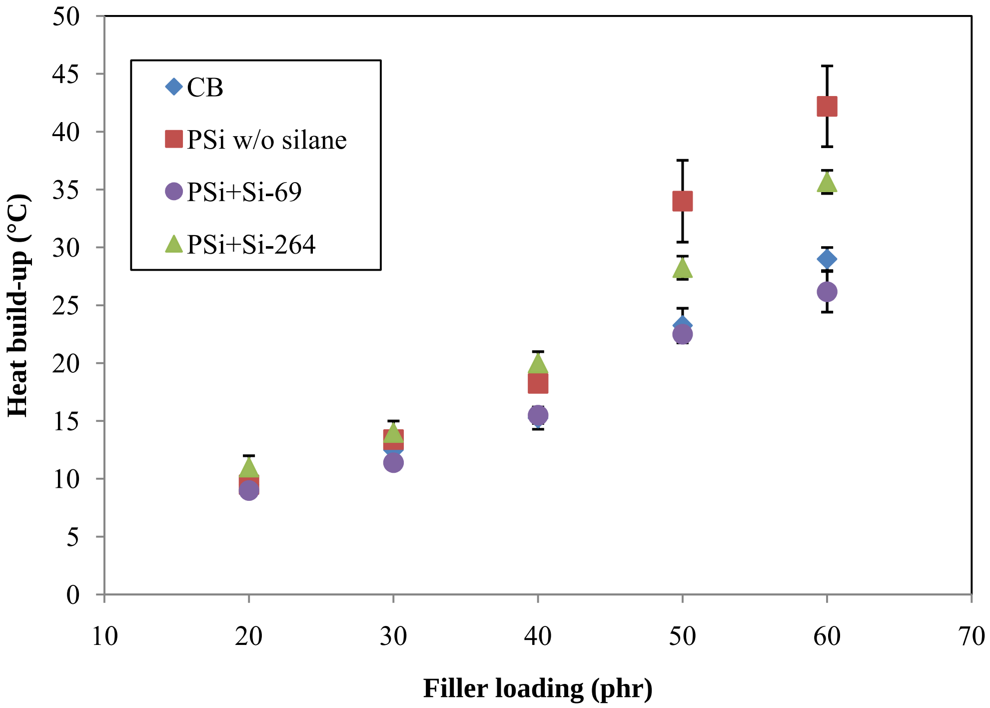

Figure 5.76 Heat build-up (HBU) of CR vulcanizates with various filler loadings

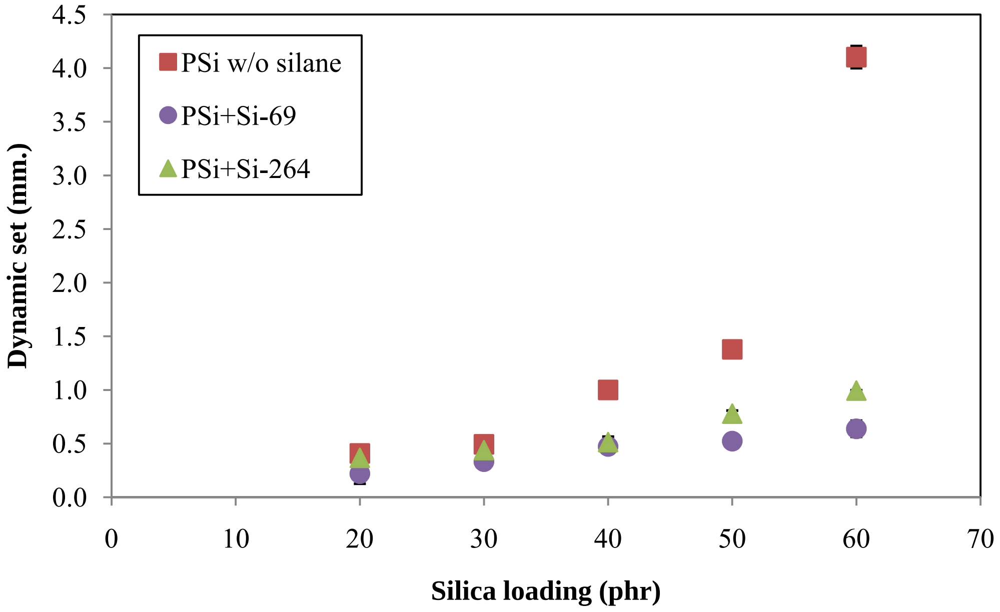

Figure 5.77 Dynamic set of CR vulcanizates with various PSi loadings

Compared with Si-264, Si-69 provides the rubber vulcanizates with lower HBU. This could be due to the greater crosslink density (see Figure 5.61) accompanied with the lower magnitude of physical interaction (as revealed in the Figure 5.65). Furthermore, the improvement in the dynamic set of PSi-filled CR vulcanizates by SCA treatment is remarkable. The results are in line with results of crosslink density and HBU.

5.4.8 Abrasion resistance

Figure 5.78 represents the effects of SCA on abrasion resistance of rubber vulcanizates. The addition of SCA significantly raises the abrasion resistance (i.e., the reduction of abrasion loss). This improvement is caused by several factors, including increases in rubber–filler interaction, PSi dispersion, and crosslink density.

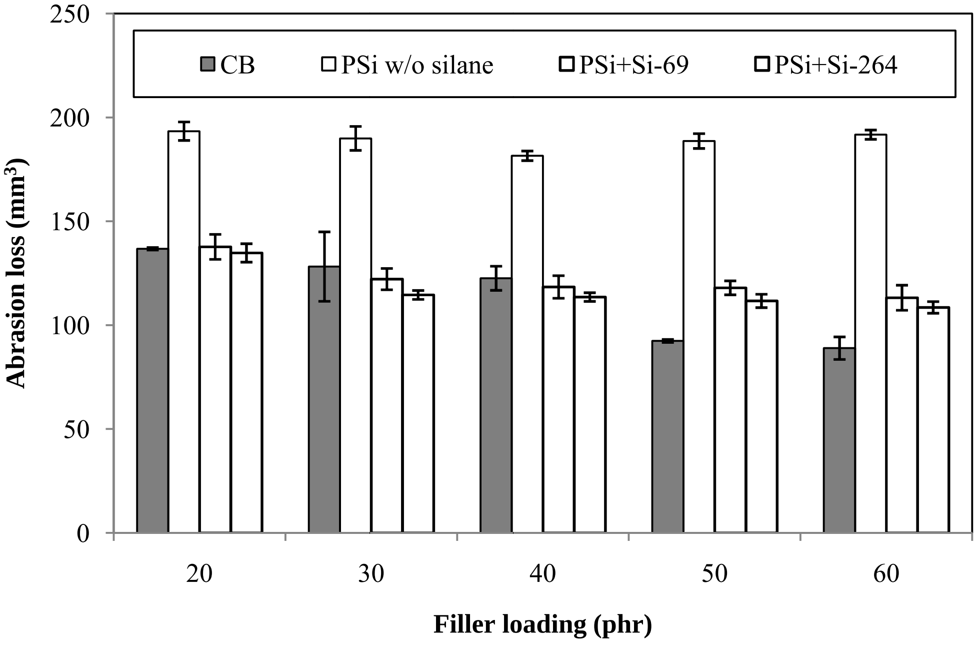

Figure 5.78 Abrasion loss of CR vulcanizates with various filler loadings

Surprisingly, compared with Si-69, the Si-264 silane illustrates greater abrasion resistance. The results obtained are in disagreement with the crosslink density and tensile strength results. The explanation of this contradiction is still unclear. However, it should be noted that, apart from hardness and tensile strength, the dynamic properties could govern the abrasion resistance.

As mentioned elsewhere, the system with lower tan δ would provide the higher elasticity to the rubber compound [82-83]. This leads theoretically to the greater abrasion resistance. From the results obtained, at given temperature, PSi-filled CR with Si-264 treatment shows the higher tan δ value and should theoretically provide the lower in abrasion resistance. Results obtained are not in agreement with the abrasion results. The exactly explanation is not known at present.

Furthermore, the greater abrasion resistance found in CB-filled CR is due probably to the higher magnitude of crosslink density (as illustrated in Figure 5.73). It is evident that, with filler loading up to 40 phr, SCA-treated PSi provides similar magnitude of abrasion resistance to CB. However, by further loading, CB still gives further improvement while PSi exhibits no significant enchantment. It is believed that both higher magnitudes of crosslink density and filler dispersion provided by CB are responsible.

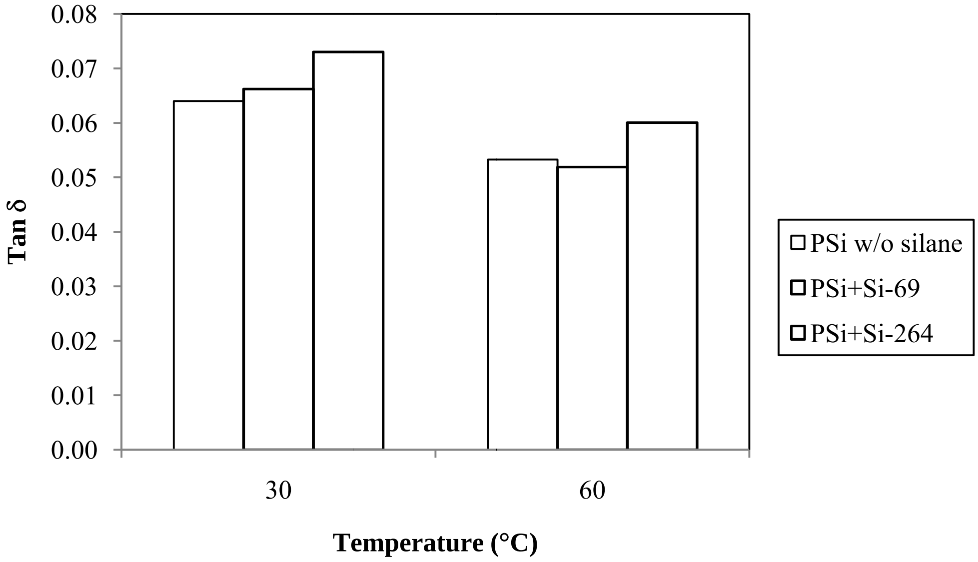

Figure 5.79 Tan δ at 30 and 60 °C of PSi-filled CR vulcanizates with and without SCA treatment (PSi is kept constant at 40 phr)

CHAPTER VI

CONCLUSION

Part 1: A study of metal oxide effect on cure characteristics and mechanical properties of CR vulcanizates.

The crosslink density increases with increasing metal oxide until 4 and 5 phr of MgO and ZnO, respectively. The results agree with the general formula usually used to vulcanize CR rubber. In the case of PbO, the magnitude of crosslink density is relatively low which could be summarized that the MgO and ZnO contribute to the crosslink of CR more effectively than PbO. The scorch time (t_{s2}) of the composites increases with increasing loading of MgO and decreases with increasing loading of ZnO and PbO.

Hardness, tensile strength and modulus at 100% strain are in good accordance with the crosslink density. However, the reduction of tensile strength at high loading of MgO and ZnO are due to the excessive crosslink density. Additionally, the compression set and heat build-up are resulted from the increase in post-curing effect and molecular restriction, respectively. The development in abrasion resistance with increasing MgO and ZnO could be attributed to the increment in crosslink density.

The crosslink density of CR vulcanizates increases with increasing total loading of metal oxide (while MgO to ZnO loading ratio is kept constant at 4:5). The hardness and M100 are in good accordance with the crosslink density. However, the reduction in tensile strength and abrasion resistance of CR vulcanizates with increasing total loading of metal oxide could be explained in terms of poor dispersion and distribution of metal oxides associate with the excessive crosslink density. Furthermore, the poor compression set and heat build-up of CR vulcanizates at high total loading of metal oxides are caused by post-curing effect and molecular restriction, respectively.

Part 2: A study of sulfur effect on cure characteristics and mechanical properties of CR vulcanizates.

Sulfur has an important role in vulcanization process for CR compound. The CR compounds accompanied with sulfur and metal oxide reveal the greater magnitude of crosslink density than those without sulfur. Additionally, the CR composites in non-sulfur system also provide longer scorch time.

Hardness, tensile strength and M100 are in good accordance with the results of crosslink density in a way that the change in these properties via metal oxide loading is caused by crosslink density, and the addition of sulfur could develop the magnitude of these properties.

The presence of sulfur added in CR vulcanizates leads to the poorer thermal aging resistance and, thus, poorer compression set and heat build-up at elevated temperature. Additionally, CR vulcanizates without sulfur added offer the greater abrasion resistance than those with the presence of sulfur. The results obtained are in contradiction with the crosslink density, hardness, tensile strength, and tanδ value.

Part 3: A study of reinforcing filler effect on cure characteristics, mechanical properties, and phase morphology of CR vulcanizates.

The crosslink density increases continuously with increasing filler loading which could be attributed to the development of interaction between the CR and filler. The crosslink density as determined by torque difference reveals the greater amount of crosslink density in PSi-filled CR than that in CB-filled CR. Meanwhile, the crosslink density as determined by Flory-Rehner equation shows the contrary results.

The addition of filler leads to the development of mechanical properties, such as hardness, tensile strength, M100 and abrasion resistance. However, the reduction in tensile strength and abrasion at high filler loading could be due to the excessive crosslink density and/or incomplete filler dispersion leading to the presence of flaws in vulcanizates. In the case of heat build-up and compression set, the poorer properties are due probably to the increased energy dissipation via: (i) the increased crosslink density; (ii) a disruption of psudo–network and (iii) dilution effect.

Part 4: A study of silane coupling agent effect on cure characteristics, mechanical properties and phase morphology of CR vulcanizates.

The crosslink density of CR vulcanizates increases with increasing precipitated silica (PSi) loading, regardless of the silane coupling agent (SCA) added. However, there are contrary results of crosslink density which determined by torque difference and Flory-Rehner concept.

The use of silane coupling agent in PSi-filled CR vulcanizates appears to significantly improve the filler-rubber interaction which leads to the development of mechanical properties (i.e., hardness, tensile properties, abrasion resistance compression set, heat- build up, etc.) and morphology of CR vulcanizates.

REFERENCES

1. Klingender RC. Handbook of specialty elastomers, 1st ed. United States of America: Taylor & Francis Group; 2008, pp 2-37
2. sites.google.com/site/helpingarm
3. www.iqsdirectory.com/rubber-rollers
4. Schatzel RA, Cassell GW. Synthetic Elastic Polymers in the Cable Industry. Industrial and engineering chemistry 1939; 31: 945-949
5. www.brederoshaw.com/solutions/Polychloroprene.htm
6. Hofmann W. Vulcanization and vulcanizing agents, 1st ed. United Kingdom: Maclaren and son Ltd; 1967
7. Das A, Naskar N, Basu DK. Thiophosphoryl disulfides as crosslinking agents for chloroprene rubber. Journal of Applied Polymer Science 2004; 91: 1913-1919
8. Kato H, Fujita H. Some novel systems for crosslinking polychloroprene. Rubber Chemistry and Technology 1975; 48: 19-25
9. Kato H, Fujita H. Development of synergistic curing systems for polychloroprene. Rubber Chemistry and Technology 1982; 55: 949-960
10. Khanra TK, Maiti S Adhikari BJ. Performance level of accelerator cum antioxidants in different rubbers. Journal of elastomers and plastics 1994; 26: 294- 306
11. Ismail H, Ahmad Z, Mohd Ishak ZA. Effects of cetyltrimethylammonium maleate on curing characteristics and mechanical properties of polychloroprene rubber. Polymer Testing 2003; 22: 179-183
12. Das A, Naskar N, Datta RN, Bose PP, Debnath SC. Naturally occurring amino acid: Novel curatives for chloroprene rubber. Journal of Applied Polymer Science 2006; 100: 3981–3986

13. Sahoo NG, Kumar ES, Das CK, Panda AB, Pramanik P, Nanofiller as crosslinker for halogen-containing elastomers. Macromolecular Research 2003; 11: 506-510
14. Sae-oui P, Sirisinha C, Thepsuwan U, Hatthapanit K. Dependence of mechanical and aging properties of chloroprene rubber on silica and ethylene thiourea loadings. European Polymer Journal 2007; 43: 185–193.
15. Mark HF, Gaylord NC, Bikales NM. Encyclopedia of Polymer Science and Technology volume 9, 3rd ed. New York: Wiley-interscience Publication; 2004: 189-234
16. Dick JS. Rubber technology: Compounding and testing for performance, 1st ed. Munich: Hanser publisher; 2001
17. Datta RN. Rubber curring system, 1st ed. United Kingdom: Smithers Repra Technology Ltd; 2002
18. Desai H, Hendrikse KG, Woolard CD, Vulcanization of Polychloroprene Rubber. I. A Revised Cationic Mechanism for ZnO Crosslinking. Journal of Applied Polymer Science 2007; 105: 865–876
19. Gent AN. Engineering with rubber: how to design rubber component, 2nd ed. Munich: Hensher publisher; 2001
20. Wang G, Li M, Chen X. Effects of fillers on mechanical properties of a water-swellable rubber. Journal of Applied Polymer Science 1999; 72: 577–584
21. http://iisrp.com/WebPolymers/04FinalPolychloropreneIISRP.pdf
22. Ciullo PA, N. Hewitt. Rubber formulary, 1st ed. United States of America: Noyes Publication; 1999,pp 12
23. Simpson RB. Rubber basic, 1st ed. United Kingdom: Repra Technology Ltd; 2002
24. Miyata Y, Atsumi M. Zinc oxide crosslinking reaction of Polychloroprene rubber. Rubber Chemistry and Technology 1989; 62: 1-12
25. Tinker AJ, Jones KP. Blends of Natural Rubber: Novel Techniques for Blending with Specialty Polymers, 1st ed. United Kingdom: Chapman & Hall Ltd; 1998
26. Billmeyer FW. Textbook of polymer science, 3rd ed. Canada: Wiley-interscience Publication; 1984

27. Mark JE, Erman B, Eirich FR. The science and technology of rubber, 3rd ed. United Kingdom: Elsevier Inc.; 2005
28. Rodgers B. Rubber compounding: Chemistry and Application, 1st ed. United States of America: Marcel Dekker Inc; 2004
29. White J, De SK, Naskar K. Rubber technologist's handbook volume 1, 1st ed. United Kingdom: Repra Technology Ltd; 2009
30. Ciesielski A. An introduction to rubber technology, 1st ed. United Kingdom: Repra Technology Ltd; 1999
31. http://www.dupontelastomers.com/literature/neoprene/585E7A59DA93810F6B1A7900D3712585.pdf
32. Bhowmick AK. Current topic in elastic research, 1st ed. United States of America: Taylor & Francis Group, LLC; 2008
33. Akiba M, Hashim AS, Vulcanization and crosslinking in elastomers. Program Polymer Science 1997; 22: 475-521
34. Kuntz I, Zapp RL, Pancirov RJ. The chemistry of the zinc oxide cure of halobutyl. Rubber Chemistry and Technology 1984; 57: 813-825
35. Hewitt N. Compounding precipitated silica in elastomers, 1st ed. United States of America: William Andrew Inc; 2007
36. Dick JS. Basic rubber testing : selecting methods for a rubber test program, 1st ed. United States of America: ASTM International: 2003 pp. 30 – 47
37. Mark HF, Gaylord NC, Bikales NM. Encyclopedia of Polymer Science and Technology volume 11, 3rd ed. United States of America: Wiley-interscience Publication; 2004: 189-234
38. Sae-Oui P, C Sirisinha, Hatthapanit K, Phewthongin N. Influence of Magnesium Carbonate Loading on the Compound Properties of Polychloroprene, Natural Rubber, and Their Blends. Journal of Applied Polymer Science 2008; 110: 2763–2769
39. Mark HF, Gaylord NC, Bikales NM. Encyclopedia of Polymer Science and Technology volume 10, 3rd ed. United States of America: Wiley-interscience Publication; 2004: 1-20
40. Leblanc JL. Rubber-filler interaction and rheological properties in filled compounds, Programe Polymer Science 2002; 27: pp 627-687

41. http://www.gemmechem.com/solutions/SolutionsInfo.asp?NewsID=38
42. Forrest MJ. Rubber analysis-polymers, compounds, and products, 1st ed. United Kingdom: Rapra Technology Ltd; 2001: pp 20-21 vol 12, num7
43. Varughese S, Tripathy DK. Chemical interaction between epoxidized natural rubber and silica: studies on cure characteristics and low-temperature dynamic mechanical properties. Journal of Applied Polymer Science 1992; 44: 1847–1852.
44. Manna AK, De PP, Tripathy DK, De SK, Peiffer DG. Bonding between precipitated silica and epoxidized natural rubber in the presence of silane coupling agent. Journal of Applied Polymer Science 1999; 74: 389–98.
45. Manna AK, Bhattacharyya AK, De PP, Tripathy DK, De SK, Peiffer DG. Effect of silane coupling agent on the chemo-rheological behavior of epoxidised natural rubber filled with precipitated silica. Polymer 1998; 39: 7113–7117
46. Bandyopadhyay S, De PP, Tripathy DK, De SK. Interaction between carboxylated nitrile rubber and precipitated silica: Role of (3-aminopropyl) triethoxysilane. Rubber Chemistry and Technology 1996; 69: 637–647.
47. Roychoudhury A, De PP, Roychoudhury N, Vidal A. Chemical interaction between chlorosulfonated polyethylene and silica: Effect of surface modifications of silica. Rubber Chemistry and Technology 1995; 68: 815–823
48. Sae-oui P, Sirisinha C, Thepsuwan U, Hatthapanit K. Roles of silane coupling agents on properties of silica-filled polychloroprene. European Polymer Journal 2006; 42: 479–486
49. Wang MJ. The Role of Filler Networking in Dynamic Properties of Filled Rubber. Rubber Division, American Chemical Society: United States of America, May 5-8, 1998; paper No. 48
50. Payne AR. The dynamic properties of carbon black loaded natural rubber vulcanizates. Part II. Journal of Applied Polymer Science 1962; 6: 368-372
51. Koerner H, Liu W, Alexander M, Mirau P, Dowty H, Vaia RA. Deformation–morphology correlations in electrically conductive carbon nanotube—thermoplastic polyurethane nanocomposites. Polymer 2005; 46: 4405–4420

52. Nillawong M, Sombatsompop N, Sirisinha C. Viscoelastic Properties of Nitrile Rubber Filled with Lignite Fly Ash. Journal of Applied Polymer Science 2010; 116: 3497–3502
53. Sirisinha K, Kamphunthong W. Rheological analysis as a means for determining the silane crosslink network structure and content in crosslinked polymer composites. Polymer testing 2009; 28: 636-641
54. http://www.tssilica.net/images/TOKUSIL%20BROCHURE.pdf
55. Mark JE. Physical Properties of Polymers Handbook. 2nd ed. United States of America: Springer Science Business Media, LLC 2007
56. Vergnaud JM, Rosca ID. Rubber curing and properties, 1st ed. United States of America: Taylor & Francis Group; 2009, pp.149-150
57. Barikani M, Hepburn C. Determination of Crosslink Density by Swelling in the Castable Polyurethane Elastomer Based on 1/4 – Cyclohexane Diisocyanate and para - Phenylene Diisocyanate. Iranian Journal of Polymer Science & Technology 1992; 1: pp. 1-5
58. Chatterjee K, Naskar K. Development of thermoplastic elastomers based on maleated ethylene propylene rubber (m-EPM) and polypropylene (PP) by dynamic vulcanization. eXPRESS Polymer Letters 2007; 1: 527–534
59. Brandup J, Immergut EH, Grulke EA. Polymer Handbook, 4th ed. United States of America: Wiley; 1999
60. http://en.wikipedia.org/wiki/Toluene
61. Kundu PP, Tripathy DK. Influence of Filler–Polymer Interactions on the Cure Mismatch of Dissimilar Polymeric Blends. Journal of Applied Polymer Science 1997; 64: 321–328
62. Stuart B. Polymer analysis, 1st ed. United Kingdom: Wiley; 2002
63. Brown R. Physical testing of rubber, 4th ed. United States of America: Springer Science-i-Business Media, Inc.; 2006
64. http://en.wikipedia.org/wiki/Energy-dispersive_X-ray_spectroscopy
65. http://mee-inc.com/eds.html
66. Mallon PE, McGill WJ, Shillington DP. A DSC study of the crosslinking of polychloroprene with ZnO and MgO. Journal of Applied Polymer Science 1995; 55: 705-721

67. Sombatsompop N, Kumnuantip C. Rheology, cure characteristics, physical and mechanical properties of tire tread reclaimed rubber/natural rubber compounds. Journal of Applied Polymer Science 2003; 87: 1723-1731

68. Kar KK, Bhowmick AK. High-Strain Hysteresis of Rubber Vulcanizates over a Range of Compositions, Rates, and Temperatures. Journal of Applied Polymer Science 1997; 65: 1429-1439

69. Sae-Oui P, Sirisinha C, Hatthapanita K, Thepsuwan U. Comparison of reinforcing efficiency between Si-69 and Si-264 in an efficient vulcanization system. Polymer Testing 2005; 24: 439–446

70. Sae-Oui P, Thepsuwan U, Hatthapanita K. Effect of curing system on reinforcing efficiency of silane coupling agent. Polymer Testing 2004; 23:397–403

71. Rattanasom N, Saowapark T, Deeprasertkul C. Reinforcement of natural rubber with silica/carbon black hybrid filler. Polymer Testing 2007; 26: 369–377

72. Das A, Costa FR, Wagenknecht U, Heinrich G. Nanocomposites based on chloroprene rubber: Effect of chemical nature and organic modification of nanoclay on the vulcanizate properties. European Polymer Journal 2008; 44: 3456–3465

73. Phewphong P, Sae-Oui P, Sirisinha C. Mechanism of Silica Reinforcement in CPE/NR Blends by the Use of Rheological Approaches. Journal of Applied Polymer Science 2008; 107: 2638–2645

74. White J, De SK, Naskar K. Rubber technologist's handbook volume 2, 1st ed. United Kingdom: Smithers Rapra Technology Ltd; 2009

75. Guth E, Gold O. Theory of filler reinforcement. Journal of Applied Physics 1945; 16: 20-25.

76. Fröhlich J, Niedermeier W, Luginsland H-D. The effect of filler–filler and filler–elastomer interaction on rubber reinforcement. Composites: Part A 2005; 36; 449–460

77. Edwards DC. Review Polymer-filler interactions in rubber reinforcement, Journal of material science 1990; 25: 4175-4185

78. Alliger G, Weissert FC. Annual review Elastomer Technology: Research on the relationships between molecular structure and mechanical behavior is

leading to continual improvements in performance. Industrial and Engineering Chemistry 1968; 60: 51-62

79. Lipatov YS. Polymer reinforcement, 1st ed. Canada: ChemTec Publishing; 1995
80. Choi S-S. Improvement of properties of silica-filled natural rubber compounds using polychloroprene, Journal of Applied Polymer Science 2002; 83: 2609-2616
81. Byers JT. Silane coupling agents for enhanced silica performance. Rubber World 1998; 218: 38–47
82. Barnes HA, Hutton JF, Walters K. An introduction to rheology, 3rd ed. Netherlands: Elsevier Science Publishers; 1993
83. Shaw MT, MacKnight WJ. Introduction to polymer viscoelastic, 3rd ed. Canada: John Wiley & Sons, Inc; 2005

APPENDICES

APPENDIX A

A STUDY OF METAL OXIDE EFFECT ON CURE CHARACTERISTICS AND MECHANICAL PROPERTIES OF CR VULCANIZATES

Table A1 Torque difference of CR with varied metal oxide types and loadings determined by moving die rheometer (MDR)

MgO (phr)	M_H - M_L (dN.m)	ZnO (phr)	M_H - M_L (dN.m)	PbO (phr)	M_H - M_L (dN.m)
2	14.76±0.32	2	14.89±0.15	2	9.95±0.46
3	15.59±0.55	3	15.46±0.40	3	10.09±0.50
4	16.67±0.65	4	15.80±0.40	4	10.17±0.46
5	16.19±0.74	5	16.67±0.65	5	9.41±0.41
6	16.01±1.04	6	15.35±0.61	6	9.65±0.29

Table A2 Scorch time (t_{s2}) of CR with varied metal oxide types and loadings determined by moving die rheometer (MDR)

MgO (phr)	t_{s2} (min)	ZnO (phr)	t_{s2} (min)	PbO (phr)	t_{s2} (min)
2	1.50±0.07	2	1.87±0.12	2	1.92±0.22
3	1.60±0.13	3	1.80±0.10	3	1.83±0.26
4	1.71±0.18	4	1.73±0.11	4	1.61±0.04
5	1.87±0.14	5	1.71±0.18	5	1.59±0.02
6	1.88±0.07	6	1.68±0.07	6	1.41±0.39

Table A3 Crosslink density (n) of CR with varied metal oxide types and loadings determined by Flory – Rehner equation

MgO (phr)	n ($\times 10^{-4}$mol/cm^3)	ZnO (phr)	n ($\times 10^{-4}$mol/cm^3)	PbO (phr)	n ($\times 10^{-4}$mol/cm^3)
2	9.03±0.11	2	9.57±0.02	2	7.55±0.17
3	9.65±0.08	3	9.87±0.15	3	7.93±0.25
4	10.52±0.33	4	10.01±0.25	4	8.05±0.31
5	10.30±0.17	5	10.52±0.33	5	8.18±0.20
6	10.38±0.27	6	9.77±0.15	6	8.27±0.17

Table A4 Hardness of CR vulcanizates with varied metal oxide types and loadings

MgO (phr)	Hardness (Shore A)	ZnO (phr)	Hardness (Shore A)	PbO (phr)	Hardness (Shore A)
2	69.75±0.55	2	71.39±0.69	2	68.00±0.76
3	71.77±0.37	3	71.68±0.78	3	68.15±0.55
4	73.38±0.58	4	72.58±0.60	4	68.23±0.32
5	71.52±0.39	5	73.38±0.58	5	68.38±0.23
6	71.75±0.41	6	71.06±0.70	6	68.52±0.60

Table A5 Tensile strength of CR vulcanizates with varied metal oxide types and loadings

MgO (phr)	Tensile strength (MPa)	ZnO (phr)	Tensile strength (MPa)	PbO (phr)	Tensile strength (MPa)
2	20.15±0.65	2	19.36±0.76	2	19.67±0.94
3	20.86±0.61	3	19.73±0.69	3	19.89±0.47
4	19.38±0.81	4	20.78±0.85	4	20.82±0.05
5	19.34±0.42	5	19.38±0.81	5	20.78±0.27
6	19.71±0.61	6	19.99±0.73	6	21.12±0.38

Table A6 Modulus at 100% elongation (M100) of CR vulcanizates with varied metal oxide types and loadings

MgO (phr)	M100 (MPa)	ZnO (phr)	M100 (MPa)	PbO (phr)	M100 (MPa)
2	5.18±0.59	2	5.60±0.32	2	3.75±0.14
3	5.95±0.29	3	6.08±0.31	3	4.34±0.13
4	6.22±0.68	4	6.15±0.26	4	4.50±0.22
5	6.19±0.14	5	6.22±0.68	5	4.54±0.13
6	6.14±0.36	6	5.85±0.25	6	4.21±0.10

Table A7 Compression set at 70 °C of CR vulcanizates with varied metal oxide types and loadings

MgO (phr)	Compression set (%)	ZnO (phr)	Compression set (%)	PbO (phr)	Compression set (%)
2	7.44±0.20	2	8.06±1.11	2	6.34±0.67
3	6.96±0.31	3	6.16±0.37	3	7.11±0.82
4	8.33±1.07	4	7.03±0.46	4	7.84±0.06
5	9.22±0.25	5	8.33±1.07	5	8.73±0.17
6	10.72±0.04	6	11.30±0.32	6	10.03±1.12

Table A8 Compression set at 100 °C of CR vulcanizates with varied metal oxide types and loadings

MgO (phr)	Compression set (%)	ZnO (phr)	Compression set (%)	PbO (phr)	Compression set (%)
2	18.18±0.05	2	22.28±0.16	2	21.47±1.13
3	18.28±0.05	3	19.95±0.06	3	19.69±0.78
4	19.79±1.05	4	20.44±0.11	4	20.53±0.70
5	25.67±0.12	5	19.79±1.05	5	25.67±0.38
6	24.86±0.07	6	20.38±1.65	6	26.04±0.24

Table A9 Heat build-up of CR vulcanizates with varied metal oxide types and loadings

MgO (phr)	Heat build-up (°C)	ZnO (phr)	Heat build-up (°C)	PbO (phr)	Heat build-up (°C)
2	19.5±0.7	2	21.0±0.0	2	17.0±0.0
3	21.0±0.0	3	21.0±0.0	3	15.0±0.0
4	22.0±0.0	4	22.0±0.0	4	16.0±0.0
5	22.0±0.0	5	22.0±0.0	5	17.0±0.0
6	22.0±0.0	6	18.6±0.7	6	17.5±0.8

Table A10 Abrasion loss of CR vulcanizates with varied metal oxide types and loadings

MgO (phr)	Abrasion loss (mm^3)	ZnO (phr)	Abrasion loss (mm^3)	PbO (phr)	Abrasion loss (mm^3)
2	93.28±0.38	2	96.88±1.48	2	80.79±3.70
3	92.84±4.79	3	94.09±1.28	3	82.98±3.24
4	92.44±0.72	4	93.65±0.66	4	95.03±5.62
5	100.59±2.16	5	92.44±0.72	5	92.74±3.31
6	102.65±3.08	6	94.36±2.21	6	94.96±5.01

Table A11 Elemental content of CR vulcanizates with PbO determined by EDS at specific areas

Element type	Elemental content (%)		
	Spectrum A	Spectrum B	Spectrum C
C	72.17	77.51	83.38
S	N/A	0.18	0.28
Cl	16.10	16.53	14.56
Zn	2.01	5.78	1.78
Pb	9.72	N/A	N/A

Table A12 Torque difference of CR with various total loadings of MgO and ZnO

MgO (phr)	ZnO (phr)	M_H - M_L (dN.m)
4	5	16.67±0.65
8	10	17.17±0.37
12	15	19.42±0.36
16	20	21.23±0.07
20	25	22.33±0.60

Table A13 Crosslink density (n) of CR with various total loadings of MgO and ZnO

MgO (phr)	ZnO (phr)	Crosslink density ($\times 10^{-4}$ mol/cm^3)
4	5	10.52±0.33
8	10	10.65±0.67
12	15	11.20±0.14
16	20	12.37±2.26E-04
20	25	13.96±0.13

Table A14 Hardness of CR vulcanizates with various total loadings of MgO and ZnO

MgO (phr)	ZnO (phr)	Hardness (Shore A)
4	5	73.38±0.58
8	10	74.00±0.53
12	15	75.86±0.69
16	20	77.33±1.10
20	25	78.09±0.66

Table A15 Elemental content of CR vulcanizates determined by EDS at specific areas

Element type	Elemental content (%)		
	Spectrum A	Spectrum B	Spectrum C
C	43.85	51.71	73.77
O	34.68	18.39	4.73
Mg	6.84	3.12	0.47
Cl	12.88	13.83	19.38
Zn	1.74	12.95	1.65

Table A16 Relative elastic modulus (relative G′) in 5, 10, 50 and 100 % strain at the test frequency of 0.99 rad/s of vulcanized CR with various total loadings of MgO and ZnO

MgO (phr)	ZnO (phr)	Carbon black (phr)	Volume fraction of metal oxides and CB	Relative G’				
				Guth-Gold Equation	Experimental			
					at 5% strain	at 10% strain	at 50% strain	at 100% strain
0	0	0	0.00	1.00	1.00	1.00	1.00	1.00
4	5	50	0.26	2.63	5.02	4.49	2.92	2.20
8	10	50	0.28	2.77	5.18	4.63	2.98	2.28
12	15	50	0.29	2.90	5.65	4.86	2.97	2.25
16	20	50	0.30	3.04	6.29	5.37	3.19	2.42
20	25	50	0.31	3.17	7.31	6.08	3.58	2.70

Table A17 Tensile strength and Modulus at 100% elongation (M100) of CR vulcanizates with various total loadings of MgO and ZnO

MgO (phr)	ZnO (phr)	Tensile strength (MPa)	M100 (MPa)
4	5	19.38±0.81	6.22±0.68
8	10	16.23±0.37	6.39±0.02
12	15	16.18±0.63	6.48±0.71
16	20	15.57±0.83	6.76±0.31
20	25	15.37±0.75	6.81±0.10

Table A18 %Compression set at 70 and 100 °C of CR vulcanizates with various total loadings of MgO and ZnO

MgO (phr)	ZnO (phr)	Compression set (%)	
		@ 70 °C	@100°C
4	5	8.33±1.07	19.79±1.05
8	10	10.09±0.78	24.30±1.20
12	15	10.26±0.53	27.74±0.75
16	20	10.52±0.27	30.65±0.82
20	25	10.62±0.95	28.97±1.32

Table A19 Heat build-up of CR vulcanizates with various total loadings of MgO and ZnO

MgO (phr)	ZnO (phr)	Heat build-up (°C)
4	5	23.3±1.5
8	10	24.3±0.6
12	15	26.0±1.8
16	20	27.0±1.7
20	25	27.7±2.7

Table A20 Abrasion loss of CR vulcanizates with various total loadings of MgO and ZnO

MgO (phr)	ZnO (phr)	Abrasion loss (mm^3)
4	5	92.44±0.72
8	10	118.43±0.71
12	15	136.41±1.37
16	20	142.56±5.93
20	25	145.83±7.13

APPENDIX B

A STUDY OF SULFUR EFFECT ON CURE CHARACTERISTICS AND MECHANICAL PROPERTIES OF CR VULCANIZATES

Table B1 Torque difference of CR in sulfur and non-sulfur systems with varied metal oxide types and loadings determined by moving die rheometer (MDR)

MgO (phr)	M_H - M_L (dN.m)		ZnO (phr)	M_H - M_L (dN.m)	
	Sulfur	Non-sulfur		Sulfur	Non-sulfur
2	14.76±0.32	13.23±0.55	2	14.89±0.15	14.12±0.24
3	15.59±0.55	14.30±0.41	3	15.46±0.40	14.65±0.42
4	16.67±0.65	15.60±0.69	4	15.80±0.40	15.49±0.29
5	16.19±0.74	15.38±0.37	5	16.67±0.65	15.60±0.69
6	16.01±1.04	16.26±0.26	6	15.35±0.61	15.07±0.63

Table B2 Scorch time (t_{s2}) of CR in sulfur and non-sulfur systems with varied metal oxide types and loadings determined by moving die rheometer (MDR)

MgO (phr)	Scorch time (min)		ZnO (phr)	Scorch time (min)	
	Sulfur	Non-sulfur		Sulfur	Non-sulfur
2	1.50±0.07	1.88±0.18	2	1.87±0.12	2.23±0.17
3	1.60±0.13	1.91±0.03	3	1.80±0.10	2.16±0.23
4	1.71±0.18	1.94±0.03	4	1.73±0.11	1.98±0.05
5	1.87±0.14	2.00±0.07	5	1.71±0.18	1.94±0.03
6	1.882±0.07	2.05±0.09	6	1.68±0.07	1.93±0.03

Table B3 Crosslink density of CR in sulfur and non-sulfur systems with varied metal oxide types and loadings determined by Flory-Rehner equation

MgO (phr)	n (×10^{-4} mol/cm^3)		ZnO (phr)	n (×10^{-4} mol/cm^3)	
	Sulfur	Non-sulfur		Sulfur	Non-sulfur
2	9.03±0.11	8.93±0.41	2	9.57±0.02	9.37±0.12
3	9.65±0.08	9.75±0.03	3	9.87±0.15	9.65±0.15
4	10.52±0.33	9.96±0.22	4	10.01±0.25	9.72±0.15
5	10.30±0.17	10.17±0.13	5	10.52±0.33	9.96±0.22
6	10.38±0.27	10.27±0.03	6	9.77±0.15	10.11±0.17

Table B4 Hardness of CR in sulfur and non-sulfur systems with varied loadings of MgO and ZnO

MgO (phr)	Hardness (Shore A)		ZnO (phr)	Hardness (Shore A)	
	Sulfur	Non-sulfur		Sulfur	Non-sulfur
2	69.76±0.55	69.08±0.75	2	71.39±0.69	68.95±0.42
3	71.77±0.37	69.57±0.30	3	71.68±0.78	70.22±0.25
4	73.38±0.58	71.30±0.36	4	72.58±0.60	70.35±0.33
5	73.32±0.50	70.76±0.64	5	73.38±0.58	70.68±0.37
6	73.53±0.26	71.67±0.30	6	71.06±0.70	70.05±0.35

Table B5 Tensile strength of CR vulcanizates in sulfur and non – sulfur systems with various loadings of MgO and ZnO

MgO (phr)	Tensile strength (MPa)		ZnO (phr)	Tensile strength (MPa)	
	Sulfur	Non-sulfur		Sulfur	Non-sulfur
2	20.15±0.65	17.26±0.57	2	19.36±0.76	17.25±0.74
3	20.86±0.61	17.65±0.64	3	19.73±0.69	19.29±0.65
4	19.38±0.81	19.29±0.97	4	20.78±0.85	19.66±0.94
5	19.34±0.42	16.37±0.53	5	19.38±0.81	19.29±0.97
6	19.71±0.61	15.55±0.57	6	19.99±0.73	19.18±0.85

Table B6 Modulus at 100% elongation (M100) of CR vulcanizates in sulfur and non – sulfur systems with various loadings of MgO and ZnO

MgO (phr)	M100 (MPa)		ZnO (phr)	M100 (MPa)	
	Sulfur	Non-sulfur		Sulfur	Non-sulfur
2	5.18±0.59	4.96±0.24	2	5.60±0.32	5.48±0.30
3	5.95±0.29	5.90±0.17	3	6.08±0.31	6.06±0.27
4	6.22±0.68	6.18±0.32	4	6.15±0.26	6.14±0.59
5	6.19±0.14	5.86±0.28	5	6.22±0.68	6.18±0.32
6	6.14±0.36	6.20±0.22	6	5.85±0.25	6.22±0.45

Table B7 Compression set of CR vulcanizates at 70°C in sulfur and non – sulfur systems with various loadings of MgO and ZnO

MgO (phr)	Compression set at 70°C (%)		ZnO (phr)	Compression set at 70°C (%)	
	Sulfur	Non-sulfur		Sulfur	Non-sulfur
2	7.44±0.20	5.82±1.13	2	8.06±1.11	7.50±0.39
3	6.96±0.31	6.61±0.41	3	6.16±0.37	6.69±0.43
4	8.33±1.07	9.57±0.75	4	7.03±0.46	9.04±0.07
5	9.22±0.25	8.53±0.81	5	8.33±1.07	9.57±0.75
6	10.72±0.04	8.48±0.78	6	11.30±0.32	6.26±1.03

Table B8 Compression set of CR vulcanizates at 100°C in sulfur and non – sulfur systems with various loadings of MgO and ZnO

MgO (phr)	Compression set at 100°C (%)		ZnO (phr)	Compression set at 100°C (%)	
	Sulfur	Non-sulfur		Sulfur	Non-sulfur
2	18.18±0.05	14.19±0.71	2	22.28±0.16	11.37±1.33
3	18.28±0.05	12.65±0.86	3	19.95±0.06	12.81±0.86
4	19.79±1.05	12.74±0.14	4	20.44±0.11	13.06±0.30
5	25.67±0.12	14.12±0.34	5	19.79±1.05	11.75±1.53
6	24.86±0.07	14.69±0.59	6	20.38±1.65	13.3±0.81

Table B9 Heat build-up (HBU) of CR vulcanizates in sulfur and non – sulfur systems with various loadings of MgO and ZnO

MgO (phr)	Heat build-up (°C)		ZnO (phr)	Heat build-up (°C)	
	Sulfur	Non-sulfur		Sulfur	Non-sulfur
2	19.5±0.7	21.5±0.7	2	21.0±0.0	20.5±0.6
3	21.0±0.0	20.7±0.6	3	21.0±0.0	20.7±1.2
4	22.0±0.0	23.0±1.0	4	22.0±0.0	21.0±0.0
5	22.0±0.0	21.5±0.7	5	22.0±0.0	23.0±1.0
6	22.0±0.0	22.7±1.2	6	18.6±0.7	22.3±0.6

Table B10 Abrasion loss of CR vulcanizates in sulfur and non – sulfur systems with various loadings of MgO and ZnO

MgO (phr)	Abrasion loss (mm^3)		ZnO (phr)	Abrasion loss (mm^3)	
	Sulfur	Non-sulfur		Sulfur	Non-sulfur
2	96.88±1.48	92.07±0.97	2	96.88±1.48	92.50±0.81
3	94.09±1.28	91.63±1.00	3	94.09±1.28	91.36±5.13
4	93.65±0.66	90.91±0.95	4	93.65±0.66	90.82±2.69
5	92.44±0.72	97.66±0.75	5	92.44±0.72	90.91±0.95
6	94.36±2.21	106.15±3.04	6	94.36±2.21	90.63±1.75

Table B11 Tan δ at 30°C of CR vulcanizates with and without sulfur (ZnO is kept constant at 5 phr)

MgO content (phr)	Tan δ	
	Sulfur system	Non-sulfur system
2	0.097796	0.104762
6	0.091494	0.100696

Table B12 Tan δ as a function of temperature in CR vulcanizates with MgO 2 phr/ ZnO 5 phr in sulfur and non – sulfur systems determined by DMTA

Sulfur				Non-sulfur			
Temp (°C)	Tanδ	Temp (°C)	Tanδ	Temp (°C)	Tanδ	Temp (°C)	Tanδ
25.0	0.10074	63.2	0.07406	25.1	0.10893	63.4	0.08146
25.2	0.09977	64.7	0.07121	25.3	0.10956	64.7	0.08002
27.2	0.09913	66.0	0.07163	27.2	0.10727	66.1	0.07966
28.7	0.09937	67.4	0.07052	28.7	0.10664	67.6	0.07934
30.0	0.09780	68.8	0.07107	30.0	0.10476	68.8	0.07965
31.4	0.09650	70.2	0.06986	31.4	0.10489	70.1	0.07920
32.8	0.09602	71.8	0.07126	32.8	0.10326	71.6	0.07913
34.2	0.09418	73.2	0.07104	34.3	0.10176	73.1	0.07997
35.7	0.09135	74.4	0.07010	35.6	0.10070	74.6	0.07815
36.9	0.09154	75.7	0.06936	37.0	0.09964	75.9	0.07792
38.3	0.09083	77.3	0.06946	38.4	0.09835	77.1	0.08012
39.6	0.08711	78.7	0.07205	39.8	0.09705	78.5	0.07902
41.0	0.08845	80.0	0.06882	41.1	0.09599	80.0	0.07783
42.4	0.08694	81.3	0.06795	42.6	0.09524	81.5	0.07823
43.9	0.08569	82.9	0.06851	44.0	0.09460	83.0	0.07686
45.4	0.08313	84.4	0.06802	45.3	0.09117	84.2	0.07724
46.7	0.08461	85.5	0.06812	46.7	0.09099	85.7	0.07538
48.1	0.08179	86.9	0.06778	48.2	0.09155	86.9	0.07500
49.3	0.08155	88.5	0.06689	49.5	0.09041	88.3	0.07536
50.8	0.08029	89.7	0.06581	50.9	0.08846	89.7	0.07517
52.2	0.07957	91.2	0.06670	52.3	0.08763	91.2	0.07439
53.6	0.07801	92.7	0.06683	53.6	0.08715	92.5	0.07464
55.0	0.07765	93.8	0.06736	55.0	0.08547	94.1	0.07483
56.4	0.07597	95.3	0.06489	56.5	0.08381	95.2	0.07421
57.8	0.07601	96.8	0.06340	57.9	0.08202	96.4	0.07353
59.3	0.07576	98.3	0.06312	59.0	0.08349	97.9	0.07358
60.6	0.07527	99.3	0.06399	60.6	0.08266	99.4	0.07272
62.0	0.07428			62.0	0.08160		

Table B13 Tanδ as a function of temperature in CR vulcanizates with MgO 6 phr/ ZnO 5 phr in sulfur and non – sulfur systems determined by DMTA

Sulfur				Non-sulfur			
Temp (°C)	Tanδ	Temp (°C)	Tanδ	Temp (°C)	Tanδ	Temp (°C)	Tanδ
25.0	0.09403	63.3	0.06698	25.0	0.10278	63.3	0.07193
25.2	0.09265	64.8	0.06719	25.2	0.10342	64.7	0.07211
27.2	0.09338	66.1	0.06751	27.3	0.10233	66.0	0.06978
28.7	0.09311	67.7	0.06751	28.6	0.10087	67.4	0.07015
30.0	0.09149	69.0	0.06732	30.0	0.10070	68.9	0.07044
31.4	0.09022	70.3	0.06688	31.4	0.09891	70.3	0.06985
32.9	0.08855	71.8	0.06613	32.8	0.09599	71.9	0.06836
34.3	0.08689	73.2	0.06592	34.2	0.09575	73.3	0.06754
35.7	0.08620	74.4	0.06608	35.6	0.09405	74.3	0.06869
36.9	0.08539	75.8	0.06475	36.9	0.09292	75.8	0.06788
38.3	0.08390	77.3	0.06440	38.3	0.09172	77.2	0.06884
39.7	0.08300	78.6	0.06565	39.7	0.08951	78.4	0.06719
41.2	0.08205	80.0	0.06514	41.0	0.08835	80.1	0.06644
42.4	0.07965	81.5	0.06420	42.4	0.08784	81.2	0.06686
43.9	0.07857	82.8	0.06381	43.9	0.08522	82.8	0.06685
45.3	0.07749	84.3	0.06423	45.3	0.08481	84.2	0.06709
46.7	0.07640	85.6	0.06264	46.6	0.08302	85.5	0.06544
48.2	0.07553	86.9	0.06336	48.1	0.08179	86.9	0.06551
49.5	0.07419	88.4	0.06250	49.5	0.08098	88.4	0.06552
50.8	0.07407	89.6	0.06306	50.8	0.08004	89.7	0.06535
52.2	0.07197	91.1	0.06124	52.3	0.07904	91.0	0.06500
53.7	0.07083	92.5	0.06156	53.7	0.07797	92.6	0.06642
55.1	0.07087	94.0	0.06170	55.0	0.07730	93.9	0.06526
56.4	0.07107	95.3	0.06218	56.5	0.07557	95.3	0.06273
57.9	0.06971	96.7	0.06132	57.8	0.07540	96.5	0.06316
59.2	0.06904	98.3	0.06057	59.2	0.07480	98.3	0.06506
60.7	0.06833	99.5	0.06021	60.6	0.07279	99.4	0.06295
61.9	0.06766			61.8	0.07262		

APPENDIX C

A STUDY OF REINFORCING FILLER EFFECT ON CURE CHARACTERISTICS, MECHANICAL PROPERTIES AND PHASE MORPHOLOGY OF CR VULCANIZATES

Table C1 Torque difference of CR with varied filler types and loadings determined by moving die rheometer (MDR)

Carbon black (phr)	M_H - M_L (dN.m)	Precipitated silica (phr)	M_H - M_L (dN.m)
20	10.81±0.39	20	10.65±0.35
30	11.58±0.12	30	15.72±0.45
40	13.66±0.63	40	22.17±0.10
50	16.67±0.65	50	27.72±1.00
60	19.59±0.02	60	28.21±0.77
70	20.24±1.17		

Table C2 Crosslink density of CR vulcanizates with varied filler types and loadings determined by Flory-Rehner equation

Carbon black (phr)	n ($\times 10^{-4}$ mol/cm^3)	Precipitated silica (phr)	n ($\times 10^{-4}$ mol/cm^3)
20	4.76±0.03	20	3.20±0.09
30	6.09±0.12	30	3.83±0.03
40	8.11±0.13	40	4.27±0.18
50	10.38±0.68	50	4.82±0.23
60	12.84±0.28	60	5.42±0.31
70	14.58±0.22		

Table C3 Relative elastic modulus (relative G′) in 5, 10, 50 and 100 % strain at the test frequency of 0.99 rad/s of vulcanized CR with various precipitated silica (PSi) loadings

PSi (phr)	Volume fraction of PSi	Relative G’				
		Guth-Gold Equation	Experimental			
			at 5% strain	at 10% strain	at 50% strain	at 100% strain
0	0	1.00	1.00	1.00	1.00	1.00
20	0.11	1.44	2.37	2.30	1.88	1.66
30	0.16	1.73	5.01	4.30	2.43	1.93
40	0.20	2.04	12.48	9.37	3.87	2.82
50	0.24	2.37	30.36	18.01	5.30	3.63
60	0.27	2.70	59.84	35.80	9.88	6.35

Table C4 Relative elastic modulus (relative G′) in 5, 10, 50 and 100 % strain at the test frequency of 0.99 rad/s of vulcanized CR with various carbon black (CB) loadings

CB (phr)	Volume fraction of CB	Relative G’				
		Guth-Gold Equation	Experimental			
			at 5% strain	at 10% strain	at 50% strain	at 100% strain
0	0	1.00	1.00	1.00	1.00	1.00
20	0.12	1.49	1.69	1.76	1.59	1.41
30	0.17	1.81	2.27	2.34	1.92	1.64
40	0.21	2.15	3.25	3.22	2.41	1.98
50	0.25	2.50	4.53	4.28	2.88	2.27
60	0.29	2.86	7.42	6.83	4.07	3.19
70	0.32	3.22	11.15	9.76	5.25	4.07

Table C5 Hardness of CR vulcanizates with various filler (carbon black (CB) and precipitated silica (PSi)) loadings

Carbon black (phr)	Hardness (Shore A)	Precipitated silica (phr)	Hardness (Shore A)
20	57.68±0.20	20	55.75±0.27
30	59.92±0.38	30	61.50±0.44
40	65.97±0.20	40	66.25±0.61
50	73.38±0.58	50	73.40±0.74
60	77.68±0.41	60	79.75±1.19
70	81.18±0.49		

Table C6 Tensile strength of CR vulcanizates with various filler (Carbon black (CB) and Precipitated silica (PSi)) loadings

CB (phr)	Tensile strength (MPa)	PSi (phr)	Tensile strength (MPa)
20	17.49±0.54	20	16.38±0.58
30	17.71±0.72	30	17.35±0.42
40	18.56±0.36	40	17.98±0.42
50	19.85±0.68	50	18.56±0.66
60	18.76±0.80	60	18.06±0.33
70	17.45±0.52		

Table C7 Modulus at 100% elongation (M100) of CR vulcanizates with various filler (carbon black (CB) and precipitated silica (PSi)) loadings

CB (phr)	M100 (MPa)	PSi (phr)	M100 (MPa)
20	1.84±0.03	20	1.45±0.05
30	2.98±0.06	30	1.98±0.03
40	4.14±0.09	40	2.09±0.10
50	6.36±0.26	50	2.43±0.16
60	8.66±0.47	60	2.91±0.08
70	12.07±0.60		

Table C8 Compression set at 70°C and 100°C of CR vulcanizates with various CB and PSi loadings

CB (phr)	Compression set (%)		PSi (phr)	Compression set (%)	
	70 °C	100 °C		70 °C	100 °C
20	9.02±0.61	15.64±0.30	20	10.36±0.55	21.70±0.09
30	7.85±1.39	17.96±0.69	30	14.34±0.81	27.50±1.48
40	7.71±0.58	14.42±1.23	40	14.60±0.71	28.13±1.3
50	8.33±1.07	19.79±1.05	50	21.42±0.71	36.49±0.11
60	8.71±1.14	21.33±1.05	60	21.75±0.94	37.34±0.33
70	11.53±0.50	20.45±0.75			

Table C9 Heat build-up of CR vulcanizates with various CB and PSi loadings

CB (phr)	Heat build-up (°C)	PSi (phr)	Heat build-up (°C)
20	9.5±0.7	20	9.5±0.6
30	12.5±0.7	30	13.0±0.6
40	15.3±1.0	40	18.2±0.5
50	23.3±1.5	50	34.0±3.5
60	29.0±1.0	60	33.6±1.5
70	29.5±0.7		

Table C10 Abrasion loss of CR vulcanizates with various CB and PSi loadings

CB (phr)	Abrasion loss (mm^3)	PSi (phr)	Abrasion loss (mm^3)
20	136.78±0.58	20	193.37±4.44
30	128.19±16.70	30	189.90±5.76
40	122.58±5.81	40	181.53±2.32
50	92.44±0.72	50	188.62±3.58
60	88.94±5.41	60	191.70±2.24
70	96.67±3.27		

Table C11 Elemental content of PSi-filled CR vulcanizates determined by EDS at specific areas

Element type	Elemental content (%)	
	Spectrum A	Spectrum B
C	32.27	50.95
O	35.43	13.18
Mg	9.59	0.64
Si	7.80	10.76
Cl	12.98	22.03
Zn	1.94	2.45

APPENDIX D

A STUDY OF SILANE COUPLING AGENT (SCA) EFFECT ON CURE CHARACTERISTICS, MECHANICAL PROPERTIES AND PHASE MORPHOLOGY OF CR VULCANIZATES

Table D1 Crosslink density determined by moving die rheometer (MDR) of CR vulcanizates with varied PSi loadings in silane and non-silane systems

Precipitated silica (phr)	M_H - M_L (dN.m)		
	No silane system	Silane system	
		Si-69	Si-264
20	10.65±0.35	10.37±0.24	10.06±0.06
30	15.72±0.45	13.44±0.56	12.64±0.41
40	22.17±0.10	16.04±0.80	16.64±0.26
50	27.72±1.00	18.93±0.87	19.23±0.57
60	28.21±0.77	19.40±0.07	21.53±0.66

Table D2 Crosslink density as determined from Flory-Rehner equation in vulcanizates with various loadings of PSi

Precipitated silica (phr)	n (×10^{-4} mol/cm^3)		
	No silane system	Silane system	
		Si-69	Si-264
20	3.20±0.09	4.45±0.01	4.26±0.08
30	3.83±0.03	5.86±0.10	5.44±0.14
40	4.27±0.18	7.47±0.04	6.08±0.03
50	4.82±0.23	9.37±0.23	7.76±0.21
60	5.42±0.31	11.86±0.28	9.35±0.02

Table D3 Relative elastic modulus (relative G′) at 5, 10, 50 and 100 % strain at the test frequency of 0.99 rad/s of PSi-filled CR with Si-69 as a function of PSi volume fraction

PSi (phr)	Volume fraction of PSi	Relative G’				
		Guth-Gold Equation	Experimental			
			at 5% strain	at 10% strain	at 50% strain	at 100% strain
0	0.00	1.00	1.00	1.00	1.00	1.00
20	0.11	1.44	2.79	2.81	2.46	2.14
30	0.16	1.73	3.55	3.22	2.13	1.76
40	0.20	2.04	7.21	6.90	5.03	4.14
50	0.24	2.37	13.90	11.63	6.25	4.83
60	0.27	2.70	20.09	17.29	9.58	7.50

Table D4 Relative elastic modulus (relative G′) at 5, 10, 50 and 100 % strain at the test frequency of 0.99 rad/s of PSi-filled CR with Si-264 as a function of PSi volume fraction

PSi (phr)	Volume fraction of PSi	Relative G’				
		Guth-Gold Equation	Experimental			
			at 5% strain	at 10% strain	at 50% strain	at 100% strain
0	0.00	1.00	1.00	1.00	1.00	1.00
20	0.11	1.44	2.33	2.38	2.01	1.75
30	0.16	1.73	4.05	3.59	2.27	1.88
40	0.20	2.04	5.22	4.57	2.74	2.21
50	0.24	2.37	9.33	6.92	3.20	2.55
60	0.27	2.70	19.37	14.44	6.71	5.16

Table D5 Elemental content of CR vulcanizates with Si -69 determined by EDS at specific areas

Element type	Elemental content (%)	
	Spectrum A	Spectrum B
C	23.70	49.96
O	34.97	12.72
Mg	19.57	0.46
Si	2.79	11.67
Cl	11.90	22.81
Zn	7.07	2.37

Table D6 Elemental content of CR vulcanizates with Si -264 determined by EDS at specific areas

Element type	Elemental content (%)		
	Spectrum A	Spectrum B	Spectrum C
C	31.32	48.63	51.91
O	44.31	20.50	16.39
Mg	15.50	2.65	0.68
Si	2.72	6.68	10.08
Cl	5.10	17.05	19.44
Zn	1.05	4.48	1.50

Table D7 Hardness of CR vulcanizates with various loadings of filler

Filler Loading (phr)	Hardness (Shore A)			
	Carbon black	Precipitated silica		
		No silane system	Silane system	
			Si-69	Si-264
20	57.68±0.20	55.75±0.27	56.08±0.80	55.74±0.51
30	59.92±0.38	61.50±0.44	64.59±0.86	60.09±0.85
40	65.97±0.20	66.25±0.61	70.35±0.70	70.13±0.77
50	73.38±0.58	73.40±0.74	80.50±0.89	79.83±0.94
60	77.68±0.41	79.75±1.19	81.63±0.52	81.65±0.76

Table D8 Tensile strength of vulcanizates with various loadings of filler

Filler loading (phr)	Tensile strength (MPa)			
	Carbon black	Precipitated silica		
		No silane system	Silane system	
			Si-69	Si-264
20	17.49±0.54	16.38±0.58	15.30±0.42	16.53±0.09
30	17.71±0.72	17.35±0.42	17.70±0.50	17.59±0.58
40	18.56±0.36	17.98±0.42	20.35±1.05	19.89±0.44
50	19.85±0.68	18.56±0.66	21.51±0.85	18.49±0.52
60	18.76±0.80	18.06±0.33	18.28±0.32	18.39±0.75

Table D9 Modulus at 100% elongation (M100) of vulcanizates with various filler loadings

Filler loading (phr)	Modulus at 100% elongation (MPa)			
	Carbon black	Precipitated silica		
		No silane system	Silane system	
			Si-69	Si-264
20	1.84±0.03	1.45±0.05	1.76±0.03	1.40±0.29
30	2.98±0.06	1.98±0.03	2.59±0.14	2.47±0.05
40	4.14±0.09	2.09±0.10	3.50±0.23	2.78±0.10
50	6.36±0.26	2.43±0.16	4.98±0.38	4.58±0.08
60	8.66±0.47	2.91±0.08	6.40±0.17	5.68±0.14

Table D10 %Compression at 70°C of CR vulcanizates with various filler loadings

Filler loading (phr)	Compression at 70°C (%)			
	Carbon black	Precipitated silica		
		No silane system	Silane system	
			Si-69	Si-264
20	9.02±0.61	10.36±0.55	7.41±0.44	10.88±0.70
30	7.85±1.39	14.34±0.81	10.82±0.95	11.88±0.81
40	7.71±0.58	14.60±0.71	11.96±0.74	14.39±0.54
50	8.33±1.07	21.42±0.71	13.69±0.50	15.21±0.88
60	8.71±1.14	21.75±0.94	14.98±0.51	16.22±0.92

Table D11 %Compression at 100°C of CR vulcanizates with various filler loadings

Filler loading (phr)	Compression at 100°C (%)			
	Carbon black	Precipitated silica		
		No silane system	Silane system	
			Si-69	Si-264
20	15.64±0.30	21.70±0.09	18.69±1.31	20.53±0.47
30	17.96±0.69	27.50±1.48	23.31±1.41	21.90±1.62
40	14.42±1.23	28.13±1.3	24.13±0.26	23.87±0.42
50	19.79±1.05	36.49±0.11	26.57±1.04	26.57±1.04
60	21.33±1.05	37.34±0.33	27.54±2.13	27.54±2.13

Table D12 Heat build-up (HBU) of CR vulcanizates with various filler loadings

Filler loading (phr)	Heat build-up (°C)			
	Carbon black	Precipitated silica		
		No silane system	Silane system	
			Si-69	Si-264
20	9.5±0.7	9.5±0.6	9.0±0.0	11.0±1.4
30	12.5±0.7	13.4±0.6	11.4±0.6	14.0±0.0
40	15.3±1.0	18.3±0.5	15.5±0.7	20.0±0.0
50	23.3±1.5	34.0±3.5	22.5±0.6	28.3±0.5
60	29.0±1.0	33.6±1.5	26.2±1.8	35.7±0.6

Table D13 Dynamic set of CR vulcanizates with various PSi loadings

PSi loading (phr)	Dynamic set (mm.)		
	No silane system	Silane system	
		Si-69	Si-264
20	0.41±0.02	0.22±0.09	0.37±0.07
30	0.49±0.03	0.33±0.02	0.44±0.02
40	1.05±0.05	0.47±0.06	0.52±0.05
50	1.38±0.03	0.52±0.05	0.78±0.03
60	4.10±0.10	0.63±0.08	0.99±0.00

Table D14 Abrasion loss of CR vulcanizates with various filler loadings

Filler loading (phr)	Abrasion loss (mm^3)			
	Carbon black	Precipitated silica		
		No silane system	Silane system	
			Si-69	Si-264
20	136.78±0.58	193.37±4.44	137.70±6.01	134.77±4.41
30	128.19±16.70	189.90±5.76	122.18±5.12	114.567±2.14
40	122.58±5.81	181.53±2.32	118.40±5.43	113.54±2.08
50	92.44±0.72	188.62±3.58	117.97±3.35	111.67±3.21
60	88.94±5.41	191.70±2.24	113.20±6.02	108.54±2.79

Table D15 Tan δ at 30 and 60 °C of PSi-filled CR vulcanizates with and without SCA treatment (PSi is kept constant at 40 phr)

CR compound	Tan δ	
	At 30 °C	At 60 °C
PSi-40 w/o silane	0.064009	0.053254
PSi+Si-69	0.066221	0.051899
PSi+Si-264	0.073022	0.060052

Table D16 Tan δ as a function of temperature in PSi-filled CR vulcanizates determined by DMTA

1st				2nd			
Temp (°C)	Tanδ	Temp (°C)	Tanδ	Temp (°C)	Tanδ	Temp (°C)	Tanδ
20.0	0.06832	61.1	0.05220	20.0	0.07041	61.2	0.05250
20.1	0.07026	62.5	0.05268	20.2	0.07090	62.5	0.05211
22.2	0.06825	64.0	0.05196	22.2	0.06921	63.8	0.05212
23.6	0.06737	65.3	0.05260	23.6	0.06872	65.2	0.05283
25.0	0.06693	66.7	0.05175	25.0	0.06838	66.8	0.05307
26.4	0.06583	68.0	0.05098	26.4	0.06584	68.1	0.05307
27.8	0.06599	69.4	0.05200	27.8	0.06526	69.5	0.05335
29.2	0.06425	71.0	0.05173	29.2	0.06546	70.8	0.05336
30.6	0.06371	72.2	0.05166	30.6	0.06430	72.3	0.05231
31.9	0.06394	73.6	0.05162	31.9	0.06318	73.6	0.05243
33.3	0.06244	75.0	0.05233	33.3	0.06152	75.0	0.05278
34.7	0.06098	76.5	0.05380	34.7	0.06047	76.5	0.05301
36.1	0.06015	77.9	0.05327	36.1	0.06096	77.9	0.05333
37.5	0.06080	79.3	0.05321	37.5	0.05981	79.3	0.05410
38.9	0.05918	80.6	0.05342	38.9	0.05979	80.7	0.05299
40.3	0.05874	82.2	0.05420	40.3	0.05943	81.8	0.05404
41.7	0.05762	83.6	0.05375	41.7	0.05857	83.2	0.05459
43.0	0.05728	84.8	0.05301	43.1	0.05686	84.6	0.05330
44.3	0.05687	85.9	0.05356	44.5	0.05720	86.1	0.05499
45.8	0.05638	87.5	0.05403	45.8	0.05715	87.5	0.05454
47.2	0.05461	89.0	0.05350	47.2	0.05597	89.0	0.05377
48.7	0.05482	90.3	0.05473	48.6	0.05611	90.2	0.05480
50.0	0.05402	91.8	0.05484	50.0	0.05526	91.8	0.05527
51.5	0.05495	93.1	0.05471	51.4	0.05486	93.1	0.05472
52.8	0.05366	94.4	0.05473	52.8	0.05432	94.5	0.05538
54.3	0.05334	95.9	0.05484	54.2	0.05376	95.7	0.05593
55.5	0.05331	97.3	0.05453	55.5	0.05465	97.1	0.05577
56.8	0.05272	98.5	0.05503	56.8	0.05419	98.4	0.05452
58.4	0.05328	99.5	0.05489	58.3	0.05359	99.6	0.05496
59.6	0.05340			59.8	0.05311		

Table D17 Tan δ as a function of temperature in PSi-filled CR vulcanizates with silane treatment determined by DMTA

Si-69				Si-264			
Temp (°C)	Tanδ	Temp (°C)	Tanδ	Temp (°C)	Tanδ	Temp (°C)	Tanδ
20.0	0.06982	61.0	0.05126	20.0	0.08136	61.0	0.05896
20.2	0.07011	62.5	0.05112	20.2	0.08158	62.5	0.05936
22.2	0.07059	63.9	0.05012	22.2	0.07902	63.8	0.05844
23.6	0.06973	65.4	0.04964	23.6	0.07864	65.3	0.05763
25.0	0.06941	66.7	0.05005	25.0	0.07866	66.7	0.05740
26.4	0.06880	68.2	0.05028	26.4	0.07674	68.0	0.05741
27.9	0.06847	69.4	0.04892	27.8	0.07537	69.4	0.05720
29.2	0.06708	70.7	0.04833	29.2	0.07477	70.9	0.05678
30.6	0.06622	72.3	0.04879	30.6	0.07302	72.1	0.05616
31.9	0.06495	73.6	0.05011	31.9	0.07393	73.6	0.05722
33.3	0.06506	75.1	0.04966	33.3	0.07322	74.9	0.05691
34.7	0.06351	76.5	0.04964	34.7	0.07147	76.3	0.05636
36.1	0.06286	77.8	0.04855	36.1	0.07098	77.8	0.05592
37.5	0.06218	79.2	0.04956	37.5	0.06975	79.3	0.05586
38.9	0.06125	80.7	0.04900	38.8	0.07082	80.7	0.05588
40.3	0.06045	81.9	0.04984	40.3	0.06906	81.8	0.05653
41.7	0.05994	83.4	0.04962	41.7	0.06796	83.4	0.05667
43.2	0.05853	84.7	0.04923	43.1	0.06587	84.8	0.05586
44.4	0.05804	86.0	0.04929	44.4	0.06640	86.2	0.05697
45.7	0.05668	87.5	0.04939	45.8	0.06486	87.4	0.05673
47.1	0.05703	88.7	0.04901	47.1	0.06388	88.8	0.05638
48.7	0.05535	90.3	0.05033	48.6	0.06291	90.7	0.05710
50.0	0.05479	91.7	0.05062	50.1	0.06337	91.4	0.05512
51.4	0.05454	93.0	0.04939	51.5	0.06204	93.0	0.05678
52.8	0.05346	94.3	0.04973	52.8	0.06160	94.4	0.05543
54.1	0.05370	95.8	0.05099	54.2	0.06046	95.9	0.05605
55.6	0.05281	97.3	0.05018	55.6	0.05954	97.3	0.05597
57.0	0.05262	98.7	0.04999	56.9	0.06017	98.5	0.05611
58.3	0.05211	99.6	0.05133	58.4	0.05961	99.8	0.05755
59.6	0.05190			59.7	0.06005		

APPENDIX E

EFFECTS OF TAN δ AND CROSSLINK DENSITY ON HEAT BUILD-UP (HBU) OF CR VULCANIZATES

Table E.1 Crosslink density, tan δ and heat build-up (HBU) of CR vulcanizates filled with various loadings of MgO

MgO content (phr)	Crosslink density; n* ($\times 10^{-4}$ mol/cm^3)	tanδ	HBU (°C)
2	9.03±0.11	0.0640	19.5±0.71
4	10.52±0.33	0.0611	22.0±0.00
6	10.38±0.27	0.0602	22.0±0.02

* = As determined from the Flory-Rehner equation

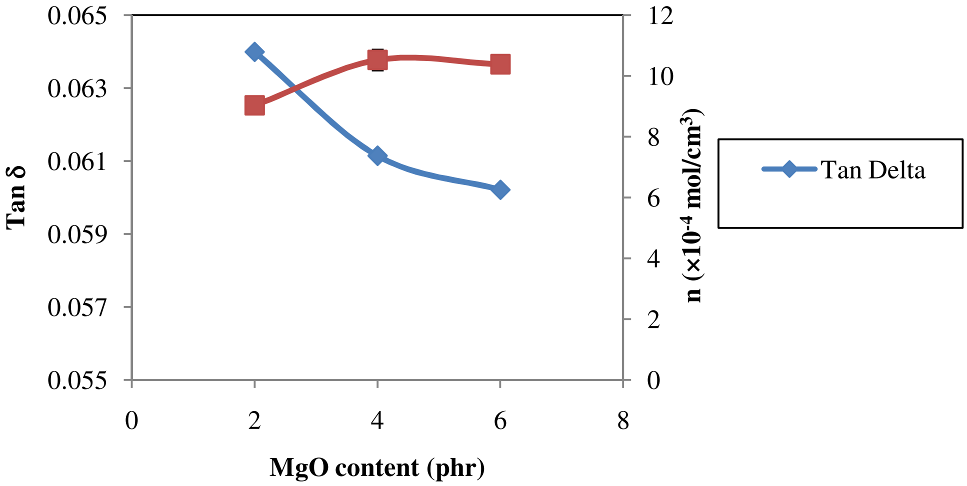

Figure E.1 Relationship among tanδ at 99.5 °C, MgO loading and crosslink density of CR vulcanizates

The hysteresis factor (tanδ) and crosslink density of CR vulcanizates with various loadings of MgO are shown in Figure E.1. Evidently, the tanδ decreases with increasing MgO content, i.e., with increasing crosslink density, and then levels off. Unexpectedly, the HBU is found to increase with increasing crosslink density. It is known that the HBU is proportional to hysteretic process or loss modulus (G″). As shown in Equation E.1, with increasing crosslink density giving rise to the decrease in tanδ and the increase in elastic modulus (G′), the increase in HBU observed would be dominated by the increase in G′ (i.e., molecular restriction).

$$G'' = G' \times \tan\delta \quad \text{[Equation E.1]}$$

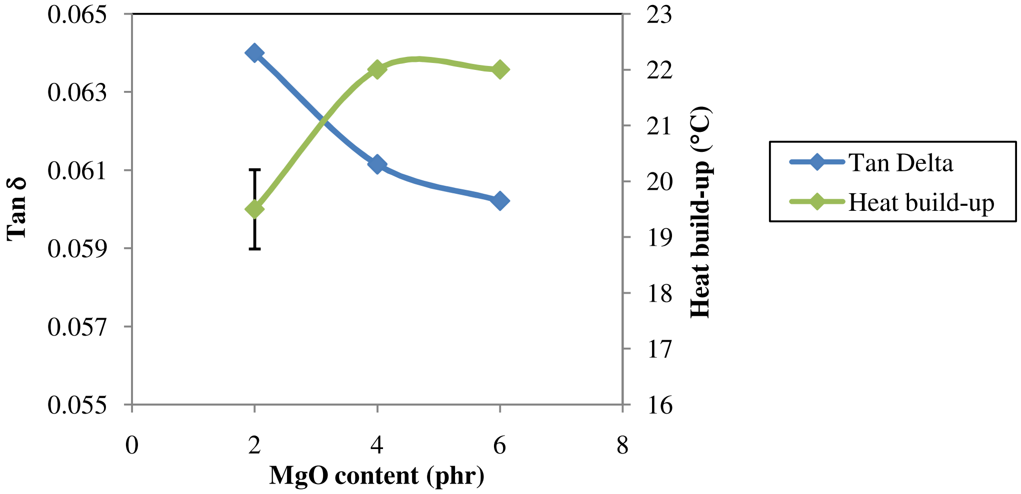

Figure E.2 The relationship between tanδ at 99.5 °C and HBU properties of CR vulcanizates

BIOGRAPHY

NAME	Miss Yotwadee Chokanandsombat
DATE OF BIRTH	18 Jan 1984
PLACE OF BIRTH	Bangkok Thailand
INSTITUTIONS ATTENDED	Mahidol University, 2003-2006: Bachelor of Science (Chemistry) Mahidol University, 2007-2010: Master of Science (Polymer science and technology)
HOME ADDRESS	37/159 Petchakasem Road, Nongkangpoo Sub-district, Nongkham District, Bangkok, THAILAND 10160
	Tel. 081-753-2503
	E-mail: khunlah@hotmail.com